MODELING AND CONTROL OF KITE ENERGY SYSTEMS
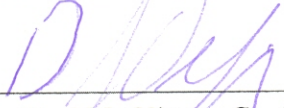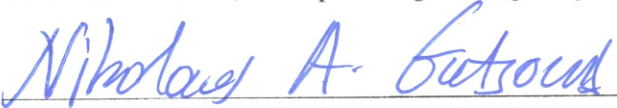
by

Haocheng Li

A dissertation submitted to the Faculty of

WORCESTER POLYTECHNIC INSTITUTE

in partial fulfillment of the requirements for the degree of

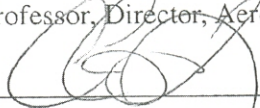DOCTOR OF PHILOSOPHY IN AEROSPACE ENGINEERING.

April 2017
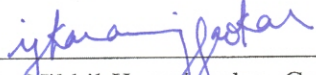
APPROVED:

Dr. Michael A. Demetriou, Co-Advisor
Professor, Aerospace Engineering Program.

Dr. David J. Olinger, Co-Advisor
Associate Professor, Aerospace Engineering Program.

Dr. Nikolaos A. Gatsonis, Committee Member
Professor, Director, Aerospace Engineering Program

Chris Vermillion, Committee Member
Assistant Professor, Department of Mechanical Engineering and Engineering Science
University of North Carolina at Charlotte

Dr. Nikhil Karanjgaokar, Graduate Committee Representative
Assistant Professor, Aerospace Engineering Program.

Abstract

Kite energy systems are an emerging renewable energy technology. Unlike conventional turbines, kite energy systems extract wind power using tethered kites which can move freely in the wind or underwater in an ocean current. Due to the mobility, kite power systems can harvest power from regions with higher and steadier power density by moving in high-speed cross flow motion. An airborne kite energy system harnesses wind power at an altitude higher than the conventional wind turbines, while an undersea kite energy system extracts power close to the ocean surface.

In this dissertation, the physical limitation, mathematical modeling, and control system design of the kite energy systems are studied. First, three major physical effects that are acting on the kite energy systems are investigated, including potential force, steady aero-/hydro-dynamic force and added mass effects. Furthermore, the dissipativity of the steady aero-/hydro-dynamic forces with respect to the apparent velocity is established. Based on this analysis, the power generation limit of the kite energy systems is studied. A power limit formulation is given which generalize the two-dimensional result to three-dimensional case.

The different physical phenomenon is modeled in different coordinate systems, the difference of the density, viscosity between air and water are significant, and the kite energy system can operate in two distinct modes. To combine different physical effects into a single simulation framework, the equivalences of the kite model in different coordinate systems are established through kinematic analysis. Using these equivalent relations, a unified simulation model for airborne and undersea kite energy systems are derived.

The control system design of kite energy systems is also investigated. The resulting equations of motion of kite energy systems are highly nonlinear. Therefore, Lyapunov methods are used to

analyze the system behavior. Three different techniques are reviewed, including Lyapunov analysis for autonomous and non-autonomous systems, the ultimate boundedness and input-to-state stability and passivity methods. For the fixed tether length kite energy systems, the ultimate boundedness of the kite translation is established through the dissipativity of the steady aero-/hydro-dynamic force. For the variable tether length kite energy system, the input-to-state analysis is used to design the tether tension that guaranteed the boundedness of the kite translation. In both cases, the Lyapunov based methods are used to design kite rotational control systems which result in PD type control signals. Although this control scheme generates consecutive power cycles for kite energy systems. It is shown that the kite aero-/hydro-dynamical performance is unstable in the simulation which could result in unsteady power generation.

To provide a steadier performance in kite translation and power output, the relative dynamics of the kite translation is first proposed. In this model, the kite apparent speed and attitudes, the angle of attack and side-slip angle, are used to describe the kite translation. A nonlinear control scheme is designed to regulate the angle of attack and side-slip angle using back-stepping methods by using the kite angular velocity and control inputs. However, due to the magnitude limit of the angular velocity, the residual error of the apparent attitude tracking remain large for the large desired angle of attack and side-slip angle.

To achieve a better power harvesting and aero-/hydro-dynamics performance, the geometric properties of kite angle of attack and side-slip angle are studied. A geometric attitudes trajectory is constructed to track given apparent attitudes. A rotational control system is designed based on the back-stepping and sliding mode methods for the desired geometric attitude, and the high gain observer is applied to acquire the information needed for the rotational control signal. Through the geometric apparent attitudes tracking control algorithm, the angle of attack and side-slip angle act as direct control inputs to the kite translational motion. The kite translational dynamics under the geometric apparent attitude tracking is studied. These dynamics give the possibility of controlling the kite translational motion only through the rotational control scheme.

Contents

List of Figures

Chapter 1

Introduction

Modern industrial society is driven by a large amount of energy. It has been estimated that the total consumption of global energy is equivalent to 9301 million tonnes of oil in 2013, which is equal to 12.3 Terawatts. The combustion of fossil fuel provides over 86% of the total energy consumption. Despite its great economical advantage and high energy density, the carbon emission during the burning of fossil fuel has a significant social and environmental impact. To achieve sustainable development of modern society, various alternative energy technologies have been developed including nuclear, hydrokinetic, biomass, solar, wind and geothermal energy. Among all these alternative options, wind and hydrokinetic energies are considered in this thesis. It is also important to notice that the solar energy sources are distributed on earth with great disparities which greatly limit the commercialization of such renewable power plants. Similar to the solar power systems, the conventional wind power plants are also limited by the low power density and global disparity of the energy sources. To access to the high wind power density, huge towers are required in a conventional wind power systems. Currently, the largest wind turbine is the Enercon E-126, with the hub height of 135 meters and the rotor diameter of 127 meters. The uncertainty of the wind power system, such as the variation of the wind velocity in time, also cause difficulties in utilizing the wind power. However, at higher altitudes than the conventional wind turbines, there is wind with higher velocity and consistency. Figure 1.1 shows the wind energy density, $P = \frac{1}{2}\rho_{air}W^3$, at

---

[1]Certain Materials are included under the fair use exemption of the U.S. Copy law and have been prepared according to the fair use guidelines and are restricted from the further use

7

Wind Energy Density Map

120m   600m
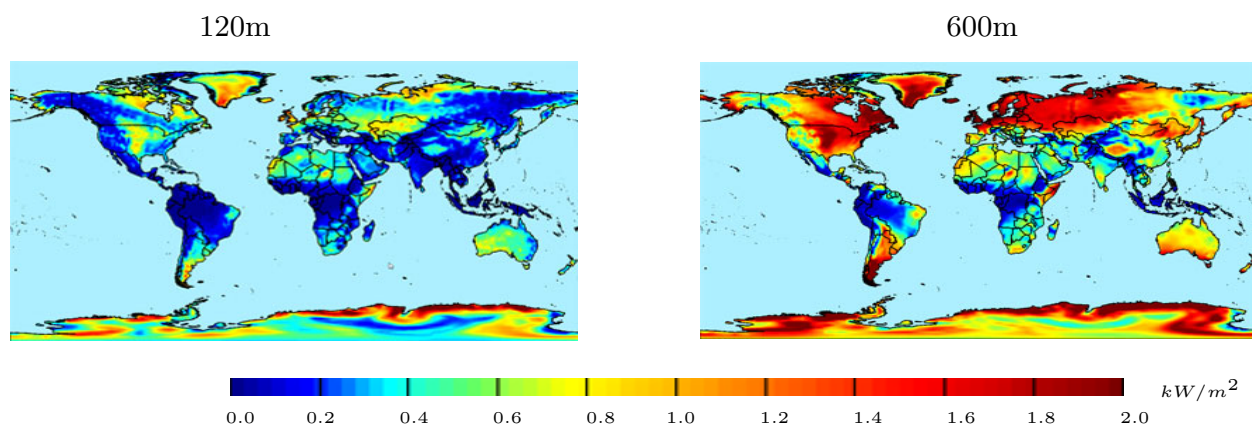
Figure 1.1: Wind Energy Density Comparison: 120m Altitudes and 600m Altitudes, From [5], Copyright Joby Energy[1]

120m altitude and 600m altitude, where ρ_{air} is the air density and W is the wind speed. To harvest the wind energy that exists at higher altitudes than the airborne wind energy systems have been considered.

1.1 Kite Energy Technology

In this dissertation, an emerging renewable energy technology, kite energy, is studied. The kite energy technologies are power generation technology using airborne or submersible kites, [6, 7]. There are three major advantages of using kite energy systems in power generation:

- The mobility of the kite energy systems allow for power generation at altitudes or depths with higher wind and current velocities,

- The mobility of the kite allow for high-speed crosswind or current motion which increase the energy density in power generation,

- Without the towering structures, the kite energy systems may achieve higher power to mass ratio and need less material investment than conventional turbines

There are three common elements in every kite energy systems: the airborne or undersea structures (also referred as kites), the tether and power generation device. Typical wind turbine,
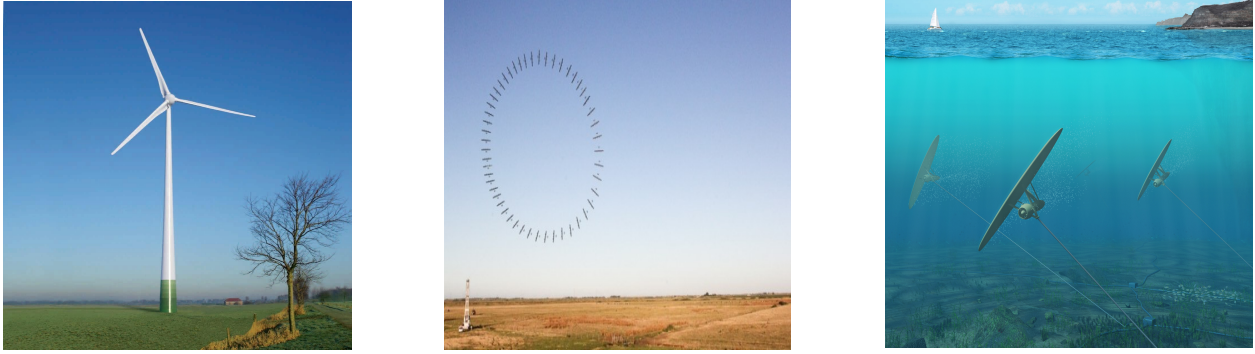
Figure 1.2: Wind Turbine System, Airborne Kite Energy System and Undersea Kite Energy System, From [1, 2], Copyright Makani, Minesto

airborne kite energy system and undersea kite energy system are shown in Figure 1.2. If the power generation device is an electric generator, the airborne kite energy system can be placed into two categories, the GroundGen and FlyGen system as shown in Figure 1.3. Among the airborne kite energy systems, the GroundGen systems (also refer to lift mode) are kite energy systems with the power generation unit on the ground, [3, 8, 9]. Either flexible kite or rigid kite can be used to provide the lifting force that needs for power generation as shown in Figure 1.4. The tether is used to connect the kite to a ground-based generator. The mechanical power of the flying kite is then transformed to electrical power by the ground-based generator. On the other hand, the similar system configuration is also applicable to the undersea kite energy system. In this work, the undersea kite connected to a floating platform is considered which is anchored to the seabed. A detailed illustration of the undersea kite configuration is shown in Figure 1.5.
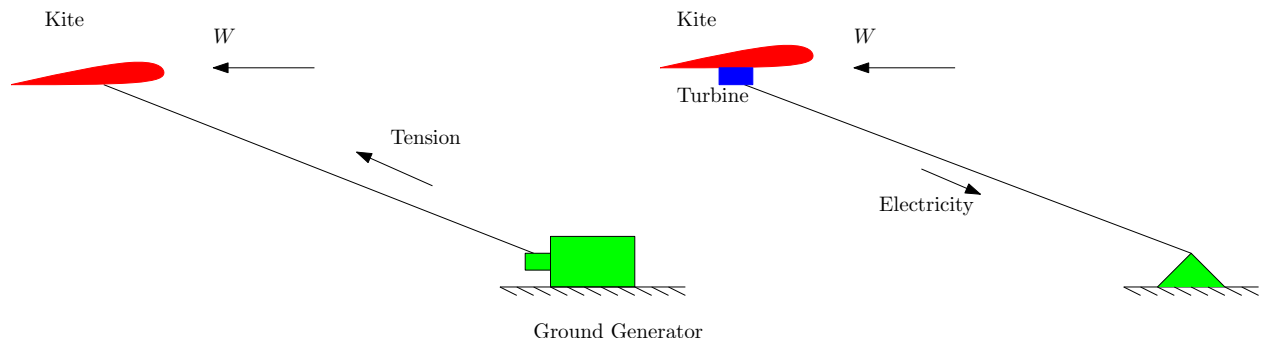
Figure 1.3: GroundGen and FlyGen Airborne Kite Energy Systems

There are two motion phases during the kite motion in a GroundGen system, the generation and retraction phase. In generation phase, the kite is controlled to produce high lift and power is

9

Figure 1.4: Rigid and Flexible GroundGen Airborne Kite Energy System, From [3, 4], Copyright Ampyx, Delft University of Technology
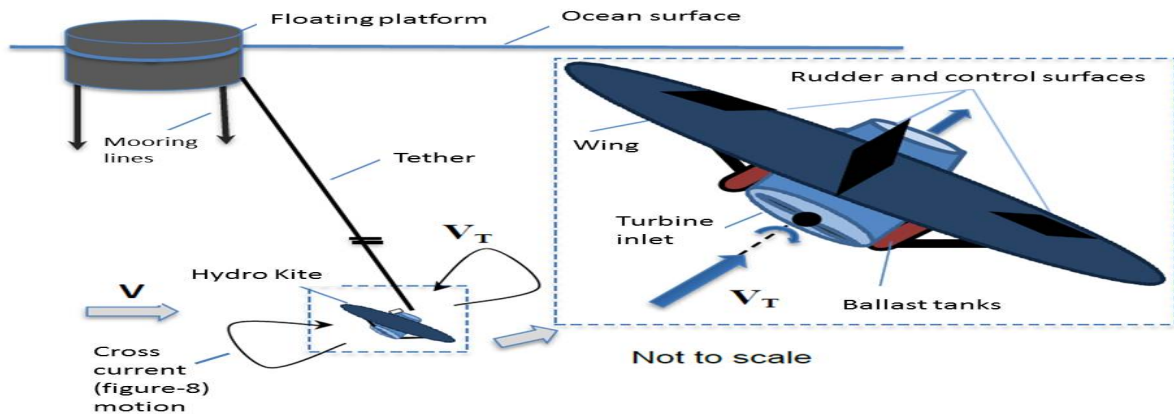
Figure 1.5: System configuration of undersea kite energy system

generated as the kite reels out the tether. In retraction phase, the kite is controlled to produce low lift force, and part of the generated power is used to reel in the tether to an initial position for next power generation phase. The illustration of power and traction phase of a GroundGen system is shown in Figure 1.6. The goal of a GroundGen airborne kite energy system is to maximize the net power output which is the difference between the power output of the power generation phase and power consumption in retraction phase.

On the other hand, the FlyGen airborne kite energy system is a kite system with onboard turbine generator for power generation as shown in [1] where the turbine is also used as propeller during the takeoff and landing operation. Since the airborne kite needs to provide the high lift force as well as support the turbines, these systems use rigid kite(or glider). The constant length tether in FlyGen airborne kite energy system is used to constrain the kite motion and conduct the generated power to the ground. Other than the electricity generation, there is airborne kite energy system that use the tether tension to drive the marine or ground vehicles. The towing kite system
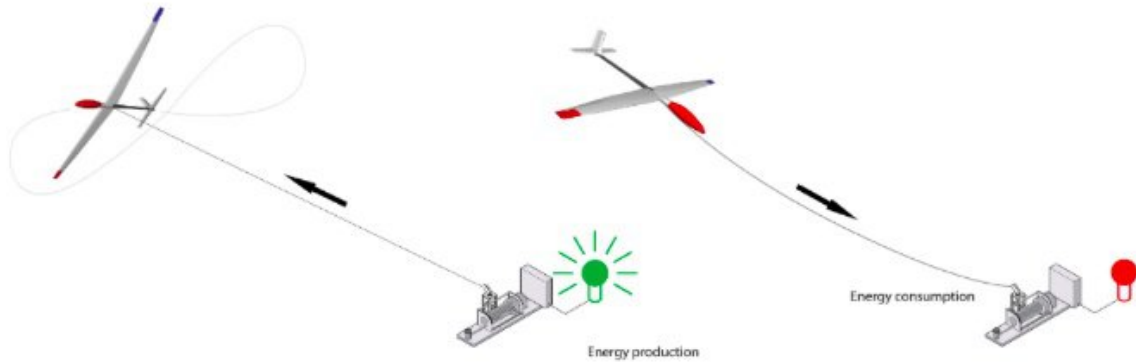
Figure 1.6: Airborne Kite Energy System: Power and Recover Phases,from Ref [1,3], Copyright Ampyx and Makani

in such vehicle propulsion case is almost identical to the GroundGen airborne kite system. The airborne propulsion system is especially promising in the naval transport application where the cost crucially depends on the fuel price. Moreover, the lifting force generated by the airborne kite can also be used in the pumping system.

The balloon-type system configuration is also developed for power generation. In such system, the wind turbine is supported by the buoyancy force of the balloon, and the high power output is achieved by flying at high altitudes. The tether is used to constrain the balloon motion and conduct the generated power to the ground. Theoretically, such system can stay at the high altitude indefinitely without power consumption.

However, these systems required a high volume to keep floating and significant tether in the case of strong wind. The FlyGen type of kite energy systems can also be used in the undersea circumstance, which is also referred as the Tethered Undersea Kite System (TUSK). Similar to the FlyGen airborne systems, the undersea turbine generates power in cross current motion, [2]. Undersea kites can be connected either to the seabed or floating platforms. Due to greater density and viscosity of the water compared to air, it is more efficient to produce power using turbine than using tether tension in water.

In summary, there are three major concepts in the kite energy system: the flexible kite system, the rigid glider system, and balloon systems. A low weight flexible kite system generates either

electrical or mechanical power in a moderate speed motion through tether tension. A high weight rigid kite system can generate power in a high-speed cross wind motion in the air or a cross current motion undersea. Either turbines or tether tension can be used to generate power in the airborne case. However, the turbine is often used to produce power undersea. The major characteristics of these three system configurations are summarized in Table 1.1

	Flexible Kite	Rigid Kite	Balloon
Weight	Low	High	Moderate
Speed	Moderate	High	Static
Power Generation	Tension	Tension/Turbine	Turbine
Power Output	Mechanical/Electrical	Electrical	Electrical
Application	Airborne	Airborne/Undersea	Airborne

Table 1.1: Comparison of Different System Configurations

1.2   Literature Reviews

Depending on the power generation configurations, there is two major control mechanisms in the kite and balloon energy systems: tether control mechanism and control surfaces mechanism. For a flexible kite energy system, only the tether control mechanism is applicable where the input of the system is typically the tether length difference. On the other hand, both tether control mechanism and control surface mechanism can be used in the rigid kite system. In a control surfaces mechanism, the input to the system is the deflection of the control surfaces. The control system configurations have a significant influence on the kite dynamics. If the kite systems are controlled by the tether mechanism, the kite translation and rotation can not be treated as independent motions. In this case, the simplified kite dynamics are usually studied. If the control surfaces mechanisms are used, the translational and rotational motion can be treated as independent motions. The tether tension and control moment acting on the kite can be treated as independent inputs.

In [10], two flexible kite energy system configurations, the *yo-yo* configuration and the *carousel* configuration, are investigated by numerical simulation. The control systems are designed using nonlinear model predictive method and set membership function approximation. In [11], the evaluation of control system performance, the optimization power generating cycles are studied using

simplified power equations. The proposed optimal operation cycles are simulated by nonlinear model predictive control strategy. In [12], the authors investigated the controlled kite application on the naval transportation. To maximize the boat speed, a constrained optimization problem was formulated based on the simplified kite and boat translational dynamics. A predictive control strategy was carried out to a realistic dynamic model of the system in the presence of wind turbulence. The detailed kinematics of the towing kite system is discussed in [13]. The control system of the kite is designed based on the simplification of nonlinear kinematics. The quaternion is then used to modify the kinematic relation in [14]. The optimization control techniques are developed for maximum power generation.

A study of sensor fusion techniques is presented in [15]. The estimation algorithms for kite position and velocity angle were proposed. The developing of the control-oriented velocity dynamics was presented in [16]. The proposed model was identified from the experiments, and proportional controls are applied to achieve the figure eight kite operations. The power optimization control technique is studied in [17]. The sensitivity of the tether tension for generalized path parameterization was analyzed, and an algorithm is designed for maximizing the tension force. On the other hand, the control design for the tether tension in the retraction phase was presented in [18]. The time delay effects in velocity angle dynamics are studied in [19]; a cascade control architecture is implemented for velocity direction tracking. The model-based adaptive control method is applied for time-varying wind conditions. The time delay input model for the kite energy system is considered in [20]. A path-tracking receding horizon LQR controller and on-line estimation of the system parameters are considered. In [21], a range-inertial estimation scheme is proposed base on the sensor fusion estimation.

In [22, 23], the flexible kite system dynamics are modeled using Euler-Lagrange approach. Both kite rigid body motion and aerodynamic forces acting on the tether are considered in the system formulations. The numerical nonlinear optimal control schemes are applied to the control system design. However, the multi-body model of the kite energy system yields large dimensional dynamics which make the analytical and numerical control techniques difficult to apply. Therefore, the kite motion is projected to two-dimensional motion of the plane on an imaginary sphere in [24]. Based on this simplification, the kite heading angle and track angle are defined. The correlation

relation of kite track angle and steering input are used to form the base of control system design. The high level and low level of the kite tracking control is designed using proportion and derivative control methods. Other than the conventional PD control design for the kite system tracking and optimization, the learning method is also used for control design as presented in [25]. The core idea of the flexible kite system controls rely on the simplification of the kite dynamics into a single degree of freedom linear system. This process allows the mature control techniques to be applied to the kite control design, however the linear approximation constraint the capability of the system models.

The modeling and control problem of the balloon energy systems are addressed in [26–28]. Although the rigid body shroud dynamics are presented in [26], the operation of the balloon energy system is typically stationary. Therefore, the linearization technique is typically applicable, and the frequency domain analysis method can be applied. In [27], a Lyapunov based extreme seeking control schemes are designed, and the energy generation performance is improved. The adaptive control design based on the extreme seeking and wind speed estimation is considered in [28].

In previous research, the author has developed the Lyapunov based rotational control for the six degrees of freedom rigid kite energy system dynamics [29, 30]. The corresponding six-degree freedom system for undersea kite energy system is proposed in [31, 32]. The dynamic models of the undersea kites have then been modified to include the added mass effect with passivity-based control signal. The idea of geometric apparent attitude tracking is proposed in [33]. Using this method, the kite angle of attack and side slip angle can be regulated to the desired value if the kite apparent wind velocity can be obtained by the sensors. Moreover, the kite translational dynamics under the geometric apparent attitude tracking is proposed in [34]. In this work, the consequence of the geometric apparent attitude tracking is studied. It turns out that the geometric apparent attitude tracking decomposed the steady aerodynamic forces and provided direct actuation to the kite translation. Therefore, the translational control signals can be designed in the using backstepping methods. This work extends the previously published results by considering three more important aspects of kite energy systems. The power production limit of the kite energy system is discussed in Chapter 4 using the passivity property of the steady aerodynamic forces. The tension control signal is designed by investigating the open loop kite system dynamics in

Chapter 7. The apparent dynamic attitude tracking control design is proposed in Chapter 8.

In this dissertation, the focus is put on the rigid kite energy system with the control surface mechanism for the following reasons:

- The rigid body dynamics yields a complete description of kite translational and rotational motion;

- The complete aero-/hydro-dynamic description allows the detail studies of the kite geometric properties on the overall performance;

- It allows the complete studies of the relation between the control action and kite system motion.

1.3   Contributions

In this work, both modeling and control aspects of the kite energy systems are investigated. The crucial physical effects acting on the kite motion are considered, including the steady fluid dynamical forces, the added mass effects, and the potential forces. In the preliminary chapter, these forces are analyzed separately. The key kinematic relations are also given which provide a foundation in establishing the dynamical models of the kite energy systems. In the modeling chapter, the transformation relations of the kite system dynamics are established using results of the system kinematics. Using dynamics transformation relations, physical effects that modeled in different reference frames can be combined into a single framework of system modeling. To conclude the system modeling, the kite dynamics are expressed in matrix forms. These expressions reduce the computational complexity in simulating of the kite motion. After establishing the models of kite energy systems, the dissipativity of the steady aero-/hydro-dynamic forces is provided. Based on this property of the aero-/hydro-dynamic forces, the power limit of the kite energy system is derived. There are three major methods that will be used to control the kite motion: the passivity-based control methods, the geometric apparent attitude tracking, and the dynamical apparent attitude tracking. In passivity-based approach, the fundamental aspects of the kite translational motion are discussed such as the input to state stability and ultimately boundedness. Using

Lyapunov methods, the passivity-based control methods can be used in both airborne and undersea kite energy systems. The geometric apparent attitude tracking of kite energy systems provides a method of using kite rotational motion to achieve the desired kite apparent attitudes. A geometric attitude trajectory is proposed, and the corresponding rotational controls are derived based on sliding mode method. Based on the rotational trajectory proposed, the translational motion of the kite is further studied. This study shows that the geometric apparent attitude tracking provides additional actuation to kite translation. A simplified kite translational model is proposed based on the apparent attitude tracking. In addition to the geometric method, the apparent kite attitudes can also be controlled using kite angular velocity. By transforming the kite dynamics into relative motion frame, the kite angular velocity appears as control inputs to kite translation. Based on the back-stepping method, the apparent attitude regulator is proposed and verified by simulation.

The major contributions of this work are summarized in the following list:

- Establishing the added mass model of the kite energy systems;

- Providing the equivalent relations of the rigid body model of kite energy system in different reference frames;

- Establishing a framework of modeling for combining different physical phenomenon;

- Establishing the passivity of the steady aero-/hydro-dynamic forces;

- Establishing the power generation limits of the kite energy systems;

- Develop the passivity-based tension control for airborne and undersea kite energy systems;

- Develop the passivity-based rotational control for undersea kite energy systems;

- Proposing the apparent dynamic attitude tracking control for airborne kite energy systems;

- Proposing the geometric apparent attitude tracking law for airborne energy systems;

- Designing the rotational attitudes tracking control using back-stepping methods;

- Establishing the kite translational dynamics under the geometric apparent attitude tracking.

16

Chapter 2

Physical Fundamentals of the Kite Energy Systems

In this chapter, the fundamental perspectives of the kite energy systems are discussed. In Section 2.1, the kinematic transformation matrices between different coordinate systems are given. Important properties of the transformation matrices are also provided. From Section 2.2 to 2.4, the steady aero-/hydro-dynamic force, added mass effect, potential forces and tether tension are discussed. One important aspect of special importance, the passivity of the steady aero-/hydro-dynamic force, is given in Section 2.5. Using the passivity properties, the power limitation of the kite energy systems in three dimensional motion is derived at the last section of this chapter.

2.1   System Kinematics

To describe the rigid body motion of the kite energy system, two translational coordinate systems and two rotational coordinate systems need to be introduced as follows

Translational Coordinate Systems

– Cartesian Frame: $\mathbf{C} \doteq \begin{pmatrix} \mathbf{i}_C & \mathbf{j}_C & \mathbf{k}_C \end{pmatrix}$;   Spherical Frame: $\mathbf{S} \doteq \begin{pmatrix} \mathbf{e}_r & \mathbf{e}_1 & \mathbf{e}_2 \end{pmatrix}$,

Rotational Coordinate Systems

– Body Frame: $\mathbf{B} \doteq \begin{pmatrix} \mathbf{i}_B & \mathbf{j}_B & \mathbf{k}_B \end{pmatrix}$;   Euler Frame: $\mathbf{E} \doteq \begin{pmatrix} \mathbf{e}_\phi & \mathbf{e}_\theta & \mathbf{e}_\psi \end{pmatrix}$.

The Cartesian frame centers at the anchor point of tether, which is also the origin of the kite energy system. The x-axis is pointing to the upstream direction of the wind and the z-axis is vertical downwards. The y-axis forms a right hand coordinate system with x-axis and z-axis.

Denote the position of kite center of gravity (CG) as $\mathbf{r}_C = \begin{pmatrix} x_C & y_C & z_C \end{pmatrix}$, then the spherical coordinates of the kite $\mathbf{q} = \begin{pmatrix} r & q_1 & q_2 \end{pmatrix}$ can be defined as follows

$$\mathbf{q} = \begin{pmatrix} r & q_1 & q_2 \end{pmatrix} = \begin{pmatrix} \sqrt{x_C^2 + y_C^2 + z_C^2} & \arctan\left(\frac{y_C}{\sqrt{x_C^2 + z_C^2}}\right) & \arctan\left(\frac{x_C}{z_C}\right) \end{pmatrix}, \tag{2.1}$$

where r is the tether length, q_1 is referred as the crosswind angle and q_2 as the inclination angle. The inverse coordinate transform is given by

$$\mathbf{r}_C = \begin{pmatrix} x_C & y_C & z_C \end{pmatrix} = r \begin{pmatrix} \cos q_1 \sin q_2 & \sin q_1 & \cos q_1 \cos q_2 \end{pmatrix}. \tag{2.2}$$

Taking the derivative of equation (2.2) gives the translational velocity transformation:

$$\mathbf{V}_C = \mathbf{P}\dot{\mathbf{q}} \qquad \mathbf{P} = \begin{pmatrix} \cos q_1 \sin q_2 & -r \sin q_1 \sin q_2 & r \cos q_1 \cos q_2 \\ \sin q_1 & r \cos q_1 & 0 \\ \cos q_1 \cos q_2 & -r \sin q_1 \cos q_2 & -r \cos q_1 \sin q_2 \end{pmatrix}. \tag{2.3}$$

The body frame $\mathbf{B}$ centers at the CG of the glider and follows the North-East-Down axes convention. The kinematic relations of the kite translation is shown in Figure 2.1.

The attitude of the body frame $\mathbf{B}$ with respect to Cartesian frame $\mathbf{C}$ can be represented by three consecutive Euler angles $\boldsymbol{\Theta} = \begin{pmatrix} \phi & \theta & \psi \end{pmatrix}$. Denote the glider translational velocity measured in the body frame $\mathbf{B}$ as $\mathbf{V}_B$ and the directional cosine matrix as $\mathbf{L}_{BC}$, then the translational velocity transformation from frame $\mathbf{B}$ to $\mathbf{C}$ is given by

$$\mathbf{V}_C = \mathbf{L}_{CB}\mathbf{V}_B, \qquad \mathbf{L}_{BC} = \mathbf{L}_{CB}^T = \begin{pmatrix} c_\theta c_\psi & c_\theta s_\psi & -s_\theta \\ s_\phi s_\theta c_\psi - c_\phi s_\psi & s_\phi s_\theta s_\psi + c_\phi c_\psi & s_\phi c_\theta \\ c_\phi s_\theta c_\psi + s_\phi s_\psi & c_\phi s_\theta s_\psi - s_\phi s_\psi & c_\phi c_\theta \end{pmatrix}, \tag{2.4}$$
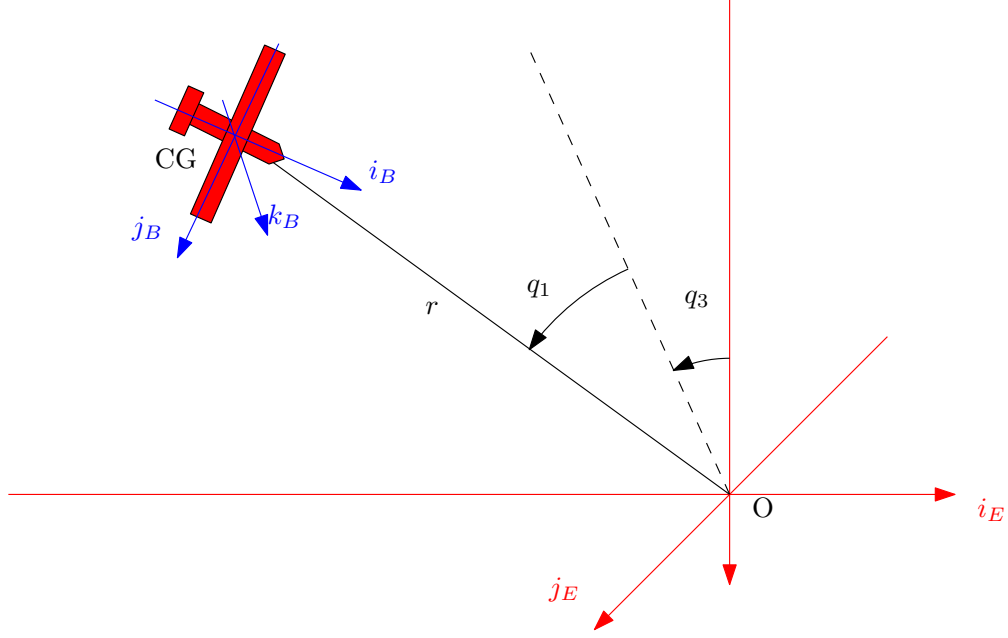
Figure 2.1: Kite Translational Kinematics
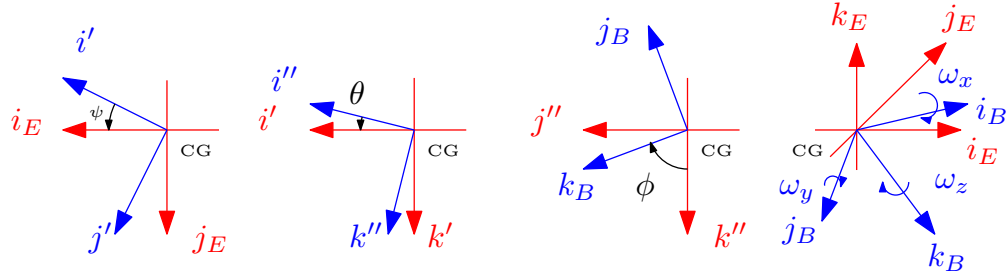
Figure 2.2: Kite Rotational Kinematics

where c and s are short hand notations of the sine and cosine function respectively. Denote the glider rotational velocity along axes in the body frame $\mathbf{B}$ as $\boldsymbol{\omega} = \begin{pmatrix} \omega_x & \omega_y & \omega_z \end{pmatrix}$, then the rotational velocity transformation from frame $\mathbf{E}$ to $\mathbf{B}$ is given by

$$\boldsymbol{\omega} = \mathbf{R}\dot{\boldsymbol{\Theta}} \qquad \mathbf{R} = \begin{pmatrix} 1 & 0 & -s_\theta \\ 0 & c_\phi & c_\theta s_\phi \\ 0 & -s_\phi & c_\theta c_\phi \end{pmatrix} \tag{2.5}$$

. The consecutive rotation of the Euler angles is shown in the Figure 2.2.

The following properties of the kinematic transformation matrices $\mathbf{L}_{BC}, \mathbf{R}$ and $\mathbf{P}$ are very important in developing a unified simulation model of kite energy systems. The directional cosine

matrix $\mathbf{L}_{BC}$ is orthogonal, that is, its transpose is its inverse

$$\mathbf{L}_{BC}^{-1} = \mathbf{L}_{BC}^{T} = \mathbf{L}_{CB}. \tag{2.6}$$

The derivative of the directional cosine matrix $\mathbf{L}_{BC}$ satisfies the following equation:

$$\dot{\mathbf{L}}_{BC} = -\mathbf{\Omega}_{\times}\mathbf{L}_{BC}, \quad \mathbf{\Omega}_{\times} = \begin{pmatrix} 0 & -\omega_z & \omega_y \\ \omega_z & 0 & -\omega_x \\ -\omega_y & \omega_x & 0 \end{pmatrix}. \tag{2.7}$$

Additionally, the Jacobian matrix of translational and rotational velocity with respect to spherical coordinates and kite attitudes satisfies the following equations:

$$\frac{\partial \mathbf{V}_C}{\partial \mathbf{q}} = \dot{\mathbf{P}}, \quad \frac{\partial \boldsymbol{\omega}}{\partial \boldsymbol{\Theta}} = \left(\dot{\mathbf{R}} + \mathbf{\Omega}_{\times}\mathbf{R}\right)^{T}. \tag{2.8}$$

These relation can be proven by substitution and they will be used in deriving the equivalence among the translational and rotational dynamics of kite energy systems.

2.2 Steady Aero-/Hydro-dynamic Forces

The steady aero-/hydro-dynamic force can be modeled using the kite angle of attack α and side slip angle β. Suppose the kite apparent current velocity is given by

$$\mathbf{V}_a = \begin{pmatrix} u_a & v_a & w_a \end{pmatrix}^{T} = \mathbf{L}_{BC}(\mathbf{V}_C - \mathbf{W}). \tag{2.9}$$

Further assume that the apparent velocity in $\mathbf{i}_B$ direction is positive, $u_a > 0$, then the angle of attack and side slip angle can be defined as:

$$\alpha = \arctan\left(\frac{w_a}{u_a}\right), \tag{2.10}$$

$$\beta = \arcsin\left(\frac{v_a}{V_a}\right), \tag{2.11}$$
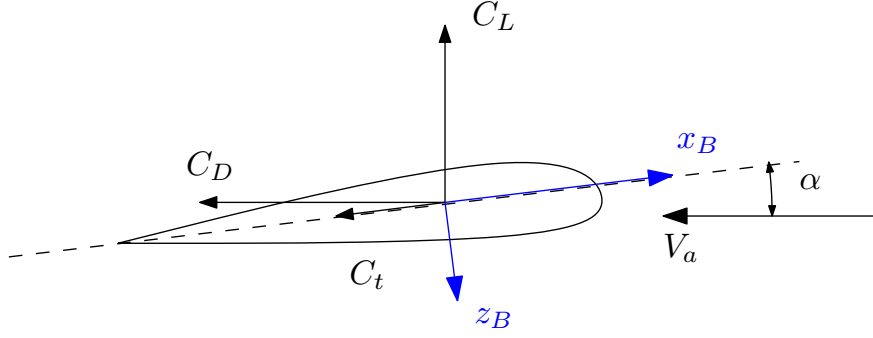
Figure 2.3: Kite lift and Drag

where $V_a = \|\mathbf{V}_a\|$ is the magnitude of the apparent current.

In general, the kite lift and drag coefficients are function of α while the side force coefficient is function of β:

$$C_L = C_L(\alpha), \qquad C_D = C_D(\alpha), \qquad C_y = C_y(\beta). \tag{2.12}$$

Along the body frame axes, the hydrodynamic coefficients are

$$\begin{pmatrix} C_x \\ C_z \end{pmatrix} = \begin{pmatrix} 1 & 0 \\ 0 & -1 \end{pmatrix} \begin{pmatrix} \sin\alpha & -\cos\alpha \\ \cos\alpha & \sin\alpha \end{pmatrix} \begin{pmatrix} C_L \\ C_D \end{pmatrix}. \tag{2.13}$$

Moreover, the turbine drag coefficient can be computed from its induction factor a as follows

$$C_t = 4a(1-a)\frac{S_t}{S}, \tag{2.14}$$

where S_t is the turbine area and S is the kite area. Then the total hydrodynamic coefficient can be computed as

$$\mathbf{C}_B = \begin{pmatrix} C_x & C_y & C_z \end{pmatrix}^T - \begin{pmatrix} C_t & 0 & 0 \end{pmatrix}^T. \tag{2.15}$$

The geometric relation of kite lift C_L, drag C_D and turbine drag C_t coefficients are shown in Figure 2.3, the side force coefficient is shown in Figure 2.4.
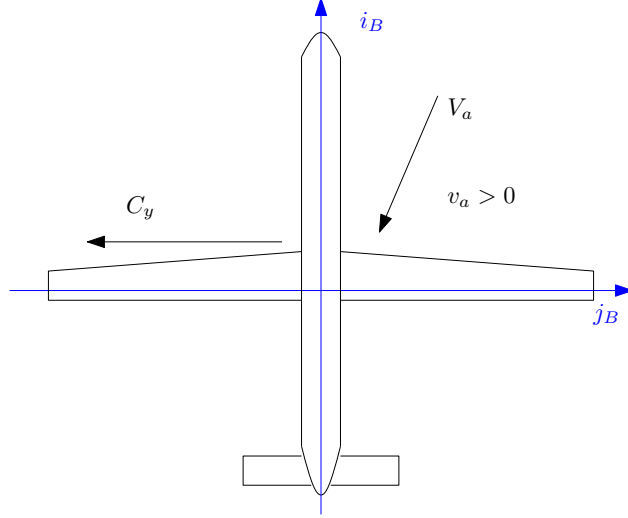
Figure 2.4: Side Force Coefficient

Using $\mathbf{C}_B$, the kite aero-/hydro-dynamic force is given by:

$$\mathbf{H}_B = \frac{1}{2}\rho_f V_a^2 S \mathbf{C}_B, \tag{2.16}$$

where ρ_f is the density of the surrounding fluid. Applying generalized force transformation, the steady aero-/hydro-dynamic force in frame $\mathbf{C}$ and $\mathbf{S}$ are

$$\mathbf{H}_C = \frac{1}{2}\rho_f V_a^2 S \mathbf{L}_{CB}\mathbf{C}_B \tag{2.17}$$

$$\mathbf{H}_S = \frac{1}{2}\rho_f V_a^2 S \mathbf{P}^T\mathbf{L}_{CB}\mathbf{C}_B \tag{2.18}$$

2.3   Added Mass Effects

While the influence of the steady flow on the kite motion can be characterized by steady aero-/hydro-dynamic force, the added mass effects characterized the influence of the unsteady flow. When accelerating with respect to the surrounding fluid, additional inertial will be introduced to the kite system as shown in Figure 2.5. By assuming the surrounding unsteady fluid field to be
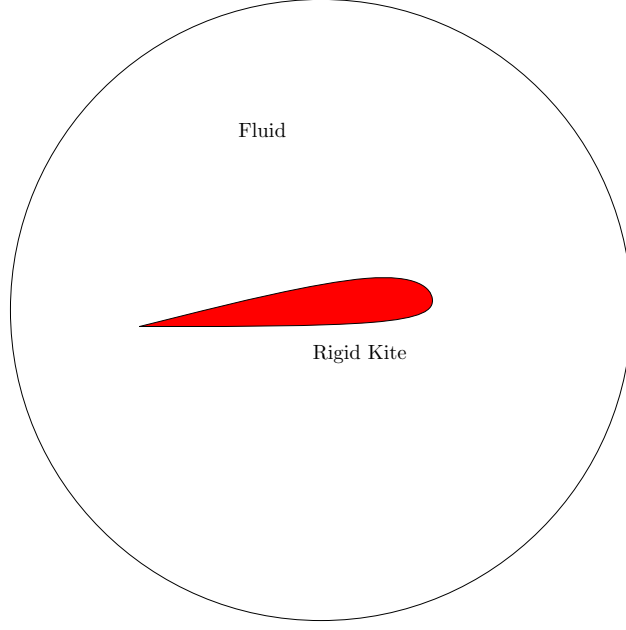
Figure 2.5: Rigid Kite and Surrounding Fluid

potential, the added mass effect can be characterized using energy approach:

$$
\begin{aligned}
T_F &= \frac{1}{2} \begin{pmatrix} \mathbf{V}_a^T & \boldsymbol{\omega}^T \end{pmatrix} \begin{pmatrix} \mathbf{M}_a & \boldsymbol{\Gamma}^T \\ \boldsymbol{\Gamma} & \mathbf{J}_a \end{pmatrix} \begin{pmatrix} \mathbf{V}_a \\ \boldsymbol{\omega} \end{pmatrix} \\
&= \frac{1}{2}\mathbf{V}_B^T\mathbf{M}_a\mathbf{V}_B + \frac{1}{2}\boldsymbol{\omega}^T\mathbf{J}_a\boldsymbol{\omega} + \boldsymbol{\omega}^T\boldsymbol{\Gamma}\mathbf{V}_B - \mathbf{V}_B^T\mathbf{M}_a\mathbf{W}_B - \boldsymbol{\omega}^T\boldsymbol{\Gamma}\mathbf{W}_B + \frac{1}{2}\mathbf{W}_B^T\mathbf{M}_a\mathbf{W}_B, \quad (2.19)
\end{aligned}
$$

where T_F is the total kinetic energy of the unsteady surrounding fluid flow and matrices $\mathbf{M}_a$ and $\mathbf{J}_a$ to be symmetric.

The force introduced by the added mass effect can be modeled using the impulse-force principle. Denote the impulse from the unsteady fluid field as follows,

$$
\boldsymbol{\eta}_t = \frac{\partial T_F}{\partial \mathbf{V}_B} = \mathbf{M}_a\mathbf{V}_B + \boldsymbol{\Gamma}^T\boldsymbol{\omega} - \mathbf{M}_a\mathbf{W}_B, \tag{2.20}
$$

$$
\boldsymbol{\eta}_r = \frac{\partial T_F}{\partial \boldsymbol{\omega}} = \mathbf{J}_a\boldsymbol{\omega} + \boldsymbol{\Gamma}\mathbf{V}_B - \boldsymbol{\Gamma}\mathbf{W}_B. \tag{2.21}
$$

Applying the Kirchoff's law, the force due to impulse $\boldsymbol{\eta}_t$ and $\boldsymbol{\eta}_r$ are

$$
\mathbf{A}_t = -\dot{\boldsymbol{\eta}}_t - \boldsymbol{\omega} \times \boldsymbol{\eta}_t, \tag{2.22}
$$

$$\mathbf{A}_r = -\,\dot{\boldsymbol{\eta}}_r - \boldsymbol{\omega} \times \boldsymbol{\eta}_r - \mathbf{V}_B \times \boldsymbol{\eta}_t. \tag{2.23}$$

Substituting equations (2.20) and (2.21) into (2.22) and (2.23), the added mass force on kite rotation and translation as $\mathbf{A}_t$ and $\mathbf{A}_r$ are given by

$$\mathbf{A}_t = -(\mathbf{M}_a \dot{\mathbf{V}}_a + \boldsymbol{\Gamma}^T \dot{\boldsymbol{\omega}}) - \boldsymbol{\omega} \times (\mathbf{M}_a \mathbf{V}_a + \boldsymbol{\Gamma}^T \boldsymbol{\omega}), \tag{2.24}$$

$$\mathbf{A}_r = -(\mathbf{J}_a \dot{\boldsymbol{\omega}} + \boldsymbol{\Gamma} \dot{\mathbf{V}}_a) - \boldsymbol{\omega} \times (\mathbf{J}_a \boldsymbol{\omega} + \boldsymbol{\Gamma} \mathbf{V}_a) - \mathbf{V}_B \times (\mathbf{M}_a \mathbf{V}_a + \boldsymbol{\Gamma}^T \boldsymbol{\omega}). \tag{2.25}$$

2.4   Potential Forces and Tether Tension

The potential energy of kite energy systems consist of two parts: the gravitational potential energy and buoyancy potential energy,

$$U = -\mathbf{G}^T \mathbf{r}_C + \mathbf{B}^T \mathbf{r}_G, \tag{2.26}$$

where $\mathbf{r}_C$ is the position vector of kite center of gravity and $\mathbf{r}_G$ is the position vector of kite center of geometry. Assume that the magnitude of buoyancy force $\mathbf{B}$ is a fraction of the magnitude of the gravity with ratio $\lambda_B \in (0,1)$. The distance between center of gravity and center of geometry in body frame is $\mathbf{d}_B$ as shown in Figure 2.6 then

$$\begin{aligned} U = & -\mathbf{G}^T \mathbf{r}_C + \lambda_B \mathbf{G}^T (\mathbf{r}_C + \mathbf{L}_{CB} \mathbf{d}_B) \\ = & -(1 - \lambda_B)\mathbf{G}^T \mathbf{r}_C + \lambda_B \mathbf{G}^T \mathbf{L}_{CB} \mathbf{d}_B. \end{aligned} \tag{2.27}$$

Since the gravitational potential energy is function of kite position r_C and attitudes $\boldsymbol{\Theta}$, the corresponding translational and rotational conservative force in frame $\mathbf{C}$ and $\mathbf{E}$ are

$$\mathbf{G}_t = -\frac{\partial U}{\partial \mathbf{r}_C}, \qquad \mathbf{G}_r = -\frac{\partial U}{\partial \boldsymbol{\Theta}}. \tag{2.28}$$

In physics, the potential energy is defined as the energy terms that only depends on the end
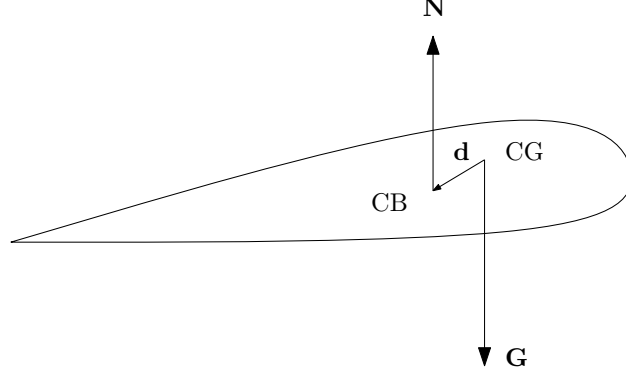
Figure 2.6: Kite Gravity and Buoyancy

point of the displacement. For constant current velocity, the last term of (2.19) depends only on the attitude of the kites, therefore, it can be treated as the velocity dependent potential,

$$U_v = -\frac{1}{2}\mathbf{W}_B^T\mathbf{M}_a\mathbf{W}_B.$$

(2.29)

Since the current velocity is constant in frame $\mathbf{C}$, therefore, the current potential energy is only function of kite attitudes. The conservative force introduced by the current potential energy in frame $\mathbf{E}$ is

$$\mathbf{G}_v = -\frac{\partial U_v}{\partial \boldsymbol{\Theta}}.$$

(2.30)

The tether tension acting on the kite energy systems depends on the configuration of the systems. In the kite energy system with variable tether length, underwater or airborne, the tether tension can be treated as an control input to the kite translation. In such case, the tether tension $\mathbf{T}$ can be designed using Lyapunov method and is independent to other physical effects. On the other hand, for the kite energy system with fixed tether length, the tether tension is a reaction to the total force acting on the tether direction. Since the tether length is fixed, the kite is moving on a sphere that centers at the system origin. The virtual work done by the tension in the normal direction of the sphere must be zero. In other words, the tether tension can be obtained by the force balance in the tether direction. In airborne kite energy systems, the tether tension is given by

$$\mathbf{T}_S = -\mathbf{P}^T\Big(\big((\mathbf{L}_{CB}\mathbf{H}_B + \mathbf{G}_t)^T\hat{\mathbf{r}}_C\big)\hat{\mathbf{r}}_C\Big),$$

(2.31)

25

where $\hat{\mathbf{r}}_C$ is the unit vector along the tether direction, $\hat{\mathbf{r}}_C = \begin{pmatrix} \cos q_1 \sin q_2 & \sin q_1 & \cos q_1 \cos q_2 \end{pmatrix}$. In addition to the steady hydrodynamic force and the gravity, the added mass effect also needs to be taken into account in computing the tether tension. Therefore, in the undersea kite systems, the tether tension is given by

$$\mathbf{T}_S = -\big((\mathbf{L}_{CB}\mathbf{H}_B + \mathbf{G}_t + \mathbf{L}_{CB}\mathbf{A}_t)^T \hat{\mathbf{r}}_C\big)\mathbf{P}^T \hat{\mathbf{r}}_C. \tag{2.32}$$

2.5   Passivity of Steady Aero-/Hydro-Dynamic Force

Section 2.2 to Section 2.4 introduced the elements that drives the kite translation, among them the steady aero-/hydro-dynamic force is crucial in stability and power limit analysis. In this section, the passivity of the kite aerodynamic force is provided. Recall that the aerodynamic force acting on the kite is given by

$$\mathbf{H}_B = \frac{1}{2}\rho_f V_a^2 S \mathbf{C}_B, \tag{2.33}$$

where the aerodynamic coefficients are

$$\begin{pmatrix} C_x \\ C_z \end{pmatrix} = \begin{pmatrix} 1 & 0 \\ 0 & -1 \end{pmatrix} \begin{pmatrix} \sin\alpha & -\cos\alpha \\ \cos\alpha & \sin\alpha \end{pmatrix} \begin{pmatrix} C_L \\ C_D \end{pmatrix}, \tag{2.34}$$

$$\mathbf{C}_B = \begin{pmatrix} C_x & C_y & C_z \end{pmatrix}^T - \begin{pmatrix} C_t & 0 & 0 \end{pmatrix}^T. \tag{2.35}$$

By expansion of equation (2.35), the aerodynamic coefficient $\mathbf{C}_B$ is given by

$$\mathbf{C}_B = \begin{pmatrix} C_L \sin\alpha - C_D \cos\alpha - C_t \\ C_y \\ -C_L \cos\alpha - C_D \sin\alpha \end{pmatrix}. \tag{2.36}$$

The kite apparent velocity can be expressed using kite angle of attack and side-slip angle

$$\mathbf{V}_a = \mathbf{L}_{BC}(\mathbf{V}_C - \mathbf{W}) = V_a \begin{pmatrix} \cos\alpha\cos\beta & \sin\beta & \sin\alpha\cos\beta \end{pmatrix}. \tag{2.37}$$

It can be proven in the following lemma that the steady aerodynamic force is passive with respect to the kite apparent velocity, i.e.

Lemma 1 (Passivity of Steady Aero-/Hydro-Dynamic force). *If the kite apparent attitude $\alpha, \beta \in (-\frac{1}{2}\pi, \frac{1}{2}\pi)$, the work done by the airflow on the kite is non positive,*

$$\mathbf{V}_a^T \mathbf{H}_B \leq 0. \tag{2.38}$$

Proof. Define the apparent aerodynamic coefficient as follows

$$C_a = C_D \cos \beta - C_y \sin \beta + C_t \cos \alpha \cos \beta. \tag{2.39}$$

Notice the kite and turbine drag coefficients are positive, therefore, the quantities $C_D \cos \beta + C_t \cos \alpha \cos \beta > 0$. Moreover, the side force coefficient C_y is in the negative direction of the v_a and the side-slip angle β is given by

$$C_y v_a < 0; \quad \beta = \sin^{-1} \left(\frac{v_a}{V_a} \right). \tag{2.40}$$

Therefore, for $\beta \in (-\frac{1}{2}\pi, \frac{1}{2}\pi)$,

$$C_y \sin \beta < 0. \tag{2.41}$$

The illustration of the passivity of the side force is shown in Figure 2.7. Hence, it can be conclude that the apparent aerodynamic coefficient C_a is positive definite. Substituting equations (2.33) - (2.37) into equation (2.38) gives that

$$
\begin{aligned}
\mathbf{V}_a^T \mathbf{H}_B &= \frac{1}{2} \rho_f \|\mathbf{V}_a\|^2 S \left(u_a (C_x - C_t) + v_a C_y + w_a C_z \right) \\
&= \frac{1}{2} \rho_f \|\mathbf{V}_a\|^3 S \left((C_x - C_t) \cos \alpha \cos \beta + C_y \sin \beta + C_z \sin \alpha \cos \beta \right) \\
&= \frac{1}{2} \rho_f \|\mathbf{V}_a\|^3 S \left(-C_D \cos \beta + C_y \sin \beta - C_t \cos \alpha \cos \beta \right) \\
&= -\frac{1}{2} \rho_f \|\mathbf{V}_a\|^3 S C_a.
\end{aligned} \tag{2.42}
$$

Hence, the steady aerodynamic force is passive with respect to the kite apparent velocity. □
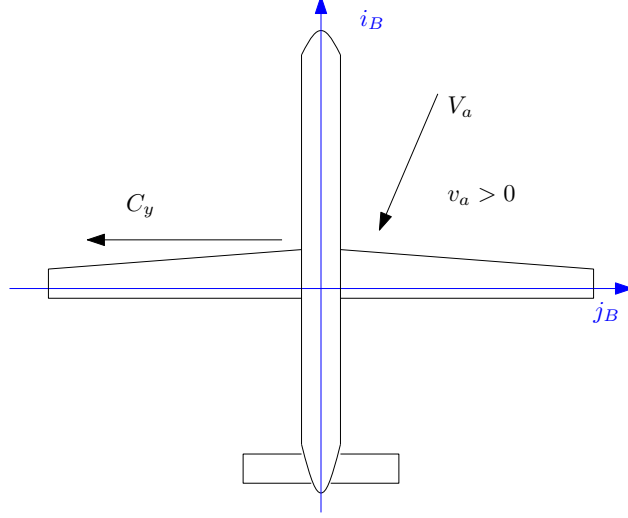
Figure 2.7: Side Force Coefficient

Though the steady aerodynamic force takes complicated form, it act as a resistance on the kite translation. This result are used to derive the power limitation of the kite energy system in the next section.

2.6 Power Generation Limit

In [35], the available power of the airborne kite energy system in a two dimensional case is given by the following equation

$$P_{wind} = \|\mathbf{W}\| F_a \cos \gamma, \tag{2.43}$$

where $\mathbf{W}$ is the wind velocity, F_a is the total aerodynamic force and γ is the angle between the direction of the force and the wind speed. The power limit of an airborne kite energy system is given by the following equation

$$P_{max} = \frac{2}{27} \rho_f \|\mathbf{W}\|^3 S C_R \left(\frac{C_R}{C_D}\right)^2 \quad \text{with} \quad C_R = \sqrt{C_L^2 + (C_D + C_t)^2}, \tag{2.44}$$

where S is the kite area and C_R is the resultant aerodynamic coefficient.

Using the similar procedure, the power limit of the kite energy system in three dimensional

28

motion can be derived. Notice that the aerodynamic force acting on the kite can be decomposed into two parts,

$$\mathbf{H}_B = \mathbf{H}_k + \mathbf{H}_t = \frac{1}{2}\rho_f\|\mathbf{V}_a\|^2 S\left(\begin{pmatrix} C_x & C_y & C_z \end{pmatrix}^T - \begin{pmatrix} C_t & 0 & 0 \end{pmatrix}^T \right). \tag{2.45}$$

Moreover, the wind velocity and aerodynamic force measured in reference frame $\mathbf{B}$ and $\mathbf{C}$ is related as follows

$$\mathbf{W}_C = \mathbf{L}_{CB}\mathbf{W}_B, \quad \mathbf{H}_C = \mathbf{L}_{CB}\mathbf{H}_B.$$

In the three dimensional case, the available power to a stationary ground station is given by

$$P_{wind} = \mathbf{W}_C^T\mathbf{H}_C = \mathbf{W}_B^T\mathbf{H}_B, \tag{2.46}$$

where the kite velocity and aerodynamic force is measured in the inertial reference frame. Equation (2.46) is a generalization of equation (2.43). Therefore, the power that available for the power generation devices is given by

$$P_a = \mathbf{W}_B^T\mathbf{H}_B + \mathbf{V}_a^T\mathbf{H}_k.$$

Using the similar method in Lemma 1,

$$\mathbf{V}_a^T\mathbf{H}_k = \frac{1}{2}\rho_f\|\mathbf{V}_a\|^3 S\left(-C_D\cos\beta + C_y\sin\beta \right) \le 0. \tag{2.47}$$

Expending equation (2.46), the total power in the wind is

$$\mathbf{W}_B^T\mathbf{H}_B = \frac{1}{2}\rho_f V_a^2 S\mathbf{W}_B^T\mathbf{C}_B \le \frac{1}{2}\rho_f V_a^2 S\|\mathbf{W}_B\|\|\mathbf{C}_B\|. \tag{2.48}$$

Consider the case when $\alpha = \beta = 0$, equation (2.36) becomes

$$\mathbf{C}_B = \begin{pmatrix} -C_D - C_t & 0 & -C_L \end{pmatrix}, \tag{2.49}$$

since the side force on the kite is zero when $\beta = 0$. Moreover, the equations (2.47) and (2.48) can be further simplified as follows

$$\mathbf{V}_a^T \mathbf{H}_k = -\frac{1}{2}\rho_f V_a^3 S C_D \tag{2.50}$$

$$\mathbf{W}_B^T \mathbf{H}_B \leq \frac{1}{2}\rho_f V_a^2 S \|\mathbf{W}_B\| \sqrt{C_L^2 + (C_D + C_t)^2}. \tag{2.51}$$

Hence the maximum power of a kite energy system is given by

$$P_a \leq \frac{1}{2}\rho_f V_a^2 S \|\mathbf{W}_B\| \sqrt{C_L^2 + (C_D + C_t)^2} - \frac{1}{2}\rho_f V_a^3 S C_D. \tag{2.52}$$

Maximizing the power with respect to the kite apparent speed V_a yields

$$\frac{\partial P_a}{\partial V_a} = \frac{1}{2}\rho_f S(2V_a\|\mathbf{W}_B\|\sqrt{C_L^2 + (C_D + C_t)^2} - 3V_a^2 C_D) = 0. \tag{2.53}$$

Therefore, the optimal value of kite apparent speed is

$$V_a^* = \frac{2}{3}\frac{\sqrt{C_L^2 + (C_D + C_t)^2}}{C_D}\|\mathbf{W}\|. \tag{2.54}$$

The maximum power of a kite energy system is then given by substituting equation (2.54) into equation (2.52)

$$P_{max} = \frac{2}{27}\rho_f\|\mathbf{W}\|^3 S C_R \left(\frac{C_R}{C_D}\right)^2 \quad \text{with} \quad C_R = \sqrt{C_L^2 + (C_D + C_t)^2}.$$

In three dimensional case, the available power to a kite energy system is

$$\begin{aligned}
P_a &= \frac{1}{2}\rho_f V_a^2 S \mathbf{W}_B^T \mathbf{C}_B + \mathbf{V}_a^T \mathbf{H}_k \\
&= \frac{1}{2}\rho_f V_a^2 S \Big(W_x(C_L \sin\alpha - C_D \cos\alpha - C_t) + W_y C_y - W_z(C_L \cos\alpha + C_D \sin\alpha) \\
&\quad + V_a(-C_D \cos\beta + C_y \sin\beta)\Big).
\end{aligned}$$

The global maximum value of the available power is difficult to obtain using analytical method.

However, an upper bound of the available power can be obtained as follows

$$W_x(C_L \sin \alpha - C_D \cos \alpha) - W_z(C_L \cos \alpha + C_D \sin \alpha) \leq \sqrt{W_x^2 + W_z^2}\sqrt{C_L^2 + C_D^2}. \quad (2.55)$$

Therefore, the upper bound of the available energy of kite system is

$$P_a \leq \frac{1}{2}\rho_f V_a^2 S\Big(- W_x C_t + W_y C_y + \sqrt{W_x^2 + W_z^2}\sqrt{C_L^2 + C_D^2} + V_a(-C_D \cos \beta + C_y \sin \beta)\Big). \quad (2.56)$$

When β is small, the maximum available power takes the following form,

$$P_a \leq \frac{1}{2}\rho_f V_a^2 S\Big(- W_x C_t + W_y C_y + \sqrt{W_x^2 + W_z^2}\sqrt{C_L^2 + C_D^2} + V_a(-C_D + C_y \beta)\Big). \quad (2.57)$$

Under the small angle assumption, side force coefficient is a linear function of β,

$$C_y = C_{y,\beta}\beta. \quad (2.58)$$

From the passivity of the kite aerodynamic force, the coefficient $C_{y,\beta} < 0$, therefore, P_a is concave in β. The maximum value of P_a is obtained when the first order derivative attains zero,

$$\frac{\partial P_a}{\partial \beta} = W_y C_{y,\beta} + 2V_a C_{y,\beta}\beta. \quad (2.59)$$

The optimal value β^* must satisfies the following condition,

$$\beta^* = -\frac{W_y}{2V_a}. \quad (2.60)$$

Substituting equation (2.60) into equation (2.57) gives that

$$\max_{\beta} P_a \leq \frac{1}{2}\rho_f V_a^2 S\Big(- V_a C_D + \sqrt{W_x^2 + W_z^2}\sqrt{C_L^2 + C_D^2} - W_x C_t - C_{y,\beta}\frac{W_y^2}{4V_a}\Big). \quad (2.61)$$

Taking the derivative with respect to V_a, the upper bound of available power is given by

$$\frac{\partial P_a(V_a)}{\partial V_a} = \frac{1}{2}\rho_f S(-3V_a^2 C_D + 2V_a(\sqrt{W_x^2 + W_z^2}\sqrt{C_L^2 + C_D^2} - W_x C_t) - \frac{1}{4}C_{y,\beta}W_y^2). \quad (2.62)$$

That is the optimal value of V_a can be solved from the following equation,

$$-3(V_a^*)^2 C_D + 2V_a^*(\sqrt{W_x^2 + W_z^2}\sqrt{C_L^2 + C_D^2} - W_x C_t) - \frac{1}{4}C_{y,\beta}W_y^2 = 0. \quad (2.63)$$

Using the roots formula of quadratic equation,

$$V_a^* = -\frac{2C_t W_x - 2\sqrt{C_D^2 + C_L^2}\sqrt{W_x^2 + W_z^2} \pm \sqrt{\Delta}}{6C_D} \quad (2.64)$$
$$\Delta = 4(\sqrt{W_x^2 + W_z^2}\sqrt{C_L^2 + C_D^2} - W_x C_t)^2 - 3C_D C_{y,\beta} W_y^2.$$

By passivity of the aerodynamic force $C_{y,\beta} < 0$, therefore the following inequality holds

$$\sqrt{\Delta} > |2C_t W_x - 2\sqrt{C_D^2 + C_L^2}\sqrt{W_x^2 + W_z^2}|.$$

Thus the positive solution of the optimal value V_a^* is given by

$$V_a^* = -\frac{2C_t W_x - 2\sqrt{C_D^2 + C_L^2}\sqrt{W_x^2 + W_z^2} - \sqrt{\Delta}}{6C_D}$$
$$\Delta = 4(\sqrt{W_x^2 + W_z^2}\sqrt{C_L^2 + C_D^2} - W_x C_t)^2 - 3C_D C_{y,\beta} W_y^2.$$

To simplify the notation, denote scaled wind speed as follows

$$W_1 = \sqrt{W_x^2 + W_z^2}\sqrt{C_L^2 + C_D^2} - W_x C_t, \quad (2.65)$$
$$W_2 = \sqrt{-3C_D C_{y,\beta} W_y^2}. \quad (2.66)$$

The optimal kite apparent speed then become

$$V_a^* = -\frac{2W_1 - \sqrt{4W_1^2 + W_2^2}}{6C_D}. \quad (2.67)$$

32

Substituting equation (2.67) into equation (2.61) gives the maximum available power

$$\max P_a = \frac{1}{2}\rho_f S \frac{(2W_1 + \sqrt{4W_1^2 + W_2^2})(2W_1^2 + W_2^2 + W_1\sqrt{4W_1^2 + W_2^2})}{108C_D^2} \tag{2.68}$$

$$W_1 = \sqrt{W_x^2 + W_z^2}\sqrt{C_L^2 + C_D^2} - C_t W_x$$

$$W_2 = \sqrt{-3C_D C_{y,\beta} W_y^2}.$$

Consider the case when $W_y = 0$, the maximum power is given by

$$P_{max} = \frac{2}{27}\rho_f S \frac{W_1^3}{C_D^2}. \tag{2.69}$$

It is important to notice if $\alpha = 0$, the quantity W_1 becomes

$$W_1 = \sqrt{W_x^2 + W_z^2}\sqrt{C_L^2 + (C_D + C_t)^2}.$$

Therefore, the power limit formulation becomes

$$P_{max} = \frac{2}{27}\rho_f \|\mathbf{W}\|^3 S C_R \left(\frac{C_R}{C_D}\right)^2 \quad \text{with} \quad C_R = \sqrt{C_L^2 + (C_D + C_t)^2},$$

which agrees with the two dimensional case as in [6, 35]. In this chapter, the physical fundamentals of the kite energy systems is studied. In the next chapter, the dynamics and simulation models of the kite energy systems will be established.

Chapter 3

Dynamics of Kite Energy Systems

In this chapter, the nonlinear rigid body dynamics of kite energy systems are derived in different reference frames using Euler-Lagrange approach. Using kinematic relations, the equivalence between the system dynamics of kite energy system in different frames are established. These equivalences are used to combined different physical phenomenon into a unified mathematical model. Two simulation models of the kite energy systems for airborne and undersea cases are developed to increase the computational efficiency.

3.1   Lagrange Dynamics and Transformation

Assume the generalized coordinates is denoted by $\mathbf{h}$ and the corresponding kinetic energy is T_h, then the Euler-Lagrange equation is given by

$$\frac{d}{dt}\left(\frac{\partial T_h}{\partial \dot{\mathbf{h}}}\right) - \frac{\partial T_h}{\partial \mathbf{h}} = \mathbf{Q}_h, \tag{3.1}$$

where $\mathbf{Q}_h$ includes conservative and non-conservative generalized forces. Denote the kite mass as m and tether line density as ρ_t, then the translational kinetic energy of the airborne kite system in frame $\mathbf{C}$ is given by

$$T_t^C = \frac{1}{2}(m + \frac{1}{3}\rho_t r)\|\mathbf{V}_C\|^2. \tag{3.2}$$

Applying the Euler-Lagrange equation (2.9) to (2.10) yields the Newtonian dynamics

$$(m + \frac{1}{3}\rho_t r)\dot{\mathbf{V}}_C = \mathbf{Q}_C.$$

(3.3)

Additionally, the translational kinetic energy of the kite energy system in frame $\mathbf{B}$ is given by

$$T_t^B = \frac{1}{2}(m + \frac{1}{3}\rho_t r)\|\mathbf{V}_B\|^2.$$

(3.4)

Applying equation (3.1) to (3.4), the translational dynamics in frame $\mathbf{B}$ becomes

$$(m + \frac{1}{3}\rho_t r)(\dot{\mathbf{V}}_B + \boldsymbol{\omega} \times \mathbf{V}_B) = \mathbf{Q}_B.$$

(3.5)

The relation between $\mathbf{Q}_B$ and $\mathbf{Q}_C$ is given by

$$\mathbf{Q}_C = \frac{\partial \mathbf{r}_B}{\partial \mathbf{r}_C}\mathbf{Q}_B.$$

Using L'Hôpital's rule gives

$$\mathbf{Q}_C = \frac{\partial \mathbf{V}_B}{\partial \mathbf{V}_C}\mathbf{Q}_B.$$

(3.6)

Recall that the kite translational velocity transformation from frame $\mathbf{B}$ to frame $\mathbf{C}$ is given by

$$\mathbf{V}_C = \mathbf{L}_{CB}\mathbf{V}_B.$$

According to equation (3.6), the generalized force in frame $\mathbf{C}$ is

$$\mathbf{Q}_C = \mathbf{L}_{CB}\mathbf{Q}_B.$$

(3.7)

Therefore, the generalized force in frame $\mathbf{C}$ is a rotation of the generalized force in frame $\mathbf{B}$. Similarly, the following theorem holds for the left hand side of the Euler-Lagrange equation.

Theorem 1. *If the kinetic energy of kite systems in frame C and B are given by equations* (3.2) *and*

(3.4), *then the following relation holds:*

$$\frac{d}{dt}\left(\frac{\partial T_t^C}{\partial \mathbf{V}_C}\right) - \frac{\partial T_t^C}{\partial \mathbf{r}_C} = \mathbf{L}_{CB}\left(\frac{d}{dt}\left(\frac{\partial T_t^B}{\partial \mathbf{V}_B}\right) - \frac{\partial T_t^B}{\partial \mathbf{r}_B}\right). \tag{3.8}$$

Proof. Using the kinematic relation

$$\dot{\mathbf{L}}_{CB} = \mathbf{L}_{CB}\mathbf{\Omega}_\times,$$

the translational acceleration of the kite is given by

$$\begin{aligned}
\dot{\mathbf{V}}_C &= \left(\dot{\mathbf{L}}_{CB}\mathbf{V}_B + \mathbf{L}_{CB}\dot{\mathbf{V}}_B\right) \\
&= \left(\mathbf{L}_{CB}\mathbf{\Omega}_\times\mathbf{V}_B + \mathbf{L}_{CB}\dot{\mathbf{V}}_B\right).
\end{aligned}$$

The translational acceleration in frame **C** is the rotation of translational acceleration in frame **B**:

$$\dot{\mathbf{V}}_C = \mathbf{L}_{CB}(\dot{\mathbf{V}}_B + \boldsymbol{\omega} \times \mathbf{V}_B). \tag{3.9}$$

Pre-multiplying equation (3.9) with $m + \frac{1}{3}\rho_t r$ yields:

$$(m + \frac{1}{3}\rho_t r)\dot{\mathbf{V}}_C = \mathbf{L}_{CB}(m + \frac{1}{3}\rho_t r)(\dot{\mathbf{V}}_B + \boldsymbol{\omega} \times \mathbf{V}_B). \tag{3.10}$$

Equation (3.8) holds immediately. □

Equations (3.10) imply that the kite translational dynamics in frame **C** is a rotation of kite translational dynamics in frame **B**. Using the kinematic relation

$$\mathbf{V}_C = \mathbf{P}\dot{\mathbf{q}},$$

the generalized force transformation in frame **S** is given by

$$\mathbf{Q}_S = \frac{\partial \mathbf{r}_C}{\partial \mathbf{q}}\mathbf{Q}_C = \frac{\partial \mathbf{V}_C}{\partial \dot{\mathbf{q}}}\mathbf{Q}_C.$$

The generalized force transformation from frame $\mathbf{C}$ to $\mathbf{S}$ becomes:

$$\mathbf{Q}_S = \mathbf{P}^T \mathbf{Q}_C. \tag{3.11}$$

In terms of spherical coordinates, the kinetic energy of the kite is given by

$$T_t^S = \frac{1}{2}(m + \frac{1}{3}\rho_t r)\|\mathbf{P}\dot{\mathbf{q}}\|^2. \tag{3.12}$$

Similar to the generalized force transformation, the left hand side of the Euler-Lagrange equation satisfies the following relation as shown in Theorem 2.

Lemma 2. *If the kinetic energy of the kite energy system in frame C and S are given by equation* (3.2) *and* (3.12), *then:*

$$\frac{d}{dt}\left(\frac{\partial T_t^S}{\partial \dot{\mathbf{q}}}\right) - \frac{\partial T_t^S}{\partial \mathbf{q}} = \mathbf{P}^T\left(\frac{d}{dt}\left(\frac{\partial T_t^C}{\partial \mathbf{V}_C}\right) - \frac{\partial T_t^C}{\partial \mathbf{r}_C}\right). \tag{3.13}$$

Proof. Using the kinematic relation of translational velocity

$$\frac{\partial \mathbf{V}_C}{\partial \mathbf{q}} = \dot{\mathbf{P}}.$$

The Euler-Lagrange equation in the spherical frame becomes,

$$\begin{aligned}
\frac{d}{dt}\left(\frac{\partial T_S}{\partial \dot{\mathbf{q}}}\right) - \frac{\partial T_S}{\partial \mathbf{q}} &= (m + \frac{1}{3}\rho_t r)\left(\frac{d}{dt}(\mathbf{P}^T\mathbf{P}\dot{\mathbf{q}}) - \frac{\partial \mathbf{V}_C^T}{\partial \mathbf{q}}\mathbf{P}\dot{\mathbf{q}}\right) \\
&= (m + \frac{1}{3}\rho_t r)\left(\dot{\mathbf{P}}^T\mathbf{P}\dot{\mathbf{q}} + \mathbf{P}^T\dot{\mathbf{P}}\dot{\mathbf{q}} + \mathbf{P}^T\mathbf{P}\ddot{\mathbf{q}} - \dot{\mathbf{P}}^T\mathbf{P}\dot{\mathbf{q}}\right) \\
&= (m + \frac{1}{3}\rho_t r)\mathbf{P}^T(\dot{\mathbf{P}}\dot{\mathbf{q}} + \mathbf{P}\ddot{\mathbf{q}}).
\end{aligned}$$

The acceleration transformation between frame $\mathbf{C}$ and $\mathbf{S}$ is

$$\frac{d}{dt}\left(\frac{\partial T_t^C}{\partial \mathbf{V}_C}\right) - \frac{\partial T_t^C}{\partial \mathbf{r}_C} = \dot{\mathbf{V}}_C = \dot{\mathbf{P}}\dot{\mathbf{q}} + \mathbf{P}\ddot{\mathbf{q}}. \tag{3.14}$$

Therefore, the transformation relation (3.13) holds immediately. $\qquad\square$

The translational system dynamics transformation (3.8) and (3.13) can be illustrated using the Figure 3.1. The kite translational dynamics in frame **C** is a rotation of kite translational dynamics in frame **B**. The kite translational dynamics in frame **S** is a projection of the kite translational dynamics in frame **C**.
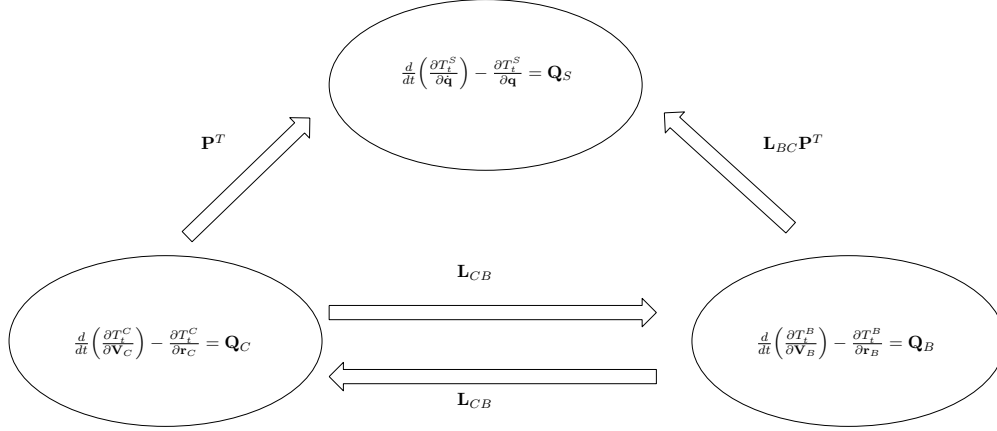
Figure 3.1: Translational Dynamics Transformations

Additionally, the generalized velocity transformation between frame **B** and **E** is given by,

$$\boldsymbol{\omega} = \mathbf{R}\dot{\boldsymbol{\Theta}}.$$

Then the generalized force transformation between frame **B** and **E** can be obtained from the virtual work principle

$$\mathbf{M}_E = \frac{\partial \boldsymbol{\omega}}{\partial \dot{\boldsymbol{\Theta}}}\mathbf{M}_B, \tag{3.15}$$

where $\mathbf{M}_E$ and $\mathbf{M}_B$ are the moment acting on the rotational motion in Euler and Body frame respectively.

Lemma 3. *If the rotational kinetic energy of the kite energy system in frame **B** and **E** are given by*

$$T_r^B = \frac{1}{2}\boldsymbol{\omega}^T\mathbf{J}\boldsymbol{\omega}, \qquad T_r^E = \frac{1}{2}\dot{\boldsymbol{\Theta}}^T\mathbf{R}^T\mathbf{J}\mathbf{R}\dot{\boldsymbol{\Theta}}. \tag{3.16}$$

*Then the equivalence of rotational dynamics between frame **B** and **E***

$$\frac{d}{dt}\left(\frac{\partial T_r^E}{\partial \dot{\boldsymbol{\Theta}}}\right) - \frac{\partial T_r^E}{\partial \boldsymbol{\Theta}} = \mathbf{R}^T \frac{d}{dt}\left(\frac{\partial T_r^B}{\partial \boldsymbol{\omega}}\right). \tag{3.17}$$

Proof. The Euler-Lagrange equation in body frame gives the Euler rotational dynamics

$$\frac{d}{dt}\left(\frac{\partial T_r^B}{\partial \boldsymbol{\omega}}\right) = \mathbf{J}\dot{\boldsymbol{\omega}} + \boldsymbol{\omega} \times \mathbf{J}\boldsymbol{\omega}. \tag{3.18}$$

Using rotational kinematic relation

$$\frac{\partial \boldsymbol{\omega}}{\partial \boldsymbol{\Theta}} = \left(\dot{\mathbf{R}} + \boldsymbol{\Omega}_\times \mathbf{R}\right)^T.$$

The Euler-Lagrange equation of the rotational dynamics in frame **E** can be obtained by

$$\begin{aligned}
\frac{d}{dt}\left(\frac{\partial T_r^E}{\partial \dot{\boldsymbol{\Theta}}}\right) - \frac{\partial T_r^E}{\partial \boldsymbol{\Theta}} &= \frac{d}{dt}(\mathbf{R}^T \mathbf{J}\mathbf{R}\dot{\boldsymbol{\Theta}}) - (\dot{\mathbf{R}} + \boldsymbol{\Omega}_\times \mathbf{R})^T \mathbf{J}\mathbf{R}\dot{\boldsymbol{\Theta}} \\
&= \dot{\mathbf{R}}^T \mathbf{J}\mathbf{R}\dot{\boldsymbol{\Theta}} + \mathbf{R}^T \mathbf{J}\dot{\mathbf{R}}\dot{\boldsymbol{\Theta}} + \mathbf{R}^T \mathbf{J}\mathbf{R}\ddot{\boldsymbol{\Theta}} - \dot{\mathbf{R}}^T \mathbf{J}\mathbf{R}\dot{\boldsymbol{\Theta}} - \mathbf{R}^T \boldsymbol{\Omega}_\times^T \mathbf{J}\mathbf{R}\dot{\boldsymbol{\Theta}} \\
&= \mathbf{R}^T \mathbf{J}\dot{\mathbf{R}}\dot{\boldsymbol{\Theta}} + \mathbf{R}^T \mathbf{J}\mathbf{R}\ddot{\boldsymbol{\Theta}} + \mathbf{R}^T \boldsymbol{\Omega}_\times \mathbf{J}\mathbf{R}\dot{\boldsymbol{\Theta}} \\
&= \mathbf{R}^T \left(\mathbf{J}(\dot{\mathbf{R}}\dot{\boldsymbol{\Theta}} + \mathbf{R}\ddot{\boldsymbol{\Theta}}) + \boldsymbol{\Omega}_\times \mathbf{J}\mathbf{R}\dot{\boldsymbol{\Theta}}\right).
\end{aligned}$$

The angular acceleration of the kite is

$$\dot{\boldsymbol{\omega}} = \dot{\mathbf{R}}\dot{\boldsymbol{\Theta}} + \mathbf{R}\ddot{\boldsymbol{\Theta}} \tag{3.19}$$

hence, the rotational dynamics in Euler frame can be further simplified as

$$\frac{d}{dt}\left(\frac{\partial T_r^E}{\partial \dot{\boldsymbol{\Theta}}}\right) - \frac{\partial T_r^E}{\partial \boldsymbol{\Theta}} = \mathbf{R}^T(\mathbf{J}\dot{\boldsymbol{\omega}} + \boldsymbol{\omega} \times \mathbf{J}\boldsymbol{\omega}). \tag{3.20}$$

$$\square$$

The rotational dynamics transformation is shown the Figure 3.2. The rotational dynamics of kite in frame **E** is a projection of the kite rotational dynamics in frame **B**.
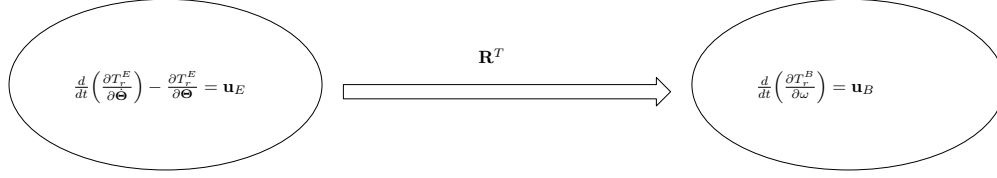
Figure 3.2: Rotational Dynamics Transformation

With the equivalent relations of the kite system dynamics as given in Lemmas 2 and 3, all the major physical effects can be combined into a unified simulation model. In next section, the model of airborne kite energy systems, which simpler than the undersea kite energy systems, will be derived.

3.2   Simulation Model of Airborne Kite Systems

In modeling the airborne kite energy systems, the added mass and buoyancy force is negligible. In general, the model of airborne kite translation is given by

$$(m + \frac{1}{3}\rho_t r)\mathbf{P}^T\dot{\mathbf{V}}_C = \mathbf{P}^T\mathbf{L}_{CB}\mathbf{H}_C + \mathbf{P}^T\mathbf{G}_t + \mathbf{T}_S. \tag{3.21}$$

There two major differences between the variable and fixed tether length airborne kite energy systems. In variable tether length airborne kite energy systems, the tether tension take the form $\mathbf{T}_S = \begin{pmatrix} T_S & 0 & 0 \end{pmatrix}$. In a constant tether length airborne kite energy system, the kite spherical coordinates and translational velocity transformation matrix are given by

$$\mathbf{q} = \begin{pmatrix} q_1 & q_2 \end{pmatrix}^T \quad \mathbf{P} = r\begin{pmatrix} -\sin q_1 \sin q_2 & \cos q_1 \cos q_2 \\ \cos q_1 & 0 \\ -\sin q_1 \cos q_2 & -\cos q_1 \sin q_2 \end{pmatrix}.$$

Although it can be shown in both case, the variable and constant tether length, the translational velocity transformation satisfies the same kinematic relations. The constant tether length assumption implies that the force is balanced in the tether direction, that is $\mathbf{T}_S = \mathbf{0}$. Using the kinematic

relation of the kite motion, the translational acceleration of the kite is given by

$$\mathbf{V}_C = \mathbf{P}\dot{\mathbf{q}}, \quad \dot{\mathbf{V}}_C = \mathbf{P}\ddot{\mathbf{q}} + \dot{\mathbf{P}}\dot{\mathbf{q}}.$$

Therefore, the equation of translational motion can be put into a more fundamental form

$$(m + \frac{1}{3}\rho_t r)\mathbf{P}^T\mathbf{P}\ddot{\mathbf{q}} + (m + \frac{1}{3}\rho_t r)\mathbf{P}^T\dot{\mathbf{P}}\dot{\mathbf{q}} = \mathbf{P}^T\mathbf{L}_{CB}\mathbf{H}_B + \mathbf{P}^T\mathbf{G}_t + \mathbf{T}_S. \tag{3.22}$$

Using the following notation,

$$\mathbf{M}_t(\mathbf{q})\ddot{\mathbf{q}} + \mathbf{C}_t(\mathbf{q},\dot{\mathbf{q}})\dot{\mathbf{q}} = \mathbf{P}^T\mathbf{L}_{CB}\mathbf{H}_C + \mathbf{P}^T\mathbf{G}_t + \mathbf{T}_S,$$

$$\mathbf{M}_t(\mathbf{q}) = (m + \frac{1}{3}\rho_t r)\mathbf{P}^T\mathbf{P}, \quad \mathbf{C}_t(\mathbf{q},\dot{\mathbf{q}}) = (m + \frac{1}{3}\rho_t r)\mathbf{P}^T\dot{\mathbf{P}}.$$

It is clear that the following matrix is skew symmetric,

$$\dot{\mathbf{M}}_t - 2\mathbf{C}_t = (m + \frac{1}{3}\rho_t r)(\dot{\mathbf{P}}^T\mathbf{P} - \mathbf{P}^T\dot{\mathbf{P}}). \tag{3.23}$$

Equation (3.23) is very useful in developing the control system for kite energy systems.

Since the density of the air is negligible compare to the kite, the buoyancy and added mass can be assumed to be zero. Using the dynamic transformation, the rotational dynamics in frame **E** are given by

$$\mathbf{R}^T\mathbf{J}\mathbf{R}\ddot{\Theta} + \mathbf{R}^T(\mathbf{J}\dot{\mathbf{R}} + \Omega_\times\mathbf{J}\mathbf{R})\dot{\Theta} = \mathbf{u}_E. \tag{3.24}$$

Denote the $\mathbf{M}_r$ and $\mathbf{C}_r$ matrix as follows

$$\mathbf{M}_r(\Theta)\ddot{\Theta} + \mathbf{C}_r(\Theta,\dot{\Theta})\dot{\Theta} = \mathbf{u}_E$$

$$\mathbf{M}_r = \mathbf{R}^T\mathbf{J}\mathbf{R} \qquad \mathbf{C}_r = \mathbf{R}^T(\mathbf{J}\dot{\mathbf{R}} + \Omega_\times\mathbf{J}\mathbf{R})$$

In summary, the complete dynamics of airborne kite energy systems are given by

- For the variable tether length airborne kite energy system

$$\mathbf{V}_C = \mathbf{P}\dot{\mathbf{q}} \quad \mathbf{P} = \begin{pmatrix} \cos q_1 \sin q_2 & -r \sin q_1 \sin q_2 & r \cos q_1 \cos q_2 \\ \sin q_1 & r \cos q_1 & 0 \\ \cos q_1 \cos q_2 & -r \sin q_1 \cos q_2 & -r \cos q_1 \sin q_2 \end{pmatrix}, \quad \mathbf{q} = \begin{pmatrix} r \\ q_1 \\ q_2 \end{pmatrix}.$$

(3.25)

- For the fixed tether length airborne kite energy system

$$\mathbf{V}_C = \mathbf{P}\dot{\mathbf{q}} \quad \mathbf{P} = r \begin{pmatrix} -\sin q_1 \sin q_2 & \cos q_1 \cos q_2 \\ \cos q_1 & 0 \\ -\sin q_1 \cos q_2 & -\cos q_1 \sin q_2 \end{pmatrix}, \quad \mathbf{q} = \begin{pmatrix} q_1 \\ q_2 \end{pmatrix}.$$

(3.26)

- The rotational kinematic relation is given by

$$\boldsymbol{\omega} = \mathbf{R}\dot{\boldsymbol{\Theta}} \quad \mathbf{R} = \begin{pmatrix} 1 & 0 & -\sin\theta \\ 0 & \cos\phi & \cos\theta \sin\phi \\ 0 & -\sin\phi & \cos\theta \cos\phi \end{pmatrix}, \quad \boldsymbol{\Theta} = \begin{pmatrix} \phi \\ \theta \\ \psi \end{pmatrix}.$$

(3.27)

The dynamic model for kite motion simulation is given by

$$\mathbf{M}_t(\mathbf{q})\ddot{\mathbf{q}} + \mathbf{C}_t(\mathbf{q}, \dot{\mathbf{q}})\dot{\mathbf{q}} = \mathbf{P}^T\mathbf{L}_{CB}\mathbf{H}_C + \mathbf{P}^T\mathbf{G}_t + \mathbf{T}_S, \tag{3.28}$$

$$\mathbf{M}_t(\mathbf{q}) = (m + \frac{1}{3}\rho_t r)\mathbf{P}^T\mathbf{P} \quad \mathbf{C}_t(\mathbf{q}, \dot{\mathbf{q}}) = (m + \frac{1}{3}\rho_t r)\mathbf{P}^T\dot{\mathbf{P}}, \tag{3.29}$$

$$\mathbf{M}_r(\boldsymbol{\Theta})\ddot{\boldsymbol{\Theta}} + \mathbf{C}_r(\boldsymbol{\Theta}, \dot{\boldsymbol{\Theta}})\dot{\boldsymbol{\Theta}} = \mathbf{u}_E, \tag{3.30}$$

$$\mathbf{M}_r = \mathbf{R}^T\mathbf{J}\mathbf{R}, \quad \mathbf{C}_r = \mathbf{R}^T(\mathbf{J}\dot{\mathbf{R}} + \boldsymbol{\Omega}_\times\mathbf{J}\mathbf{R}). \tag{3.31}$$

3.3 Simulation Model of Undersea Kite Systems

For the undersea kite energy systems, more complex physical effects need to be taken into account. Due to the high density of the water, a typical undersea kite system is the one with fixed

tether length, therefore, the translational velocity transformation relation is given by

$$\mathbf{V}_C = \mathbf{P}\dot{\mathbf{q}} \quad \mathbf{P} = r \begin{pmatrix} -\sin q_1 \sin q_2 & \cos q_1 \cos q_2 \\ \cos q_1 & 0 \\ -\sin q_1 \cos q_2 & -\cos q_1 \sin q_2 \end{pmatrix} \quad \mathbf{q} = \begin{pmatrix} q_1 \\ q_2 \end{pmatrix},$$

$$\mathbf{V}_B = \mathbf{L}_{BC}\mathbf{V}_C \quad \mathbf{L}_{BC} = \begin{pmatrix} c_\theta c_\psi & c_\theta s_\psi & -s_\theta \\ s_\phi s_\theta c_\psi - c_\phi s_\psi & s_\phi s_\theta s_\psi + c_\phi c_\psi & s_\phi c_\theta \\ c_\phi s_\theta c_\psi + s_\phi s_\psi & c_\phi s_\theta s_\psi - s_\phi s_\psi & c_\phi c_\theta \end{pmatrix}.$$

The complete system dynamics including the added mass effect and buoyancy is given by the following equations.

$$\mathbf{M}_t(\mathbf{q})\ddot{\mathbf{q}} + \mathbf{C}_t(\mathbf{q}, \dot{\mathbf{q}})\dot{\mathbf{q}} = \mathbf{P}^T\mathbf{L}_{CB}\mathbf{H}_B + \mathbf{P}^T\mathbf{G}_t + \mathbf{T}_S + \mathbf{P}^T\mathbf{L}_{CB}\mathbf{A}_t, \qquad (3.32)$$

$$\mathbf{M}_r(\mathbf{\Theta})\ddot{\mathbf{\Theta}} + \mathbf{C}_r(\mathbf{\Theta}, \dot{\mathbf{\Theta}})\dot{\mathbf{\Theta}} = \mathbf{u}_E + \mathbf{R}^T\mathbf{A}_r + \mathbf{G}_r + \mathbf{G}_v. \qquad (3.33)$$

As shown in the previous chapter, the added mass effect is modelled by:

$$\mathbf{A}_t = -(\mathbf{M}_a\dot{\mathbf{V}}_a + \mathbf{\Gamma}^T\dot{\boldsymbol{\omega}}) - \boldsymbol{\omega} \times (\mathbf{M}_a\mathbf{V}_a + \mathbf{\Gamma}^T\boldsymbol{\omega}),$$

$$\mathbf{A}_r = -(\mathbf{J}_a\dot{\boldsymbol{\omega}} + \mathbf{\Gamma}\dot{\mathbf{V}}_a) - \boldsymbol{\omega} \times (\mathbf{J}_a\boldsymbol{\omega} + \mathbf{\Gamma}\mathbf{V}_a) - \mathbf{V}_B \times (\mathbf{M}_a\mathbf{V}_a + \mathbf{\Gamma}^T\boldsymbol{\omega}).$$

If the current velocity is constant, the time derivative of the current velocity that measured in frame **B** can be

$$\dot{\mathbf{W}}_B = -\mathbf{\Omega}_\times\mathbf{W}_B \qquad (3.34)$$

Therefore, the added mass effect can be expressed as follows

$$\mathbf{A}_t = -\left(\mathbf{M}_a(\dot{\mathbf{V}}_B + \mathbf{\Omega}_\times\mathbf{W}_B) + \mathbf{\Gamma}^T\dot{\boldsymbol{\omega}}\right) - \boldsymbol{\omega} \times (\mathbf{M}_a\mathbf{V}_a + \mathbf{\Gamma}^T\boldsymbol{\omega}) \qquad (3.35)$$

$$\mathbf{A}_r = -\left(\mathbf{J}_a\dot{\boldsymbol{\omega}} + \mathbf{\Gamma}(\dot{\mathbf{V}}_B + \mathbf{\Omega}_\times\mathbf{W}_B)\right) - \boldsymbol{\omega} \times (\mathbf{J}_a\boldsymbol{\omega} + \mathbf{\Gamma}\mathbf{V}_a) - \mathbf{V}_B \times (\mathbf{M}_a\mathbf{V}_a + \mathbf{\Gamma}^T\boldsymbol{\omega}) \qquad (3.36)$$

Regroup the expression as follows,

$$\mathbf{A}_t = -(\mathbf{M}_a\dot{\mathbf{V}}_B + \boldsymbol{\Gamma}^T\dot{\boldsymbol{\omega}}) - \boldsymbol{\Omega}_\times(\mathbf{M}_a\mathbf{V}_B + \boldsymbol{\Gamma}^T\boldsymbol{\omega}) + (\boldsymbol{\Omega}_\times\mathbf{M}_a - \mathbf{M}_a\boldsymbol{\Omega}_\times)\mathbf{W}_B$$

$$\mathbf{A}_r = -(\mathbf{J}_a\dot{\boldsymbol{\omega}} + \boldsymbol{\Gamma}\dot{\mathbf{V}}_B) - \boldsymbol{\Omega}_\times(\mathbf{J}_a\boldsymbol{\omega} + \boldsymbol{\Gamma}\mathbf{V}_B) - \mathbf{V}_B \times (\mathbf{M}_a\mathbf{V}_B + \boldsymbol{\Gamma}^T\boldsymbol{\omega})$$

$$+ ([\mathbf{V}_B]_\times\mathbf{M}_a + \boldsymbol{\Omega}_\times\boldsymbol{\Gamma} - \boldsymbol{\Gamma}\boldsymbol{\Omega}_\times)\mathbf{W}_B$$

The translational and rotational velocity transformations are given by the following equations,

$$\mathbf{V}_B = \mathbf{L}_{BC}\mathbf{P}\dot{\mathbf{q}} \qquad \boldsymbol{\omega} = \mathbf{R}\dot{\boldsymbol{\Theta}}$$

Moreover, the time derivative of the direct cosine matrix satisfies that

$$\dot{\mathbf{L}}_{BC} = -\boldsymbol{\Omega}_\times\mathbf{L}_{BC} \quad \boldsymbol{\Omega}_\times = \begin{pmatrix} 0 & -\omega_z & \omega_y \\ \omega_z & 0 & -\omega_x \\ -\omega_y & \omega_x & 0 \end{pmatrix}$$

therefore the acceleration transformations are given by

$$\dot{\mathbf{V}}_B = -\boldsymbol{\Omega}_\times\mathbf{L}_{BC}\mathbf{P}\dot{\mathbf{q}} + \mathbf{L}_{BC}\dot{\mathbf{P}}\dot{\mathbf{q}} + \mathbf{L}_{BC}\mathbf{P}\ddot{\mathbf{q}} \qquad \dot{\boldsymbol{\omega}} = \dot{\mathbf{R}}\dot{\boldsymbol{\Theta}} + \mathbf{R}\ddot{\boldsymbol{\Theta}} \qquad (3.37)$$

By substitution, the equations of motion in spherical coordinates and Euler angles are given by

$$\mathbf{A}_t = -\Big(\mathbf{M}_a(-\boldsymbol{\Omega}_\times\mathbf{L}_{BC}\mathbf{P}\dot{\mathbf{q}} + \mathbf{L}_{BC}\dot{\mathbf{P}}\dot{\mathbf{q}} + \mathbf{L}_{BC}\mathbf{P}\ddot{\mathbf{q}}) + \boldsymbol{\Gamma}^T(\dot{\mathbf{R}}\dot{\boldsymbol{\Theta}} + \mathbf{R}\ddot{\boldsymbol{\Theta}})\Big)$$

$$- \boldsymbol{\Omega}_\times(\mathbf{M}_a\mathbf{L}_{BC}\mathbf{P}\dot{\mathbf{q}} + \boldsymbol{\Gamma}^T\mathbf{R}\dot{\boldsymbol{\Theta}}) + (\boldsymbol{\Omega}_\times\mathbf{M}_a - \mathbf{M}_a\boldsymbol{\Omega}_\times)\mathbf{W}_B$$

$$= -\mathbf{M}_a\mathbf{L}_{BC}\mathbf{P}\ddot{\mathbf{q}} - \boldsymbol{\Gamma}^T\mathbf{R}\ddot{\boldsymbol{\Theta}} + \Big((\mathbf{M}_a\boldsymbol{\Omega}_\times - \boldsymbol{\Omega}_\times\mathbf{M}_a)\mathbf{L}_{BC}\mathbf{P} - \mathbf{M}_a\mathbf{L}_{BC}\dot{\mathbf{P}}\Big)\dot{\mathbf{q}}$$

$$- (\boldsymbol{\Gamma}^T\dot{\mathbf{R}} + \boldsymbol{\Omega}_\times\boldsymbol{\Gamma}^T\mathbf{R})\dot{\boldsymbol{\Theta}} + (\boldsymbol{\Omega}_\times\mathbf{M}_a - \mathbf{M}_a\boldsymbol{\Omega}_\times)\mathbf{W}_B \qquad (3.38)$$

$$\mathbf{A}_r = -\Big(\mathbf{J}_a(\dot{\mathbf{R}}\dot{\boldsymbol{\Theta}} + \mathbf{R}\ddot{\boldsymbol{\Theta}}) + \boldsymbol{\Gamma}(-\boldsymbol{\Omega}_\times\mathbf{L}_{BC}\mathbf{P}\dot{\mathbf{q}} + \mathbf{L}_{BC}\dot{\mathbf{P}}\dot{\mathbf{q}} + \mathbf{L}_{BC}\mathbf{P}\ddot{\mathbf{q}})\Big) - \boldsymbol{\Omega}_\times(\mathbf{J}_a\mathbf{R}\dot{\boldsymbol{\Theta}} + \boldsymbol{\Gamma}\mathbf{L}_{BC}\mathbf{P}\dot{\mathbf{q}})$$

$$- [\mathbf{V}_B]_\times(\mathbf{M}_a\mathbf{L}_{BC}\mathbf{P}\dot{\mathbf{q}} + \boldsymbol{\Gamma}^T\mathbf{R}\dot{\boldsymbol{\Theta}}) + ([\mathbf{V}_B]_\times\mathbf{M}_a + \boldsymbol{\Omega}_\times\boldsymbol{\Gamma} - \boldsymbol{\Gamma}\boldsymbol{\Omega}_\times)\mathbf{W}_B$$

$$= -\boldsymbol{\Gamma}\mathbf{L}_{BC}\mathbf{P}\ddot{\mathbf{q}} - \mathbf{J}_a\mathbf{R}\ddot{\boldsymbol{\Theta}} + \Big((\boldsymbol{\Gamma}\boldsymbol{\Omega}_\times - \boldsymbol{\Omega}_\times\boldsymbol{\Gamma})\mathbf{L}_{BC}\mathbf{P} - \boldsymbol{\Gamma}\mathbf{L}_{BC}\dot{\mathbf{P}} - [\mathbf{V}_B]_\times\mathbf{M}_a\mathbf{L}_{BC}\mathbf{P}\Big)\dot{\mathbf{q}}$$

$$- (\mathbf{J}_a\dot{\mathbf{R}} + \boldsymbol{\Omega}_\times\mathbf{J}_a\mathbf{R} + [\mathbf{V}_B]_\times\boldsymbol{\Gamma}\mathbf{R})\dot{\boldsymbol{\Theta}} + ([\mathbf{V}_B]_\times\mathbf{M}_a + \boldsymbol{\Omega}_\times\boldsymbol{\Gamma} - \boldsymbol{\Gamma}\boldsymbol{\Omega}_\times)\mathbf{W}_B \qquad (3.39)$$

Combining the complete expression of added mass effect with the undersea kite equations of motion yields a compact form of system dynamics,

$$\mathbf{M}(\mathbf{p})\ddot{\mathbf{p}} + \mathbf{C}(\mathbf{p},\dot{\mathbf{p}})\dot{\mathbf{p}} + \mathbf{G}(\mathbf{p}) = \mathbf{u} + \mathbf{H} + \mathbf{D}, \tag{3.40}$$

where $\mathbf{p}$ is the generalized position of the undersea kite system, $\mathbf{p} = \begin{pmatrix} \mathbf{q} & \boldsymbol{\Theta} \end{pmatrix}$. The conservative force $\mathbf{G}$, control input $\mathbf{u}$, steady hydrodynamic force $\mathbf{H}$ and drift force $\mathbf{D}$ are given as follows

$$\mathbf{G}(\mathbf{p}) = \begin{pmatrix} -\mathbf{P}^T\mathbf{G}_t \\ -(\mathbf{G}_r + \mathbf{G}_v) \end{pmatrix}, \qquad \mathbf{u} = \begin{pmatrix} \mathbf{T}_S \\ \mathbf{u}_E \end{pmatrix}. \tag{3.41}$$

$$\mathbf{H} = \begin{pmatrix} \mathbf{P}^T\mathbf{L}_{CB}\mathbf{H}_B \\ \mathbf{0} \end{pmatrix}, \qquad \mathbf{D} = \begin{pmatrix} (\boldsymbol{\Omega}_\times\mathbf{M}_a - \mathbf{M}_a\boldsymbol{\Omega}_\times)\mathbf{W}_B \\ ([\mathbf{V}_B]_\times\mathbf{M}_a + \boldsymbol{\Omega}_\times\boldsymbol{\Gamma} - \boldsymbol{\Gamma}\boldsymbol{\Omega}_\times)\mathbf{W}_B \end{pmatrix}. \tag{3.42}$$

The system matrices $\mathbf{M}(\mathbf{p})$ and $\mathbf{C}(\mathbf{p},\dot{\mathbf{p}})$ are given by

$$\mathbf{M}(\mathbf{p}) = \begin{pmatrix} \mathbf{M}_{11} & \mathbf{M}_{12} \\ \mathbf{M}_{21}^T & \mathbf{M}_{22} \end{pmatrix}, \qquad \mathbf{C}(\mathbf{p},\dot{\mathbf{p}}) = \begin{pmatrix} \mathbf{C}_{11} & \mathbf{C}_{12} \\ \mathbf{C}_{21} & \mathbf{C}_{22} \end{pmatrix}. \tag{3.43}$$

where the block matrices in equation (3.43) are given by

$$\mathbf{M}_{11} = \mathbf{P}^T\mathbf{L}_{CB}\left(\mathbf{M}_a + (m + \frac{1}{3}\rho_t r)\mathbf{I}_3\right)\mathbf{L}_{BC}\mathbf{P}, \tag{3.44}$$

$$\mathbf{M}_{12} = \mathbf{P}^T\mathbf{L}_{CB}\boldsymbol{\Gamma}^T\mathbf{R}, \tag{3.45}$$

$$\mathbf{M}_{22} = \mathbf{R}^T\mathbf{J}_a\mathbf{R}, \tag{3.46}$$

$$\mathbf{C}_{11} = \mathbf{P}^T\mathbf{L}_{CB}(\boldsymbol{\Omega}_\times\mathbf{M}_a - \mathbf{M}_a\boldsymbol{\Omega}_\times)\mathbf{L}_{BC}\mathbf{P} + \mathbf{P}^T\mathbf{L}_{CB}\left(\mathbf{M}_a + (m + \frac{1}{3}\rho_t r)\mathbf{I}_3\right)\mathbf{L}_{BC}\dot{\mathbf{P}}, \tag{3.47}$$

$$\mathbf{C}_{12} = \mathbf{P}^T\mathbf{L}_{CB}(\boldsymbol{\Gamma}^T\dot{\mathbf{R}} + \boldsymbol{\Omega}_\times\boldsymbol{\Gamma}^T\mathbf{R}), \tag{3.48}$$

$$\mathbf{C}_{21} = \mathbf{R}^T\left((\boldsymbol{\Omega}_\times\boldsymbol{\Gamma} - \boldsymbol{\Gamma}\boldsymbol{\Omega}_\times + [\mathbf{V}_B]_\times\mathbf{M}_a)\mathbf{L}_{BC}\mathbf{P} + \boldsymbol{\Gamma}\mathbf{L}_{BC}\dot{\mathbf{P}}\right), \tag{3.49}$$

$$\mathbf{C}_{22} = \mathbf{R}^T\left([\mathbf{V}_B]_\times\boldsymbol{\Gamma} + \boldsymbol{\Omega}_\times(\mathbf{J} + \mathbf{J}_a)\right)\mathbf{R} + \mathbf{R}^T(\mathbf{J} + \mathbf{J}_a)\dot{\mathbf{R}}. \tag{3.50}$$

In simulation of the undersea kite motion, the inversion of generalized mass matrix $\mathbf{M}(\mathbf{p})$ is required. The first block matrix is positive definite since the $\mathbf{M}_a$ represent the added mass effect that introduced through translation motion. In other word, $\frac{1}{2}\mathbf{V}_a^T\mathbf{M}_a\mathbf{V}_a$ is the kinetic energy of the

unsteady fluid field if the kite motion is purely translation which is positive definite. Hence $\mathbf{M}_{11}$ is also invertible and the inversion of the matrix $\mathbf{M}(\mathbf{p})$ can be obtained through matrix inversion lemma.

$$\left(\mathbf{M}(\mathbf{p})\right)^{-1} = \begin{pmatrix} \mathbf{I}_3 & -\mathbf{M}_{11}^{-1}\mathbf{M}_{12} \\ \mathbf{0} & \mathbf{I}_3 \end{pmatrix} \begin{pmatrix} \mathbf{M}_{11}^{-1} & \mathbf{0} \\ \mathbf{0} & (\mathbf{M}_{22} - \mathbf{M}_{21}\mathbf{M}_{11}^{-1}\mathbf{M}_{12})^{-1} \end{pmatrix} \begin{pmatrix} \mathbf{I}_3 & \mathbf{0} \\ -\mathbf{M}_{21}\mathbf{M}_{11}^{-1} & \mathbf{I}_3 \end{pmatrix}.$$
(3.51)

Therefore, the inversion of the larger matrix $\mathbf{M}(\mathbf{p})$ is reduced to the inversion of the block matrix $\mathbf{M}_{11}$ which is smaller in size.

In summary, the complete dynamics of the undersea kite energy systems are given by

- Translational Kinematic Relation is given by

$$\mathbf{V}_C = \mathbf{P}\dot{\mathbf{q}} \quad \mathbf{P} = r \begin{pmatrix} -\sin q_1 \sin q_2 & \cos q_1 \cos q_2 \\ \cos q_1 & 0 \\ -\sin q_1 \cos q_2 & -\cos q_1 \sin q_2 \end{pmatrix}, \quad \mathbf{q} = \begin{pmatrix} q_1 \\ q_2 \end{pmatrix}.$$
(3.52)

- The rotational kinematic relation is given by

$$\boldsymbol{\omega} = \mathbf{R}\dot{\boldsymbol{\Theta}}, \quad \mathbf{R} = \begin{pmatrix} 1 & 0 & -\sin\theta \\ 0 & \cos\phi & \cos\theta\sin\phi \\ 0 & -\sin\phi & \cos\theta\cos\phi \end{pmatrix} \quad \boldsymbol{\Theta} = \begin{pmatrix} \phi \\ \theta \\ \psi \end{pmatrix}.$$
(3.53)

- The equation of motion is given by

$$\mathbf{M}(\mathbf{p})\ddot{\mathbf{p}} + \mathbf{C}(\mathbf{p},\dot{\mathbf{p}})\dot{\mathbf{p}} + \mathbf{G}(\mathbf{p}) = \mathbf{u} + \mathbf{H} + \mathbf{D}.$$
(3.54)

It is important to notice that the airborne kite energy system dynamics are special case of the undersea kite energy system dynamics with

$$\mathbf{G}_r = \mathbf{G}_v = \mathbf{0}; \quad \mathbf{M}_a = \boldsymbol{\Gamma} = \mathbf{0}.$$

In this chapter, the nonlinear dynamical model of the kite energy systems are derived. A unified simulation model is established. In next chapter, some important nonlinear control techniques will be reviewed and the outline of the rest of the dissertation will be given.

Chapter 4

Control System Design Preliminaries

In this chapter, some crucial techniques in developing the control system of nonlinear dynamical systems are reviewed. An outline of the rest of the dissertation is given in the second part of the chapter.

4.1 Lyapunov Stability Analysis

It is clear that the kite system dynamics given in (3.52)-(3.54) is nonlinear. The Lyapunov and passivity methods can be used to design the control signal for the kite energy system. Consider the following autonomous nonlinear dynamical system,

$$\dot{\mathbf{x}} = \mathbf{f}(\mathbf{x}) \tag{4.1}$$

with equilibrium at the origin, i.e. $\mathbf{f}(\mathbf{0}) = \mathbf{0}$. Then the equilibrium point $\mathbf{x} = \mathbf{0}$ is

- Stable if $\forall \epsilon > 0$, $\exists \delta > 0$ such that

$$\|\mathbf{x}(t)\| < \epsilon, \forall t \geq 0 \ \text{ if } \ \|\mathbf{x}(0)\| < \delta$$

- Unstable if is not stable.

48

- Asymptotically Stable if $\exists \delta$ such that

$$\lim_{t \to 0} \mathbf{x}(t) = \mathbf{0} \ \text{ if } \ \|\mathbf{x}(0)\| < \delta$$

It can be shown that a physical system with nonzero desired behavior can be transformed to problem (4.1) by considering the error dynamics. Lyapunov theorem gives the sufficient condition for stability of the nonlinear dynamical system, [36],

Theorem 2 (Lyapunov Theorem). *Let $\mathbf{x} = \mathbf{0}$ be a equilibrium point of system* (4.1) *and $D \subset \mathbb{R}^n$ be a domain such that $\mathbf{0} \in D$. Let $V : D \to \mathbb{R}$ be a continuous differentiable function such that*

$$V(\mathbf{0}) = 0 \tag{4.2}$$

$$V(\mathbf{x}) > 0 \quad \forall \mathbf{x} \in D - \{\mathbf{0}\} \tag{4.3}$$

$$\dot{V}(\mathbf{x}) \le 0 \quad \forall \mathbf{x} \in D \tag{4.4}$$

Then $\mathbf{x} = \mathbf{0}$ is stable. Moreover, if

$$\dot{V}(\mathbf{x}) < 0 \quad \forall \mathbf{x} \in D - \{\mathbf{0}\} \tag{4.5}$$

then $\mathbf{x} = \mathbf{0}$ is asymptotically stable.

Corollary 1 (globally asymptotically stable). *Let $\mathbf{x} = \mathbf{0}$ be a equilibrium point of system* (4.1) *and $V : \mathbb{R}^n \to \mathbb{R}$ be a continuous differentiable function such that*

$$V(\mathbf{0}) = 0 \tag{4.6}$$

$$V(\mathbf{x}) > 0 \quad \forall \mathbf{x} \ne \mathbf{0} \tag{4.7}$$

$$\lim_{\|\mathbf{x}\| \to \infty} V(\mathbf{x}) = \infty \tag{4.8}$$

$$\dot{V}(\mathbf{x}) < 0 \quad \forall \mathbf{x} \ne \mathbf{0} \tag{4.9}$$

then $\mathbf{x} = \mathbf{0}$ is globally asymptotically stable.

Often, the time derivative of the Lyapunov function is only negative semi-definiteness. In such

49

case, the invariant principle can be used to address the asymptotically stability of the nonlinear systems.

Theorem 3 (LaSalle's Invariance Principle). *Let* $\mathbf{x} = \mathbf{0}$ *be a equilibrium point of system* (4.1). *Let* $V : D \to \mathbb{R}$ *be continuous differentiable where* $D \subset \mathbb{R}^n$ *be a domain such that* $\mathbf{0} \in D$ *and* $\dot{V}(\mathbf{x}) \leq 0$ *in D. Let* $S = \{\mathbf{x} \in D | V(\mathbf{x}) = 0\}$ *and suppose that no solution can stay identically in S, other than the trivial solution* $x(t) \equiv 0$. *Then, the origin is asymptotically stable.*

Corollary 2. *Let* $\mathbf{x} = \mathbf{0}$ *be a equilibrium point of system* (4.1). *Let* $V : \mathbb{R}^n \to \mathbb{R}$ *be continuous differentiable such that* $\dot{V}(\mathbf{x}) \leq 0$ *in* $\mathbb{R}^n$. *Let* $S = \{\mathbf{x} \in \mathbb{R}^n | V(\mathbf{x}) = 0\}$ *and suppose that no solution can stay identically in S, other than the trivial solution* $x(t) \equiv 0$. *Then, the origin is globally asymptotically stable.*

For non-autonomous nonlinear systems,

$$\dot{\mathbf{x}} = \mathbf{f}(t, \mathbf{x}) \tag{4.10}$$

with the equilibrium point $\mathbf{f}(t, \mathbf{0}) = \mathbf{0}$, $\forall t > 0$. To address the stability of non-autonomous systems, the comparison functions needs to be introduced.

- A continuous function $\alpha : [0, a) \to [0, +\infty)$ is said to belong to class $\mathcal{K}$ if it is strictly increasing and $\alpha(0) = 0$.

- A continuous function $\alpha : [0, a) \to [0, +\infty)$ is said to be $\mathcal{K}_\infty$ if it is a class $\mathcal{K}$ function with $a = \infty$ and $\lim_{r \to \infty} \alpha(r) = \infty$.

- A continuous function $\beta : [0, a) \times [0, \infty) \to [0, \infty)$ is said to belong to class $\mathcal{K}\mathcal{L}$ if; for each fixed s, the mapping $\beta(r, s)$ belongs to class $\mathcal{K}$ with respect to r and, for each fixed r, the mapping $\beta(r, s)$ is decreasing with respect to s and $\lim_{s \to \infty} \beta(r, s) = 0$.

The notion of stability also need to extended for non-autonomous systems. The equilibrium point $\mathbf{x} = \mathbf{0}$ is

- Stable if $\forall \epsilon > 0, \exists \delta(\epsilon, t_0) > 0$ such that

$$\|\mathbf{x}(t)\| < \epsilon, \forall t > t_0 \text{ if } \|\mathbf{x}(t_0)\| < \delta$$

- Uniformly stable if $\forall \epsilon > 0, \exists \delta(\epsilon) > 0$, independent of t_0, such that

$$\|\mathbf{x}(t)\| < \epsilon, \forall t > t_0 \text{ if } \|\mathbf{x}(t_0)\| < \delta$$

- Unstable if it is not stable.

- Asymptotically stable if it is stable and there is a positive constant $c = c(t_0)$ such that

$$\lim_{t \to \infty} x(t) = 0 \text{ if } \|\mathbf{x}(t_0)\| < c.$$

- Uniformly asymptotically stable if it is uniformly stable and there is a positive constant c independent of t_0 such that

$$\lim_{t \to \infty} x(t) = 0 \text{ if } \|\mathbf{x}(t_0)\| < c.$$

- Globally uniformly asymptotically stable if it is uniformly stable with $\delta(\epsilon)$ can be chosen such that $\lim_{\epsilon \to \infty} \delta(\epsilon) = \infty$.

- Exponentially stable if $\exists c > 0, k > 0, \lambda > 0$ such that

$$\|\mathbf{x}(t)\| \le k \|\mathbf{x}_0(t)\| e^{-\lambda(t-t_0)}, \forall \|\mathbf{x}_0(t)\| < c$$

The Lyapunov theorem for non-autonomous systems is listed as follows,

Theorem 4. *Let* $\mathbf{x} = \mathbf{0}$ *be a equilibrium point of system* (4.10) *and* $D \subset \mathbb{R}^n$ *be a domain such that* $\mathbf{0} \in D$. *Let* $V : D \to \mathbb{R}$ *be a continuous differentiable function such that*

$$W_1(\mathbf{x}) \le V(\mathbf{x}) \le W_2(\mathbf{x}) \tag{4.11}$$

$$\frac{\partial V}{\partial t} + \frac{\partial V}{\partial \mathbf{x}}\mathbf{f}(t, \mathbf{x}) \leq 0 \tag{4.12}$$

$\forall t > 0, \mathbf{x} \in D$, where $W_1(\mathbf{x})$ and $W_2(\mathbf{x})$ are continuous positive definite functions in D. Then $\mathbf{x} = \mathbf{0}$ is uniformly stable.

Corollary 3. Let $\mathbf{x} = \mathbf{0}$ be a equilibrium point of system (4.10) and $D \subset \mathbb{R}^n$ be a domain such that $\mathbf{0} \in D$. Let $V : D \to \mathbb{R}$ be a continuous differentiable function such that

$$W_1(\mathbf{x}) \leq V(\mathbf{x}) \leq W_2(\mathbf{x}) \tag{4.13}$$

$$\frac{\partial V}{\partial t} + \frac{\partial V}{\partial \mathbf{x}}\mathbf{f}(t, \mathbf{x}) \leq -W_3(\mathbf{x}) \tag{4.14}$$

$\forall t > 0, \mathbf{x} \in D$, where $W_1(\mathbf{x}), W_2(\mathbf{x})$ and $W_3(\mathbf{x})$ are continuous positive definite functions in D. Then $\mathbf{x} = \mathbf{0}$ is uniformly asymptotically stable. Moreover, if $D = \mathcal{R}^n$ and $W_1(\mathbf{x})$ is radially unbounded then $\mathbf{x} = \mathbf{0}$ is globally uniformly asymptotically stable.

Corollary 4. Let $\mathbf{x} = \mathbf{0}$ be a equilibrium point of system (4.10) and $D \subset \mathbb{R}^n$ be a domain such that $\mathbf{0} \in D$. Let $V : D \to \mathbb{R}$ be a continuous differentiable function such that

$$k_1\|\mathbf{x}\|^a \leq V(\mathbf{x}) \leq k_2\|\mathbf{x}\|^a \tag{4.15}$$

$$\frac{\partial V}{\partial t} + \frac{\partial V}{\partial \mathbf{x}}\mathbf{f}(t, \mathbf{x}) \leq -k_3\|\mathbf{x}\|^a \tag{4.16}$$

$\forall t > 0, \mathbf{x} \in D$, where k_1, k_2, k_3 and a are positive constants. Then $\mathbf{x} = \mathbf{0}$ is exponentially stable. If the assumptions hold globally then $\mathbf{x} = \mathbf{0}$ is globally exponentially stable.

Similarly to the autonomous system, the negative definiteness of the $\dot{V}(t, \mathbf{x})$ is not always available. To address the asymptotically stability of the non-autonomous systems, the invariance-like theorem can be used.

Lemma 4. Let $\phi : \mathbb{R} \to \mathbb{R}$ be a uniformly continuous function on $[0, \infty)$. Suppose that $\lim\limits_{t \to \infty} \int_0^\infty \phi(\tau)d\tau$ exists and is finite, then

$$\lim_{t \to \infty} \phi(t) = 0.$$

Theorem 5. Let $D \subset \mathbb{R}^n$ be a domain containing $\mathbf{x} = \mathbf{0}$ and suppose $\mathbf{f}(t, \mathbf{x})$ is piecewise continuous in t and locally Lipschitz in $\mathbf{x}$, uniformly in t on $[0, \infty) \times D$. Furthermore, suppose $\mathbf{f}(t, \mathbf{0})$ is

uniformly bounded for all $t > 0$. Let $V : [0, \infty) \times D \to \mathbb{R}$ be a continuous differentiable function such that

$$W_1(\mathbf{x}) \leq V(\mathbf{x}) \leq W_2(\mathbf{x}) \tag{4.17}$$

$$\dot{V}(t, \mathbf{x}) = \frac{\partial V}{\partial t} + \frac{\partial V}{\partial \mathbf{x}} \mathbf{f}(t, \mathbf{x}) \leq W(\mathbf{x}) \tag{4.18}$$

$\forall t > 0, \mathbf{x} \in D$, where $W_1(\mathbf{x})$ and $W_2(\mathbf{x})$ continuous positive definite functions and $W(\mathbf{x})$ is a continuous positive semidefinite function on D. Choose $r > 0$ such that $B_r \subset \mathbb{R}^n$ and let $\rho < \min_{\|\mathbf{x}\|=r} W_1(\mathbf{x})$. Then, all solutions of $\dot{\mathbf{x}} = \mathbf{f}(t, \mathbf{x})$ with $\mathbf{x}(t_0) \in \{\mathbf{x} \in B_r | W_2(\mathbf{x}) \leq \rho\}$ are bounded and satisfy

$$\lim_{t \to \infty} W(\mathbf{x}(t)) = 0. \tag{4.19}$$

Moreover, if all the assumptions hold globally and $W_1(\mathbf{x})$ is radially unbounded, the statement is true for all $\mathbf{x}(t_0) \in \mathbb{R}^n$.

In this section, the Lyapunov analysis for autonomous and non-autonomous nonlinear systems is reviewed. The emphasis is put on the stability of the nonlinear system. Different stability properties are discussed. Especially, the invariance and invariance-like principles are given, which serves as remedies for the negative semi-definiteness of the time derivative of Lyapunov function. In next section, the boundedness of the system behaviors are discussed through Lyapunov analysis.

4.2   Boundedness and Input to State Stability

The following nonlinear non-autonomous dynamical system is considered in the boundedness analysis,

$$\dot{\mathbf{x}} = \mathbf{f}(t, \mathbf{x}) \tag{4.20}$$

The solution of (4.20) is said to be,

- uniformly bounded if there exists a positive constant c, independent of $t_0 \geq 0$, such that $\forall a \in (0, c), \exists \beta = \beta(a) > 0$, independent of t_0, such that

$$\|\mathbf{x}(t)\| \leq \beta, \forall t > t_0 \text{ if } \|\mathbf{x}(t_0)\| \leq a$$

- globally uniformly bounded if it is uniformly bounded with $c = \infty$.

- uniformly ultimately bounded with ultimate bound b if there exist a positive constant b and c, independent of $t_0 \geq 0$ and $\forall a \in (0, c), \exists T = T(a, b) \geq 0$, independent of t_0 such that,

$$\|\mathbf{x}(t)\| \leq b, \forall t > t_0 + T \text{ if } \|\mathbf{x}(t_0)\| \leq a$$

- globally uniformly ultimately bounded if it is uniformly ultimately bounded with $c = \infty$.

The following theorem can be used to established the ultimately boundedness of system (4.20).

Theorem 6. *Let $D \subset \mathbb{R}^n$ be a domain that contains the origin and $V : [0, \infty) \times D \to \mathbb{R}$ be a continuously differentiable function such that*

$$\alpha_1(\mathbf{x}) \leq V(t, \mathbf{x}) \leq \alpha_2(\mathbf{x}) \tag{4.21}$$

$$\frac{\partial V}{\partial t} + \frac{\partial V}{\partial \mathbf{x}} \mathbf{f}(t, \mathbf{x}) \leq -W_3(\mathbf{x}), \forall \|\mathbf{x}\| > \mu \tag{4.22}$$

$\forall t \geq 0, \mathbf{x} \in D$, where α_1 and α_2 are class $\mathcal{K}$ functions and $W_3(\mathbf{x})$ is a continuous positive definite function. Take $r > 0$ such that $B_r \subset D$ and suppose that

$$\mu < \alpha_2^{-1}(\alpha_1(r)) \tag{4.23}$$

Then, there exists a class $\mathcal{KL}$ function β and for every initial state $\mathbf{x}(t_0)$, satisfying $\|\mathbf{x}(t_0)\| \leq \alpha_2^{-1}(\alpha_1(r))$, there exists a $T \geq 0$(dependent on $\mathbf{x}(t_0)$ and μ) such that the solution of (4.20) satisfies

$$\|\mathbf{x}(t)\| \leq \beta(\|\mathbf{x}(t_0)\|, t - t_0), \forall t_0 \leq t \leq t_0 + T \tag{4.24}$$

$$\|\mathbf{x}(t)\| \leq \alpha_2^{-1}(\alpha_1(\mu)), \forall t \geq t_0 + T \qquad (4.25)$$

Moreover, if $D = \mathbb{R}^n$ and α_1 belong to class $\mathcal{K}_\infty$, then (4.24) and (4.25) hold for any initial state $\mathbf{x}(t_0)$, *with no restriction on how large μ is.*

Another important boundedness property is the boundedness of states with respect to the input to the system, consider the following nonlinear system,

$$\dot{\mathbf{x}} = \mathbf{f}(t, \mathbf{x}, \mathbf{u}) \qquad (4.26)$$

The system (4.26) is said to be

- Input to State Stability if there exist a class $\mathcal{KL}$ function β and a class $\mathcal{K}$ function γ such that for any initial state $\mathbf{x}(t_0)$ and any bounded input $\mathbf{u}(t)$, the solution $\mathbf{x}(t)$ exists for all $t > t_0$ and satisfies

$$\|\mathbf{x}(t)\| \leq \beta(\|\mathbf{x}(t_0)\|, t - t_0) + \gamma\left(\sup_{t_0 \leq \tau \leq t} \|\mathbf{u}(\tau)\| \right)$$

Then the following theorem gives a sufficient condition for input-to-state stability,

Theorem 7. *Let $V : [0, +\infty) \times \mathbb{R}^n \to \mathbb{R}$ be a continuously differentiable function such that*

$$\alpha_1(\mathbf{x}) \leq V(t, \mathbf{x}) \leq \alpha_2(\mathbf{x}) \qquad (4.27)$$

$$\frac{\partial V}{\partial t} + \frac{\partial V}{\partial \mathbf{x}}\mathbf{f}(t, \mathbf{x}) \leq -W_3(\mathbf{x}), \forall \|\mathbf{x}\| > \rho(\|\mathbf{u}\|) > 0 \qquad (4.28)$$

$\forall (t, \mathbf{x}, \mathbf{u}) \in [0, +\infty) \times \mathbb{R}^n \times \mathbb{R}^m$, *where α_1, α_2 are class $\mathcal{K}_\infty$ functions, ρ is a class $\mathcal{K}$ function, and $W_3(\mathbf{x})$ is a continuous positive definite function on $\mathbb{R}^n$. Then system (4.26) is input-to-state stable with $\gamma = \alpha_1^{-1} \circ \alpha_2 \circ \rho$.*

In this section the boundedness property of the non-autonomous nonlinear dynamical system is considered. In next section, the output structure is added into the system dynamics and the passivity will be discussed.

55

4.3 Passivity

The input-output relation $\mathbf{y} = \mathbf{h}(t, \mathbf{u})$ is said to be

- Passive if $\mathbf{u}^T\mathbf{y} \geq 0$

- Lossless if $\mathbf{u}^T\mathbf{y} = 0$

- Input strictly passive if $\mathbf{u}^T\mathbf{y} \geq \mathbf{u}^T\boldsymbol{\varphi}(\mathbf{u})$ and $\mathbf{u}^T\boldsymbol{\varphi}(\mathbf{u}) > 0, \forall \mathbf{u} \neq \mathbf{0}$

- Output strictly passive if $\mathbf{u}^T\mathbf{y} \geq \mathbf{y}^T\boldsymbol{\varphi}(\mathbf{y})$ and $\mathbf{y}^T\boldsymbol{\varphi}(\mathbf{y}) > 0, \forall \mathbf{y} \neq \mathbf{0}$

For a dynamical system represented by a state space model

$$\dot{\mathbf{x}} = \mathbf{f}(\mathbf{x}, \mathbf{u}) \tag{4.29}$$

$$\mathbf{y} = \mathbf{h}(\mathbf{x}, \mathbf{u}) \tag{4.30}$$

where $\mathbf{f} : \mathbb{R}^n \times \mathbb{R}^p \to \mathbb{R}^n$ is locally Lipschitz, $\mathbf{h} : \mathbb{R}^n \times \mathbb{R}^p \to \mathbb{R}^p$ is continuous, $\mathbf{f}(\mathbf{0}, \mathbf{0}) = \mathbf{0}$ and $\mathbf{h}(\mathbf{0}, \mathbf{0}) = \mathbf{0}$. The system (4.29)-(4.30) is said to be passive if there exists a continuously differentiable positive semidefinite function $V(\mathbf{x})$ (called the storage function) such that

$$\mathbf{u}^T\mathbf{y} \geq \dot{V} = \frac{\partial V}{\partial \mathbf{x}}\mathbf{f}(\mathbf{x}, \mathbf{u}), \forall (\mathbf{x}, \mathbf{u}) \in \mathbb{R}^n \times \mathbb{R}^p \tag{4.31}$$

Moreover, it is said to be

- lossless if $\mathbf{u}^T\mathbf{y} = \dot{V}$

- input strictly passive if $\mathbf{u}^T\mathbf{y} \geq \dot{V} + \mathbf{u}^T\boldsymbol{\varphi}(\mathbf{u})$ and $\mathbf{u}^T\boldsymbol{\varphi}(\mathbf{u}) > 0, \forall \mathbf{u} \neq \mathbf{0}$

- output strictly passive if $\mathbf{u}^T\mathbf{y} \geq \dot{V} + \mathbf{y}^T\boldsymbol{\rho}(\mathbf{y})$ and $\mathbf{y}^T\boldsymbol{\rho}(\mathbf{y}) > 0, \forall \mathbf{y} \neq \mathbf{0}$

- strictly passive if $\mathbf{u}^T\mathbf{y} \geq \dot{V} + \psi(\mathbf{x})$, where $\psi(x)$ is positive definite.

in all cases, the inequalities hold for all $(\mathbf{x}, \mathbf{u}) \in \mathbb{R}^n \times \mathbb{R}^p$.

To illustrate the relations of the passivity and stability, the zero-state observability is required. The system (4.29) and (4.30) is zero state observable if no solution of $\dot{\mathbf{x}} = \mathbf{f}(\mathbf{x}, \mathbf{0})$ can stay identically in $S = \{\mathbf{x} \in \mathbb{R}^n | \mathbf{h}(\mathbf{x}, \mathbf{0}) = \mathbf{0}\}$, other than the trivial solution $\mathbf{x} = \mathbf{0}$. The following two lemmas give the relation between the passivity and stability.

Lemma 5. *If the system* (4.29)-(4.30) *is passive with positive definite storage function* $V(\mathbf{x})$, *then the origin of* $\dot{\mathbf{x}} = \mathbf{f}(\mathbf{x}, \mathbf{0})$ *is stable.*

Lemma 6. *Consider the system* (4.29)-(4.30). *The origin of* $\dot{\mathbf{x}} = \mathbf{f}(\mathbf{x}, \mathbf{0})$ *is asymptotically stable if the system is*

- *strictly passive or*

- *output strictly passive and zero-state observable.*

Furthermore, if the storage function is radially unbounded, the origin will be globally asymptotically stable.

4.4   Outline of the System Analysis and Control Design

In previous sections, the complete system dynamics of the kite energy systems are given. To design control schemes for a kite energy system, a high level description of the kite system is needed. In an airborne kite energy system, the kite attitudes, ϕ, θ and ψ, can be treated as inputs to the aerodynamic model. The aerodynamic model of the kite energy system can be treated as a system with kite apparent velocity as input and the aerodynamic force as output. The translational kite dynamics takes the aerodynamic force as input and kite velocity as output. The cascade relation of the kite rotational, aerodynamic and translational dynamics is shown in the following Figure 4.1.

The coupling between the rotational and translational dynamics is unidirectional in airborne kite energy systems. Due to the air density, the influence of kite translational motion to rotational motion is neglected in the airborne system. On the other hand, the influence of the added mass effects on the undersea kite system is not negligible. Therefore, the coupling between kite translation and rotation is more complicated as shown in Figure 4.2
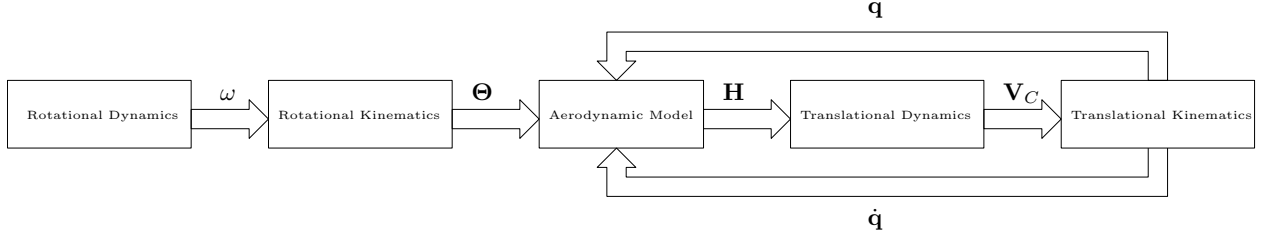
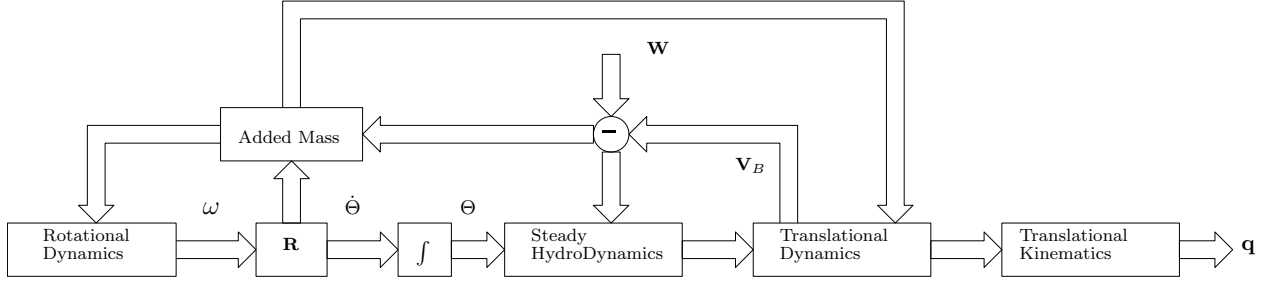*Figure 4.1: Airborne Kite Energy System Diagram (Open Loop)*

Figure 4.2: Undersea Kite Energy System Diagram (Open Loop)

Based on the analysis of open loop kite energy system dynamics, the input to state stability of the kite energy system is addressed. In passivity based system analysis, we propose that the kite mechanical energy with respect to the wind is a more suitable perspective to address the kite system stability. It can be shown in the analysis that the aerodynamic force is dissipative with respect to the kite apparent velocity. By considering the undersea kite and its surrounding fluid as an entire system, a modified PD type control signal is proposed.

Furthermore, the detail system diagram of the steady aero-/hydro-dynamical force can be shown in the following Figure 4.3. The key concept in calculating the aerodynamic force acting on the kite is the apparent attitude, angle of attack α and side slip angle β. Therefore, to analysis the influence of the aerodynamic force on the kite motion, it is important to analyze the procedure for generating angle of attack α and side slip β. It is important to realize that the kite apparent angles are spherical coordinates of the kite apparent velocity measure in the body frame, i.e.

$$\begin{pmatrix} u_a & v_a & w_a \end{pmatrix} = \|\mathbf{V}_a\| \begin{pmatrix} \cos\alpha\cos\beta & \sin\beta & \sin\alpha\cos\beta \end{pmatrix}$$

Therefore, by transforming the glider system dynamics into spherical representation of the apparent velocity, i.e. $\|\mathbf{V}_a\|, \alpha, \beta$, the kite angular velocity $\boldsymbol{\omega}$ becomes the control input to the kite translation. The rotational and translational dynamics form a cascade system. The back stepping
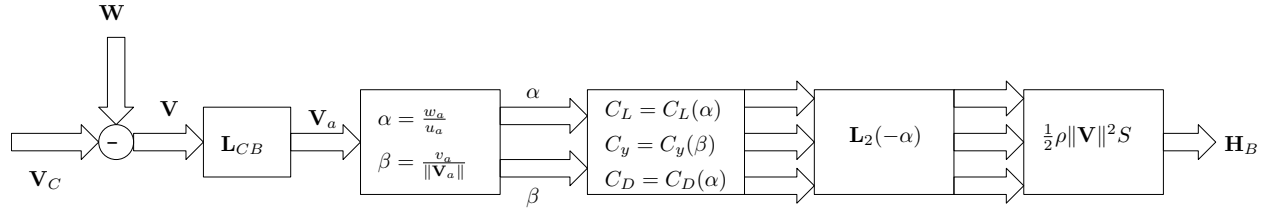
Figure 4.3: System Diagram of Aerodynamic Force

strategy can be applied on the system control design.

On the other hand, the kite apparent angles, α and β, can be treated as output from a nonlinear function that take kite apparent velocity measured in the earth Cartesian frame, $\mathbf{V}$, as inputs. An apparent attitude tracking trajectory can be obtained by solving the nonlinear process. The solution of this desired kite attitude trajectory requires the Euler angles to track a time varying attitude trajectory. To achieve the tracking behavior, two types of rotational control signals are designed based on the sliding mode method and passivity based method.

The following table summarize the dynamic model that used to simulate the kite rotational and translational motion as well as the control strategies that applied for different models.

	FlyGen Airborne	GroundGen Airborne	FlyGen Undersea
Lyapunov/Passivity Based	Section $5.1 - 5.3$	Section $5.1 - 5.3$	Section 5.4
Dynamic Attitude Tracking	section $6.1 - 6.2$		
Geometric Attitude Tracking	Section $7.1 - 7.3$	Section $7.1 - 7.3$	

In the following chapters, three control system design are proposed based on different kite system dynamics. Based on the steady aerodynamic model proposed in the previous chapter, the passivity nature of the aero-/hydro-dynamical force with respect to the kite apparent velocity is addressed. A Lyapunov based control design is proposed in the airborne kite system, the asymptotic stability of system is established using invariance principle. On the other hand, the undersea kite system dynamics are more complicated and the passivity based control design is proposed. Combining the passivity of the steady aero-/hydro-dynamical force and the passivity/Lyapunov based control design, the ultimately boundedness of the kite translation under steady aero-/hydro-dynamic perturbation is established.

As shown in the system dynamics diagram, the aerodynamic force is complicated process coupling the kite translational and rotational states as well as the wind condition. The aerodynamic

59

coupling is the reason of the under-actuation of the kite translation. To decouple the aerodynamic forces, a time varying rotational attitudes are proposed. To achieve the desired kite attitudes, a non autonomous desired rotational dynamics are proposed. The sliding mode control method is used to design the corresponding control scheme and the Lyapunov-like method is used to provide the asymptotic stability of the rotational control. In the proposed apparent attitude tracking control system, the first and second order derivatives of the kite attitudes is required. Therefore, a high gain observer is designed to provide the real time differentiation of the signals. A comparison study of the Lyapunov based control design and apparent attitude tracking control is conducted on a baseline simulation. Moreover, the apparent attitude tracking control also modified the original kite dynamics derived from the Euler-Lagrange approach. By applying the apparent attitude tracking trajectory to the kite translational dynamics, the aerodynamic force is decoupled. The kite apparent attitudes, α and β, are introduced to the translational dynamics as control inputs. A cascade kite dynamics are proposed based on the apparent attitude tracking.

In geometric apparent attitude tracking control, the rotational control signal is transformed to translational control signal through apparent attitude tracking. However, the translation actuation can also be achieved by coordinate transformation in modeling kite translational dynamics. As shown in kinematic relation, the kite apparent velocity can be used as an coordinates that describe the kite translation. By transforming the kite translational dynamics into a non-inertial body frame, the kite angular velocity appears in the system dynamics as control inputs. The rotational and translational kite dynamics form a cascade system. The back-stepping method can be used to design the control system of kite dynamics.

Chapter 5

Lyapunov Based Control Design

5.1 Passivity Analysis of Airborne Kite Energy Systems

In last chapter, the passivity property of the kite aerodynamic force is used to obtain the maximum available power of the airborne kite energy system. In this chapter, this property will be used to analysis the stability of the kite motion. For simplicity, the airborne kite energy systems are first to be analyzed. Moreover, it is assumed that the wind velocity is constant:

Assumption 1. The wind velocity $\mathbf{W}$ is constant and horizontal.

Consider the airborne kite translational dynamics in Cartesian frame $\mathbf{C}$ and rotational dynamics in body frame $\mathbf{B}$

$$(m + \frac{1}{3}\rho_t r)\dot{\mathbf{V}}_C = \mathbf{H}_C + \mathbf{G}_t + \mathbf{T}_C \tag{5.1}$$

$$\mathbf{J}\dot{\boldsymbol{\omega}} = -\boldsymbol{\omega} \times \mathbf{J}\boldsymbol{\omega} + \mathbf{u}_B \tag{5.2}$$

Define the input and output of the open loop system (5.1)-(5.2) as follows

$$\mathbf{u} = \begin{pmatrix} \mathbf{T}_C & \mathbf{u}_B \end{pmatrix}, \quad \mathbf{y} = \begin{pmatrix} \mathbf{V}_C - \mathbf{W} & \boldsymbol{\omega} \end{pmatrix} \tag{5.3}$$

The supply rate to the system is defined as the inner product of the output and input function

$$s = \mathbf{u}^T \mathbf{y} = \mathbf{T}_C^T(\mathbf{V}_C - \mathbf{W}) + \mathbf{u}_B^T \boldsymbol{\omega} \tag{5.4}$$

The storage function of the airborne kite energy system is defined as

$$V_s = \frac{1}{2}(m + \frac{1}{3}\rho_t r)\|\mathbf{V}_C - \mathbf{W}\|^2 + U + \frac{1}{2}\boldsymbol{\omega}^T \mathbf{J}\boldsymbol{\omega} \tag{5.5}$$

Taking the time derivative of the storage function along the kite system trajectory gives that

$$\dot{V}_s = (\mathbf{V}_C - \mathbf{W})^T(m + \frac{1}{3}\rho_t r)(\dot{\mathbf{V}}_C - \dot{\mathbf{W}}) - \mathbf{V}_C^T \frac{\partial U}{\partial \mathbf{r}_C} + \boldsymbol{\omega}^T \mathbf{J}\dot{\boldsymbol{\omega}} \tag{5.6}$$

Using the constant wind velocity assumption, the time derivative of V_s can be simplified as follows

$$\begin{aligned}
\dot{V}_s &= (\mathbf{V}_C - \mathbf{W})^T(m + \frac{1}{3}\rho_t r)\dot{\mathbf{V}}_C - \mathbf{V}_C^T \frac{\partial U}{\partial \mathbf{r}_C} + \boldsymbol{\omega}^T \mathbf{J}\dot{\boldsymbol{\omega}} \\
&= (\mathbf{V}_C - \mathbf{W})^T(\mathbf{H}_C + \mathbf{G}_t + \mathbf{T}_C) + \mathbf{V}_C^T \frac{\partial U}{\partial \mathbf{r}_C} + \boldsymbol{\omega}^T(-\boldsymbol{\omega} \times \mathbf{J}\boldsymbol{\omega} + \mathbf{u}_B) \\
&= (\mathbf{V}_C - \mathbf{W})^T \mathbf{H}_C + (\mathbf{V}_C - \mathbf{W})^T \mathbf{G}_t + \mathbf{V}_C^T \frac{\partial U}{\partial \mathbf{r}_C} + (\mathbf{V}_C - \mathbf{W})^T \mathbf{T}_C + \boldsymbol{\omega}^T \mathbf{u}_B
\end{aligned}$$

Based on the horizontal wind assumption, the wind velocity is perpendicular to the gravitational force, therefore, the time derivative of the storage function can be simplified as follows

$$\begin{aligned}
\dot{V}_s &= (\mathbf{V}_C - \mathbf{W})^T \mathbf{H}_C + \mathbf{V}_C^T \mathbf{G}_t + \mathbf{V}_C^T \frac{\partial U}{\partial \mathbf{r}_C} + (\mathbf{V}_C - \mathbf{W})^T \mathbf{T}_C + \boldsymbol{\omega}^T \mathbf{u}_B \\
&= (\mathbf{V}_C - \mathbf{W})^T \mathbf{H}_C + (\mathbf{V}_C - \mathbf{W})^T \mathbf{T}_C + \boldsymbol{\omega}^T \mathbf{u}_B
\end{aligned}$$

The second equality holds due to the definition of gravitational force $\mathbf{G}_t = -\frac{\partial U}{\partial \mathbf{r}_C}$. Additionally, notice the following identity

$$(\mathbf{V}_C - \mathbf{W})^T \mathbf{H}_C = (\mathbf{V}_C - \mathbf{W})^T \mathbf{L}_{CB}\mathbf{L}_{BC}\mathbf{H}_C = \mathbf{V}_a^T \mathbf{H}_B \tag{5.7}$$
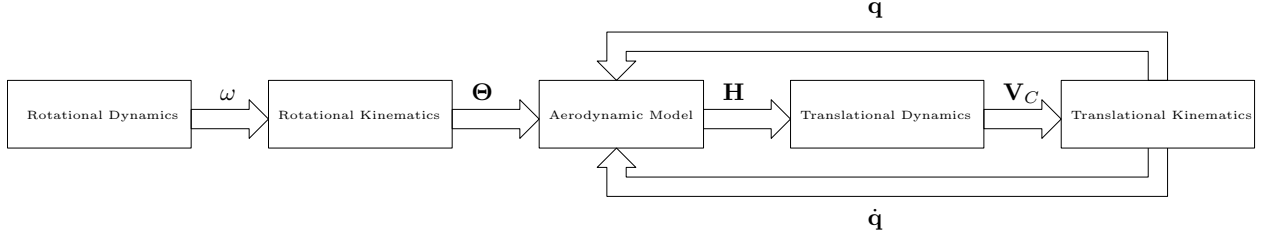
Figure 5.1: Airborne Kite Energy System Diagram (Open Loop)

Using the passivity of the steady aerodynamic force with respect to apparent velocity,

$$\mathbf{V}_a^T \mathbf{H}_B \leq 0$$

the time derivative of the storage function yield

$$\dot{V}_s \leq (\mathbf{V}_C - \mathbf{W})^T \mathbf{T}_C + \boldsymbol{\omega}^T \mathbf{u}_B \qquad (5.8)$$

Therefore, the airborne kite energy system is passive. However, the kite system dynamics (5.1) and (5.2) is under actuated, the tether can only provide the tension force in the tether direction. Therefore, no tension control signal can be design such that $\dot{V}_s$ is negative definite. On the other hand, the overall system is unidirectional coupled as shown in Figure 5.1 and the aerodynamic force is passive if $\alpha, \beta \in (-\frac{1}{2}\pi, \frac{1}{2}\pi)$. Hence, the kite rotational and translational control signal can be designed separately. The rotational control design will not influence the kite translational stability as long as the apparent angle $\alpha, \beta \in (-\frac{1}{2}\pi, \frac{1}{2}\pi)$.

5.2   Lyapunov Based Rotational Control Design

Since the kite rotational motion is independent with respect to the kite translational motion, the rotational control design is first studied in this section. Assume that the rotational transformation matrix $\mathbf{R}$ is not singular, i.e.

Assumption 2. The kite pitch angle is bounded away from the singularity, there exist a small number $\theta_\epsilon \in (0, \frac{\pi}{2})$ such that $-\frac{\pi}{2} + \theta_\epsilon \leq \theta \leq \frac{\pi}{2} - \theta_\epsilon$.

Under the assumption 2, the complete kite rotational dynamics are given the following state space model

$$\dot{\boldsymbol{\Theta}} = \mathbf{R}^{-1}\boldsymbol{\omega} \tag{5.9}$$

$$\mathbf{J}\dot{\boldsymbol{\omega}} = -\boldsymbol{\omega} \times \mathbf{J}\boldsymbol{\omega} + \mathbf{u}_B \tag{5.10}$$

Choose the rotational Lyapunov function as follows

$$V_r = \frac{1}{2}\boldsymbol{\omega}^T\mathbf{J}\boldsymbol{\omega} + \frac{1}{2}(\boldsymbol{\Theta} - \boldsymbol{\Theta}_d)^T\mathbf{K}_\Theta(\boldsymbol{\Theta} - \boldsymbol{\Theta}_d) \tag{5.11}$$

where $\mathbf{K}_\Theta$ is a positive definite design matrix and $\boldsymbol{\Theta}_d$ is constant desired kite geometric attitudes. Take the time derivative of Lyapunov function along kite rotational dynamics gives that

$$\dot{V}_r = \boldsymbol{\omega}^T\mathbf{J}\dot{\boldsymbol{\omega}} + \dot{\boldsymbol{\Theta}}^T\mathbf{K}_\Theta(\boldsymbol{\Theta} - \boldsymbol{\Theta}_d)$$

$$= \boldsymbol{\omega}^T\mathbf{u}_B + \dot{\boldsymbol{\Theta}}^T\mathbf{K}_\Theta(\boldsymbol{\Theta} - \boldsymbol{\Theta}_d)$$

$$= \dot{\boldsymbol{\Theta}}^T\left(\mathbf{R}^T\mathbf{u}_B + \mathbf{K}_\Theta(\boldsymbol{\Theta} - \boldsymbol{\Theta}_d)\right)$$

Let the control signal $\mathbf{u}_B$ satisfies the following equation,

$$\mathbf{R}^T\mathbf{u}_B + \mathbf{K}_\Theta(\boldsymbol{\Theta} - \boldsymbol{\Theta}_d) = -\mathbf{K}_\Omega\dot{\boldsymbol{\Theta}} \tag{5.12}$$

Then the derivative of rotational Lyapunov function V_r is given by

$$\dot{V}_r = -\dot{\boldsymbol{\Theta}}^T\mathbf{K}_\Omega\dot{\boldsymbol{\Theta}} \leq 0 \tag{5.13}$$

Based on the assumption, the rotational velocity transformation matrix $\mathbf{R}$ is invertible and the resulting control signal is

$$\mathbf{u}_B = -(\mathbf{R}^T)^{-1}\left(\mathbf{K}_\Theta(\boldsymbol{\Theta} - \boldsymbol{\Theta}_d) + \mathbf{K}_\Omega\dot{\boldsymbol{\Theta}}\right) \tag{5.14}$$

The closed loop system dynamics are

$$\mathbf{J}\dot{\boldsymbol{\omega}} = -\boldsymbol{\omega} \times \mathbf{J}\boldsymbol{\omega} - (\mathbf{R}^T)^{-1}\Big(\mathbf{K}_\Theta(\boldsymbol{\Theta} - \boldsymbol{\Theta}_d) + \mathbf{K}_\Omega\dot{\boldsymbol{\Theta}}\Big) \tag{5.15}$$

Using invariance principle, the invariance set of the closed loop system must satisfies that

$$\dot{\boldsymbol{\Theta}} = \mathbf{0}; \quad \boldsymbol{\omega} = \mathbf{0}; \quad \dot{\boldsymbol{\omega}} = \mathbf{0} \tag{5.16}$$

Therefore, the only closed loop dynamic trajectory that satisfies the invariant set condition is

$$\boldsymbol{\Theta} = \boldsymbol{\Theta}_d \tag{5.17}$$

The closed loop kite rotational system dynamics is asymptotically stable.

5.3 Lyapunov Based Translational Control Design

Among the airborne kite energy systems, there are two different power generation modes. In a lift mode airborne kite energy system, also known as the GroundGen system, the electricity is generated in a ground based station. On the other hand, in a drag mode airborne kite energy system, turbines are mounted on the kite or glider to generate power. In this study, we assumed that in a GroundGen system, the tether length is variable and the mechanical power is converted to the electrical power through tether tension. While in the FlyGen system, the tether length is assumed to be constant and the energy in the apparent wind is converted to electrical power through on board turbines. In both cases, the tether tension is a important factor in achieving kite power generation. In this section, the influence of the tether tension on kite motion is addressed.

In the case of variable tether length airborne kite energy system, the translational states and

velocity transformation matrix is given by

$$\mathbf{q} = \begin{pmatrix} r & q_1 & q_2 \end{pmatrix}^T \quad \mathbf{P} = \begin{pmatrix} \cos q_1 \sin q_2 & -r \sin q_1 \sin q_2 & r \cos q_1 \cos q_2 \\ \sin q_1 & r \cos q_1 & 0 \\ \cos q_1 \cos q_2 & -r \sin q_1 \cos q_2 & -r \cos q_1 \sin q_2 \end{pmatrix}$$

On the other hand, the translational velocity transformation matrix $\mathbf{P}$ and generalized coordinate $\mathbf{q}$ of a constant tether length kite energy system are given by

$$\mathbf{q} = \begin{pmatrix} q_1 & q_2 \end{pmatrix}^T \quad \mathbf{P} = r \begin{pmatrix} -\sin q_1 \sin q_2 & \cos q_1 \cos q_2 \\ \cos q_1 & 0 \\ -\sin q_1 \cos q_2 & -\cos q_1 \sin q_2 \end{pmatrix}$$

Additionally, denote the wind velocity as $\mathbf{W}$, the kite apparent velocity $\mathbf{V}_a$ and kite velocity $\mathbf{V}_C$ are given by

$$\mathbf{V}_C = \mathbf{P}\dot{\mathbf{q}}, \quad \mathbf{V}_a = \mathbf{P}\dot{\mathbf{q}} - \mathbf{W} \tag{5.18}$$

Moreover, if the wind velocity $\mathbf{W}$ is constant, the kite apparent translational dynamics takes the same form of kite absolute translational dynamics.

$$(m + \frac{1}{3}\rho_t r)\dot{\mathbf{V}}_a = \mathbf{G}_C + \mathbf{H}_C + \mathbf{T}_C \tag{5.19}$$

To facilitate the system analysis, the following two equivalent assumptions need to be made

Assumption 3. The gravitational force on the kite is bounded by a quadratic function of the kite apparent velocity, i.e.

$$\|\mathbf{G}_C\| \leq C_G \|\mathbf{V}_a\|^2 \tag{5.20}$$

Assumption 4. The kite apparent speed is not less that some nonzero minimum value, i.e.

$$\exists V_{min} > 0 \ni \|\mathbf{V}_a\| \geq V_{min} \tag{5.21}$$

66

To analyze the influence of tether tension on kite motion, the following Lyapunov function candidate is chosen,

$$V_t = \frac{1}{2}(m + \frac{1}{3}\rho_t r)\|\mathbf{V}_a\|^2 + U \tag{5.22}$$

By definition, the kite gravitational potential energy is defined by the integration of gravity with respect to kite displacement

$$U = \int \mathbf{G} d\mathbf{r}_C \tag{5.23}$$

Using the Assumption 3, the gravitational potential energy is also bounded by a quadratic function of the kite apparent velocity

$$U \leq \int \|\mathbf{G}\| d\mathbf{r} \leq C_G \|\mathbf{V}_a\|^2 r \tag{5.24}$$

Therefore, the Lyapunov function candidate (5.22) is bounded by two class $\mathcal{K}$ functions

$$\frac{1}{2}(m + \frac{1}{3}\rho_t r)\|\mathbf{V}_a\|^2 \leq V_t \leq \frac{1}{2}(m + \frac{1}{3}\rho_t r)\|\mathbf{V}_a\|^2 + C_G\|\mathbf{V}_a\|^2 r \tag{5.25}$$

Take the time derivative of the Lyapunov function $\mathbf{V}_t$ along the system trajectory gives that

$$\begin{aligned}
\dot{V}_t &= \mathbf{V}_a^T \mathbf{H}_C + \mathbf{V}_a^T \mathbf{T}_C \\
&= -\frac{1}{2}\rho_t \|\mathbf{V}_a\|^3 C_a + \mathbf{V}_a^T \mathbf{T}_C \\
&\leq -\frac{1}{2}\rho_t S\|\mathbf{V}_a\|^3 C_a + \|\mathbf{V}_a\|\|\mathbf{T}_C\|
\end{aligned} \tag{5.26}$$

To derive the tension control signal that guarantee the boundedness of the kite apparent velocity, it needs to assume that the coefficient C_a is lower bounded.

Assumption 5. There exist a positive minimum value of C_a, that is

$$\exists (C_a)_{min} > 0 \ni C_a \geq (C_a)_{min} \tag{5.27}$$

Hence, for a positive number $0 < \epsilon_a < C_a$, then the following inequality holds

$$\dot{V}_t \leq -\epsilon_a \|\mathbf{V}_a\|^3 \quad \text{if} \quad \|\mathbf{V}_a\| \geq \sqrt{\frac{2\|\mathbf{T}_C\|}{S\rho_t(C_a - \epsilon_a)}} \tag{5.28}$$

Hence the kite system dynamics (5.19) is input-to-state stable, that is there exist a class $\mathcal{KL}$ function β_a and a class $\mathcal{K}$ function γ_a such that the kite apparent velocity satisfies that

$$\|\mathbf{V}_a\| \leq \beta_a(\|\mathbf{V}_a(t_0)\|, t - t_0) + \gamma_a\left(\sup_{t_0 \leq \tau \leq t} \|\mathbf{T}_C\|\right)$$

Therefore, if the magnitude of tether tension is constant, the kite apparent velocity is bounded.

$$\|\mathbf{V}_a\| \leq \beta_a(\|\mathbf{V}_a(t_0)\|, 0) + \gamma_a(\mu_C) \quad \text{if} \quad \|\mathbf{T}_C\| \leq \mu_C \tag{5.29}$$

Moreover, if the tether tension is proportional to the apparent velocity $\|\mathbf{V}_a\|$, i.e.

$$\|\mathbf{T}_C\| = K_a\|\mathbf{V}_a\| \quad \text{for} \quad K_a > 0 \tag{5.30}$$

the kite apparent velocity $\mathbf{V}_a$ can be shown to be ultimately bounded. The derivative of the Lyapunov function (5.26) under the control signal (5.30) becomes,

$$\begin{aligned}
\dot{V}_t &\leq -\frac{1}{2}\rho_t S\|\mathbf{V}_a\|^3 C_a + \|\mathbf{V}_a\|\|\mathbf{T}_C\| \\
&= -\frac{1}{2}\rho_t S\|\mathbf{V}_a\|^3 C_a + K_a\|\mathbf{V}_a\|^2
\end{aligned} \tag{5.31}$$

The ultimately boundedness of the kite apparent velocity is given by the following inequality,

$$\dot{V}_t \leq 0 \quad \text{if} \quad \|\mathbf{V}_a\| \geq \frac{2K_a}{\rho_t S(C_a)_{min}} \tag{5.32}$$

The Lyapunov stability can be guarantee by choosing the following tension control signal

$$\|\mathbf{T}_C\| = \frac{1}{2}\rho_t S\|\mathbf{V}_a\|^2(C_a)_{min} \tag{5.33}$$

Control Signal	Formulation	System Stability
Bounded Tether Tension	$\|\mathbf{T}_C\| \leq \mu_C$	Bounded
Linear Tether Tension	$\|\mathbf{T}_C\| = K_a\|\mathbf{V}_a\|$	Ultimately Boundedness
Quadratic Tether Tension	$\|\mathbf{T}_C\| = \frac{1}{2}\rho_t\|\mathbf{V}_a\|^2(C_a)_{min}$	Lyapunov Stable

Under the control signal (5.33), the derivative of the Lyapunov function V_t becomes

$$\dot{V}_t \leq -\frac{1}{2}\rho_t S\|\mathbf{V}_a\|^3\big(C_a - (C_a)_{min}\big) \leq 0 \tag{5.34}$$

Therefore, the tether tension control design for a GroundGen airborne kite energy systems can be summarized in the following Table 5.1

For a FlyGen airborne kite energy system, the tether length is assumed to be constant. In this case, the kite translation is constrained on a half sphere with no motion in the tether direction. Therefore, the force is balance in the normal direction of the sphere. Using the virtual work principle, the kite velocity satisfies that

$$\mathbf{V}_C^T\mathbf{T}_C = 0 \tag{5.35}$$

Choose the same Lyapunov function as (5.22), the time derivative becomes

$$\begin{aligned}
\dot{V}_t &= \mathbf{V}_a^T\mathbf{H}_C + \mathbf{V}_a^T\mathbf{T}_C \\
&= \mathbf{V}_a^T\mathbf{H}_C + (\mathbf{V}_C - \mathbf{W})^T\mathbf{T}_C \\
&\leq -\frac{1}{2}\rho_t S\|\mathbf{V}_a\|^3 C_a + \|\mathbf{W}\|\|\mathbf{T}_C\|
\end{aligned} \tag{5.36}$$

It is important to notice that the tether tension can be calculated using the force balance

$$\mathbf{T}_C = -\Big((\mathbf{G}_C + \mathbf{H}_C) \cdot \hat{\mathbf{r}}_C\Big)\hat{\mathbf{r}}_C \tag{5.37}$$

where $\hat{\mathbf{r}}_C$ is the unit vector in the tether direction. Additionally, the aerodynamic coefficients on

kite is physically bounded

$$\|\mathbf{C}_B\| \leq \infty \tag{5.38}$$

Therefore, using Assumption 3, the tether tension of a FlyGen kite energy system is bounded by the following inequality

$$\|\mathbf{T}_C\| \leq \frac{1}{2}\rho_t S \|\mathbf{V}_a\|^2 (\|\mathbf{C}_B\| + C_G) \tag{5.39}$$

Therefore, kite apparent velocity is ultimately bounded,

$$\dot{V}_t \leq 0 \quad \text{if} \quad \|\mathbf{V}_a\| \geq \frac{\|\mathbf{C}_B\| + C_G}{(C_a)_{min}} \tag{5.40}$$

In summary, the apparent velocity of a FlyGen airborne kite energy system is ultimately bounded.

The key control and input parameters of a baseline simulation is given in the following table. In the baseline simulation, the Lyapunov based rotational and translational control signal is applied on a airborne kite energy system, the results shows that that the consecutive power generation and retraction motion has been achieved. In the power generation phase, we propose a switching control law which establishes cross wind kite motion by alternating desired roll, pitch, yaw trim angles Θ_d as follows, where the variables q_2^+ and q_2^- represent the right and left limit in cross wind motion.

$$\Theta_d = \begin{cases} \begin{bmatrix} \phi_d^+ & \theta_d^+ & \psi_d^+ \end{bmatrix}^T & \text{if} \quad q_2 > q_2^+ \\ \begin{bmatrix} \phi_d^- & \theta_d^- & \psi_d^- \end{bmatrix}^T & \text{if} \quad q_2 < q_2^- \end{cases}$$

In the retraction phase, on the other hand, the control goal is to establish retraction near the mid-plane ($q_2 = 0$), thus we propose the following desired roll, pitch, yaw trim angles

$$\Theta_d = \begin{bmatrix} 0 & \theta^* & 0 \end{bmatrix}^T, \theta^* < 0$$

In the following figures, the robustness of the control system design is tested through simulations. In all cases of different mass and wind speed situation, the Lyapunov based control design

70

Table 5.2: Input and Control Parameters

parameter	value	parameter	value	parameter	value
Kite Mass	15 kg	K_a	1000	$[\phi_d^+, \theta_d^+, \psi_d^+]$	$[50°, 70°, 20°]$
Kite Area	15 m^2	$\mathbf{K}_\Omega$	1000$\mathbf{I}$	$[\phi_d^-, \theta_d^-, \psi_d^-]$	$[50°, 70°, 20°]$
Tether Density	0.003 kg/m	$\mathbf{K}_\Theta$	1500$\mathbf{I}$	θ^*	$-25°$
Tether Diameter	0.002 m	$[q_2^-, q_2^+]$	$\pm11.5°$	q_1	300-600m
Wind Velocity	6 m/s				

Table 5.3: Power Output

Wind Speed(m/s)	mass(kg)	Power(kW)
	12	2.17
6	15	2.57
	18	2.56
	12	2.57
7	15	2.58
	18	2.37

achieve successively power cycles. In table 5.3, the power of these cases are listed.

5.4 Tethered Undersea Kite Systems

Using the same concepts that have been developed in the airborne kite energy systems, the kite energy generation can also be applied to the undersea circumstance. There are three major differences between the airborne and undersea kite energy systems:

- The water provide significant buoyancy than the air, which is not negligible;

- The water is much more dense and viscous than the air, therefore, there is also significant added mass effects;

- Due to the buoyancy and added mass effects, the typical configuration of the undersea kite energy system is the FlyGen system.

Similar to the FlyGen airborne kite energy systems, the undersea kite energy system consists of a fixed length tether, a rigid kite or glider and on-board turbines. To facilitate the system analysis,
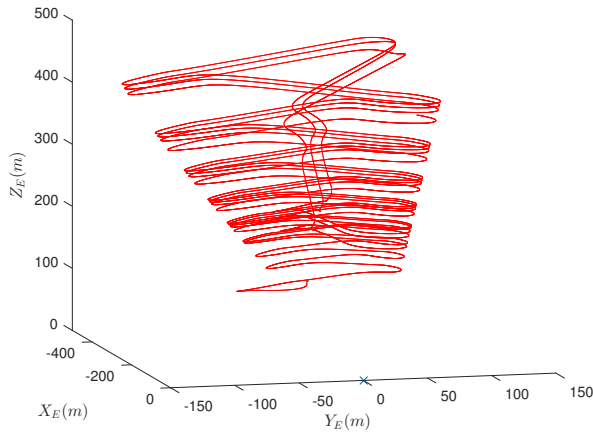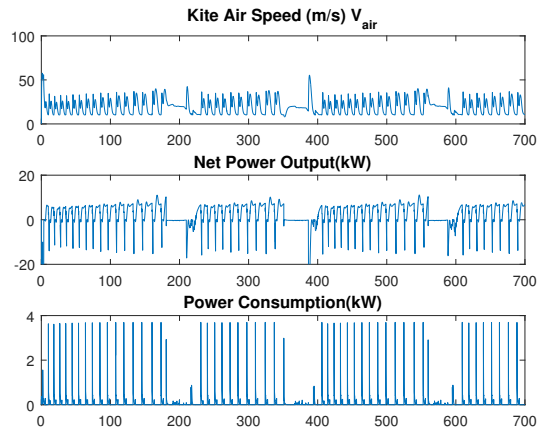
(a) Kite Spherical Coordinate Trajectory
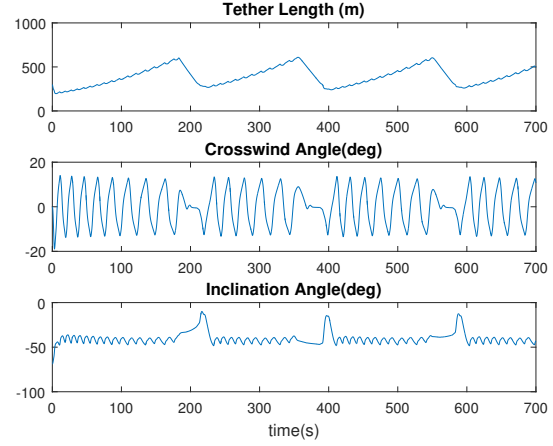
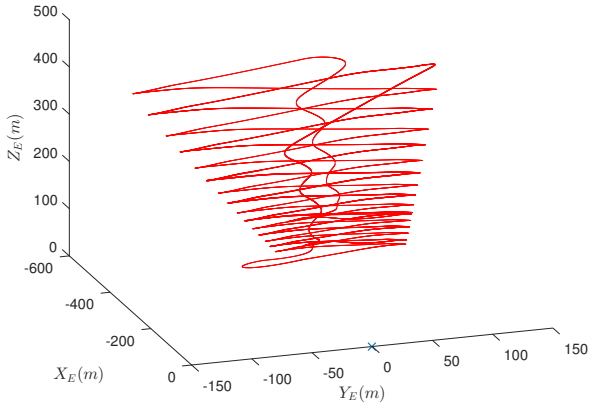*(b) Kite Spherical Coordinate Trajectory*
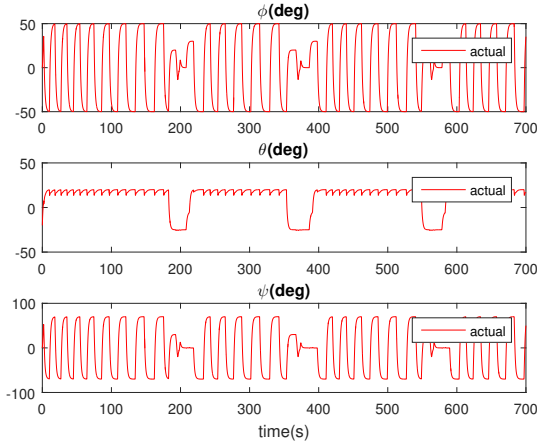
(c) Kite Aerodynamics Coefficient
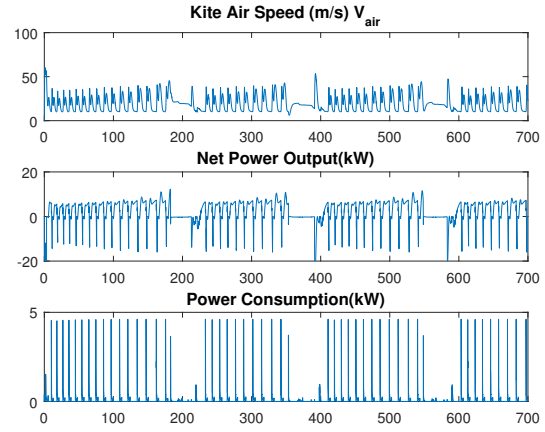
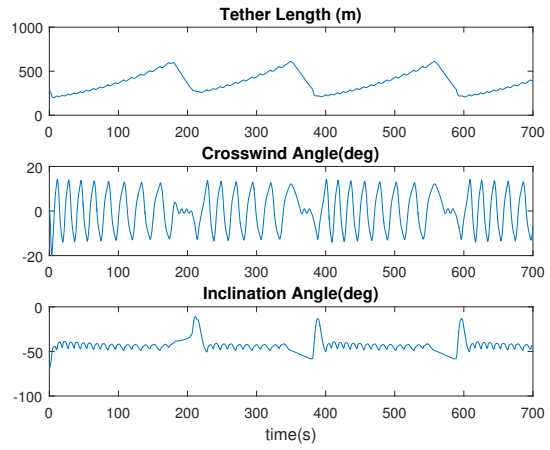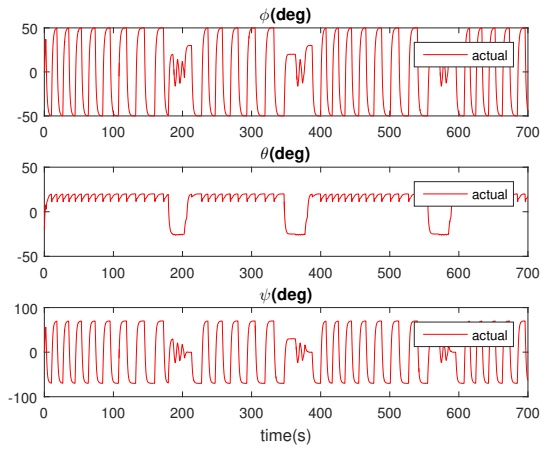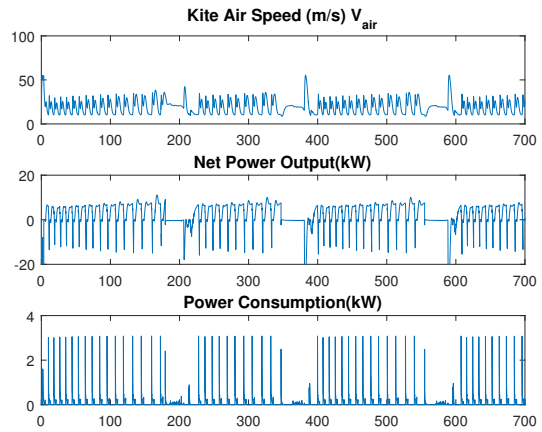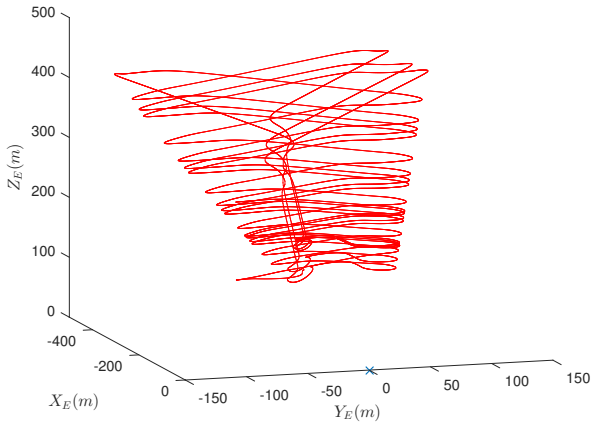*(d) Angle of attack and control tension*

Figure 5.2: Wind Speed = 6m/s, Mass = 12kg

assume that the kite geometric attitudes satisfies the Assumption 2, i.e. $\mathbf{R}$ is invertible. The complete system dynamics of the undersea kite energy systems in body frame $\mathbf{B}$ are given by

$$(m + \frac{1}{3}\rho_t r)(\dot{\mathbf{V}}_B + \boldsymbol{\omega} \times \mathbf{V}_B) = \mathbf{L}_{BC}\mathbf{G}_t + \mathbf{H}_B + \mathbf{A}_t + \mathbf{T}_B \tag{5.41}$$

$$\mathbf{J}\dot{\boldsymbol{\omega}} + \boldsymbol{\omega} \times \mathbf{J}\boldsymbol{\omega} = (\mathbf{R}^{-1})^T\mathbf{u}_E + \mathbf{A}_r + (\mathbf{R}^{-1})^T(\mathbf{G}_r + \mathbf{G}_v) \tag{5.42}$$

It is important to notice that the added mass effects are formulated in the relative motion reference frame, i.e.

$$\mathbf{A}_t = -(\mathbf{M}_a\dot{\mathbf{V}}_a + \boldsymbol{\Gamma}^T\dot{\boldsymbol{\omega}}) - \boldsymbol{\omega} \times (\mathbf{M}_a\mathbf{V}_a + \boldsymbol{\Gamma}^T\boldsymbol{\omega})$$
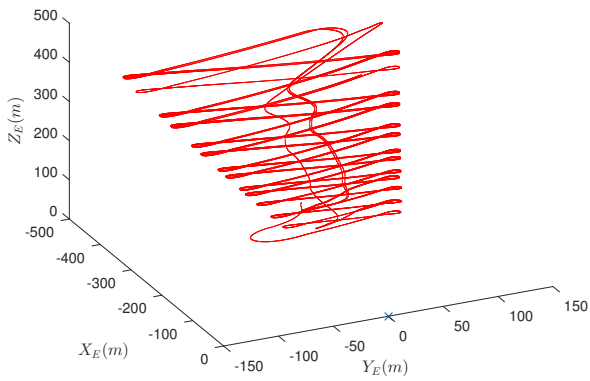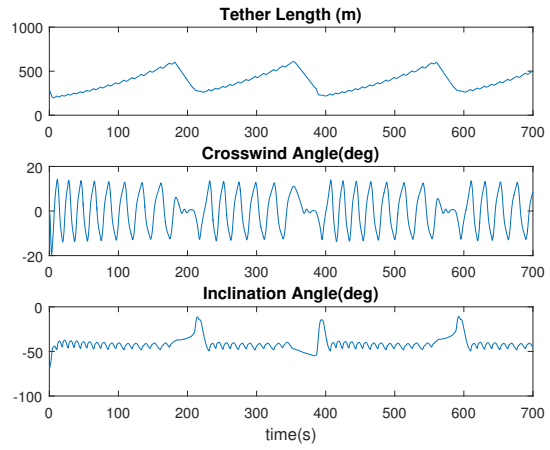
72

(a) Kite Spherical Coordinate Trajectory

(b) Kite Spherical Coordinate Trajectory
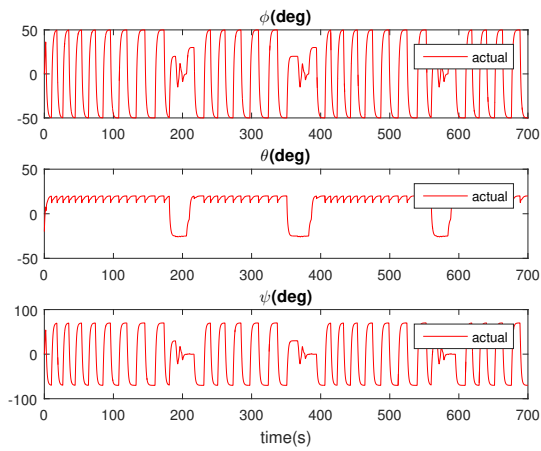
(c) Kite Aerodynamics Coefficient

(d) Angle of attack and control tension

Figure 5.3: Wind Speed = 6m/s, Mass = 15kg

(a) Kite Spherical Coordinate Trajectory

(b) Kite Spherical Coordinate Trajectory
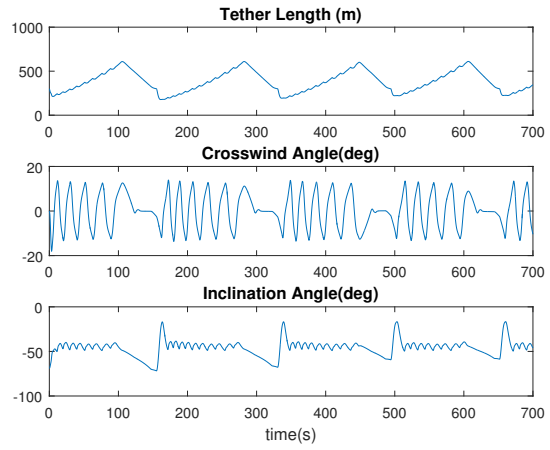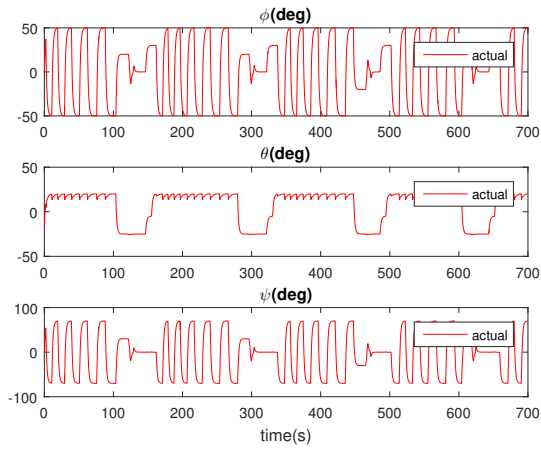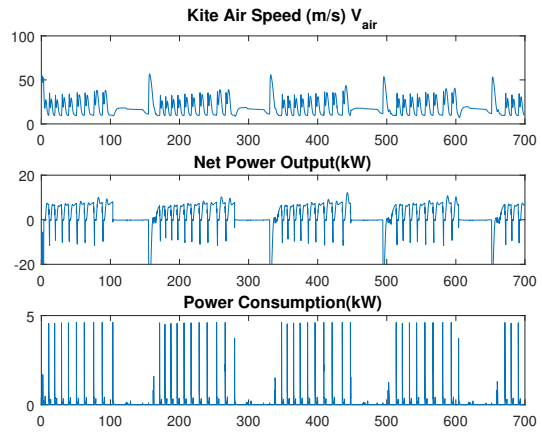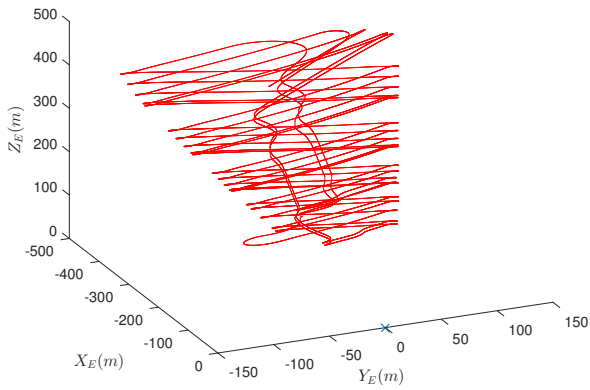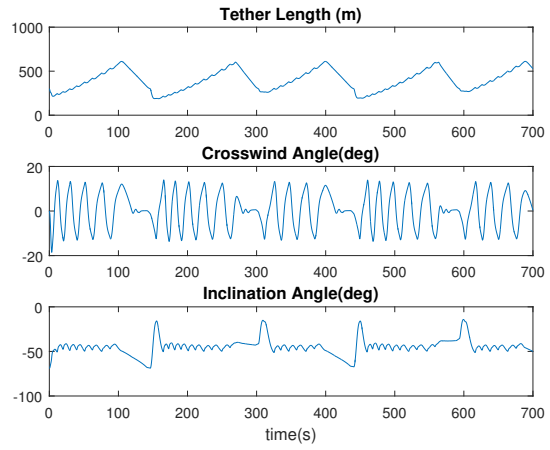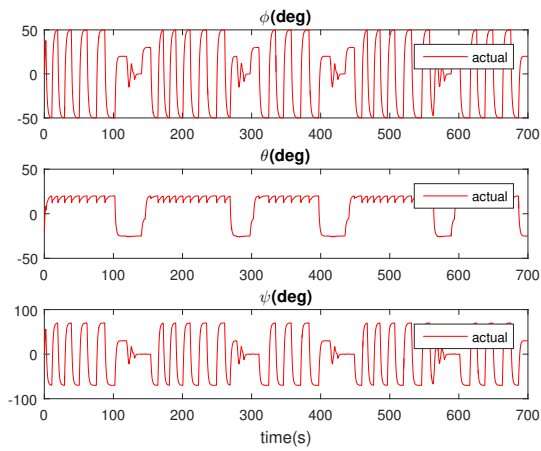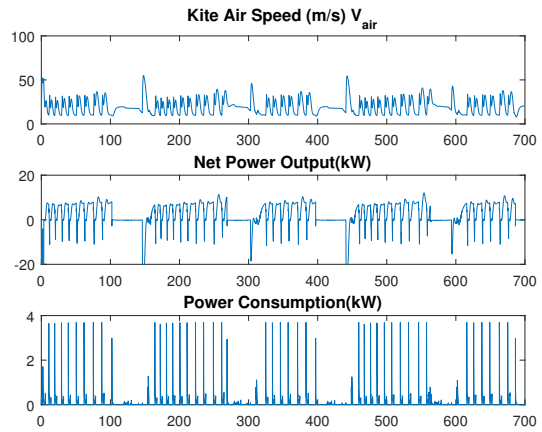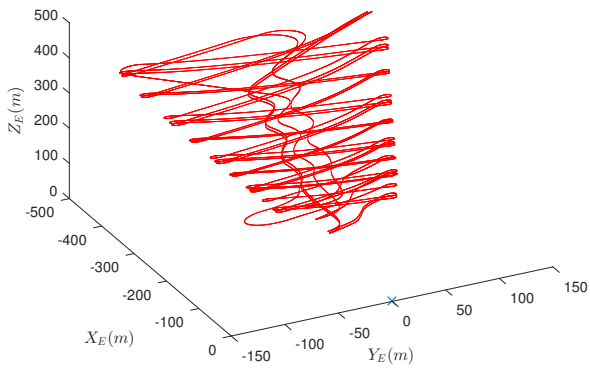

(c) Kite Aerodynamics Coefficient

(d) Angle of attack and control tension

Figure 5.4: Wind Speed = 6m/s, Mass = 18kg

(a) Kite Spherical Coordinate Trajectory

(b) Kite Spherical Coordinate Trajectory

(c) Kite Aerodynamics Coefficient

(d) Angle of attack and control tension

Figure 5.5: Wind Speed = 7m/s, Mass = 12kg

(a) Kite Spherical Coordinate Trajectory

(b) Kite Spherical Coordinate Trajectory
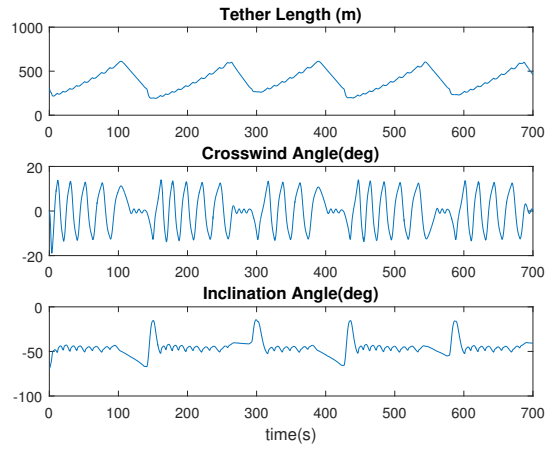

(c) Kite Aerodynamics Coefficient

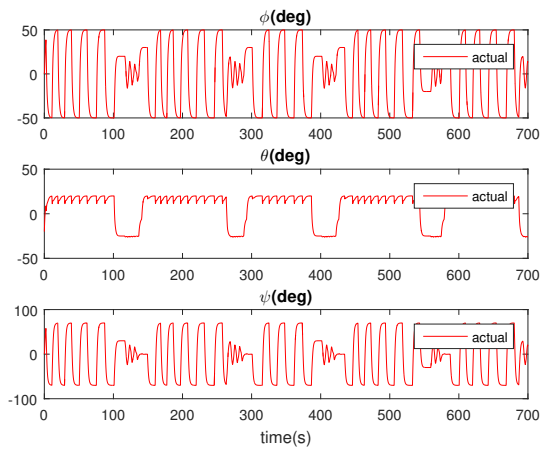*(d) Angle of attack and control tension*

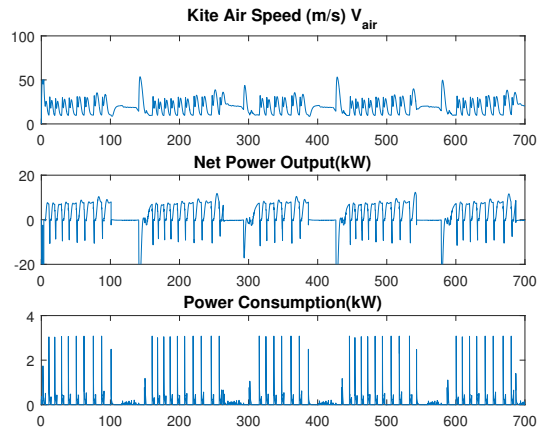*Figure 5.6: Wind Speed = 7m/s, Mass = 15kg*

(a) Kite Spherical Coordinate Trajectory

(b) Kite Spherical Coordinate Trajectory

(c) Kite Aerodynamics Coefficient

(d) Angle of attack and control tension

Figure 5.7: Wind Speed = 7m/s, Mass = 18kg

$$\mathbf{A}_r = -(\mathbf{J}_a\dot{\boldsymbol{\omega}} + \boldsymbol{\Gamma}\dot{\mathbf{V}}_a) - \boldsymbol{\omega} \times (\mathbf{J}_a\boldsymbol{\omega} + \boldsymbol{\Gamma}\mathbf{V}_a) - \mathbf{V}_B \times (\mathbf{M}_a\mathbf{V}_a + \boldsymbol{\Gamma}^T\boldsymbol{\omega})$$

To simplify the analysis, assume that the current velocity is constant, then the following lemma holds

Lemma 7. *For constant current velocity,*

$$(m + \frac{1}{3}\rho_t r)(\dot{\mathbf{V}}_B + \boldsymbol{\omega} \times \mathbf{V}_B) = (m + \frac{1}{3}\rho_t r)(\dot{\mathbf{V}}_a + \boldsymbol{\omega} \times \mathbf{V}_a) \tag{5.43}$$

Proof. By definition, the current velocity measured in body frame **B** is

$$\mathbf{W} = \mathbf{L}_{CB}\mathbf{W}_B \tag{5.44}$$

Taking the time derivative of the equation above

$$\dot{\mathbf{L}}_{CB}\mathbf{W}_B + \mathbf{L}_{CB}\dot{\mathbf{W}}_B = \mathbf{0} \tag{5.45}$$

Using the matrix identity

$$\mathbf{L}_{CB}\boldsymbol{\Omega}_\times\mathbf{W}_B + \mathbf{L}_{CB}\dot{\mathbf{W}}_B = \mathbf{0} \tag{5.46}$$

Since the velocity transformation matrix $\mathbf{L}_{CB}$ is invertible,

$$\dot{\mathbf{W}}_B = -\boldsymbol{\Omega}_\times\mathbf{W}_B \tag{5.47}$$

Substituting equation (5.47) into equation (5.43) yields

$$\begin{aligned}
&(m + \frac{1}{3}\rho_t r)(\dot{\mathbf{V}}_B + \boldsymbol{\omega} \times \mathbf{V}_B) \\
=&(m + \frac{1}{3}\rho_t r)(\dot{\mathbf{V}}_B + \boldsymbol{\omega} \times \mathbf{W}_B + \boldsymbol{\omega} \times \mathbf{V}_B - \boldsymbol{\omega} \times \mathbf{W}_B) \\
=&(m + \frac{1}{3}\rho_t r)(\dot{\mathbf{V}}_a + \boldsymbol{\omega} \times \mathbf{V}_a) \tag{5.48}
\end{aligned}$$

Thus the lemma statement holds. $\qquad\square$

Substituting equation (5.48) into equation (5.41), the dynamics of kite apparent velocity is given by

$$(m + \frac{1}{3}\rho_t r)(\dot{\mathbf{V}}_a + \boldsymbol{\omega} \times \mathbf{V}_a) = \mathbf{L}_{BC}\mathbf{G}_t + \mathbf{H}_B + \mathbf{A}_t + \mathbf{T}_B \tag{5.49}$$

On the other hand, the right hand side of the kite rotational dynamic can be rewritten as follows

$$\mathbf{J}\dot{\boldsymbol{\omega}} + \boldsymbol{\omega} \times \mathbf{J}\boldsymbol{\omega} = \mathbf{u}_B + \mathbf{A}_r + (\mathbf{R}^{-1})^T(\mathbf{G}_r + \mathbf{G}_v) \tag{5.50}$$

where $\mathbf{u}_B = (\mathbf{R}^{-1})^T\mathbf{u}_E$. Further define the augmented rotational control signal and augmented rotational added mass effect as follows

$$\mathbf{u}'_B = (\mathbf{R}^{-1})^T\mathbf{u}_E - \mathbf{W}_B \times (\mathbf{M}_a\mathbf{V}_a + \boldsymbol{\Gamma}^T\boldsymbol{\omega}) \tag{5.51}$$

$$\mathbf{A}'_r = -(\mathbf{J}_a\dot{\boldsymbol{\omega}} + \boldsymbol{\Gamma}\dot{\mathbf{V}}_a) - \boldsymbol{\omega} \times (\mathbf{J}_a\boldsymbol{\omega} + \boldsymbol{\Gamma}\mathbf{V}_a) - \mathbf{V}_a \times (\mathbf{M}_a\mathbf{V}_a + \boldsymbol{\Gamma}^T\boldsymbol{\omega}) \tag{5.52}$$

Furthermore, using the cross product identities,

$$\mathbf{V}_a \times (m + \frac{1}{3}\rho_t r)\mathbf{V}_a = \mathbf{0}$$

Equation (5.52) can be rewritten as follows

$$\mathbf{A}'_r = -(\mathbf{J}_a\dot{\boldsymbol{\omega}} + \boldsymbol{\Gamma}\dot{\mathbf{V}}_a) - \boldsymbol{\omega} \times (\mathbf{J}_a\boldsymbol{\omega} + \boldsymbol{\Gamma}\mathbf{V}_a) - \mathbf{V}_a \times \left(\mathbf{M}_a + (m + \frac{1}{3}\rho_t r)\mathbf{I}_3\mathbf{V}_a + \boldsymbol{\Gamma}^T\boldsymbol{\omega}\right) \tag{5.53}$$

Then the rotational dynamics of the undersea kite is given by

$$\mathbf{J}\dot{\boldsymbol{\omega}} + \boldsymbol{\omega} \times \mathbf{J}\boldsymbol{\omega} = \mathbf{u}'_B + \mathbf{A}'_r + (\mathbf{R}^{-1})^T(\mathbf{G}_r + \mathbf{G}_v) \tag{5.54}$$

Therefore, the undersea kite system dynamics are given by

$$\left(\mathbf{M}_a + (m + \frac{1}{3}\rho_t r)\mathbf{I}_3\right)\dot{\mathbf{V}}_a + \boldsymbol{\Gamma}^T\dot{\boldsymbol{\omega}} + \boldsymbol{\omega} \times \left(\left(\mathbf{M}_a + (m + \frac{1}{3}\rho_t r)\mathbf{I}_3\right)\mathbf{V}_a + \boldsymbol{\Gamma}^T\boldsymbol{\omega}\right)$$
$$= \mathbf{L}_{BC}\mathbf{G}_t + \mathbf{H} + \mathbf{T}_B \tag{5.55}$$

$$\dot{\boldsymbol{\Theta}} = \mathbf{R}^{-1}\boldsymbol{\omega} \tag{5.56}$$

$$(\mathbf{J} + \mathbf{J}_a)\dot{\boldsymbol{\omega}} + \boldsymbol{\Gamma}\dot{\mathbf{V}}_a + \boldsymbol{\omega} \times \left((\mathbf{J} + \mathbf{J}_a)\boldsymbol{\omega} + \boldsymbol{\Gamma}\mathbf{V}_a\right) + \mathbf{V}_a \times \left(\left(\mathbf{M}_a + (m + \frac{1}{3}\rho_t r)\mathbf{I}_3\right)\mathbf{V}_a + \boldsymbol{\Gamma}^T\boldsymbol{\omega}\right)$$

$$= \mathbf{u}_B' + (\mathbf{R}^{-1})^T(\mathbf{G}_r + \mathbf{G}_v) \tag{5.57}$$

First consider the kite apparent kinetic energy defined in the following equation

$$T_a = \frac{1}{2}\begin{pmatrix} \mathbf{V}_a^T & \boldsymbol{\omega}^T \end{pmatrix}\begin{pmatrix} \mathbf{M}_a + (m + \frac{1}{3}\rho_t r)\mathbf{I}_3 & \boldsymbol{\Gamma}^T \\ \boldsymbol{\Gamma} & (\mathbf{J} + \mathbf{J}_a) \end{pmatrix}\begin{pmatrix} \mathbf{V}_a \\ \boldsymbol{\omega} \end{pmatrix} \tag{5.58}$$

Taking the time derivative of T_a along the system trajectory (5.55) and (5.57) yields

$$\dot{T}_a = \begin{pmatrix} \mathbf{V}_a^T & \boldsymbol{\omega}^T \end{pmatrix}\begin{pmatrix} \mathbf{M}_a + (m + \frac{1}{3}\rho_t r)\mathbf{I}_3 & \boldsymbol{\Gamma}^T \\ \boldsymbol{\Gamma} & (\mathbf{J} + \mathbf{J}_a) \end{pmatrix}\begin{pmatrix} \dot{\mathbf{V}}_a \\ \dot{\boldsymbol{\omega}} \end{pmatrix}$$

$$= \begin{pmatrix} \mathbf{V}_a^T & \boldsymbol{\omega}^T \end{pmatrix}\begin{pmatrix} \mathbf{Q}_t - \boldsymbol{\omega} \times \left(\left(\mathbf{M}_a + (m + \frac{1}{3}\rho_t r)\mathbf{I}_3\right)\mathbf{V}_a + \boldsymbol{\Gamma}^T\boldsymbol{\omega}\right) \\ \mathbf{Q}_r - \mathbf{V}_a \times \left(\left(\mathbf{M}_a + (m + \frac{1}{3}\rho_t r)\mathbf{I}_3\right)\mathbf{V}_a + \boldsymbol{\Gamma}^T\boldsymbol{\omega}\right) - \boldsymbol{\omega} \times \left((\mathbf{J} + \mathbf{J}_a)\boldsymbol{\omega} + \boldsymbol{\Gamma}\mathbf{V}_a\right) \end{pmatrix}$$

where the generalized force $\mathbf{Q}_t$ and $\mathbf{Q}_r$ are given by

$$\mathbf{Q}_t = \mathbf{L}_{BC}\mathbf{G}_t + \mathbf{H} + \mathbf{T}_B \tag{5.59}$$

$$\mathbf{Q}_r = \mathbf{u}_B' + (\mathbf{R}^{-1})^T(\mathbf{G}_r + \mathbf{G}_v) \tag{5.60}$$

Using the properties of the vector triple product, the following equations hold

$$\boldsymbol{\omega}^T\left(\boldsymbol{\omega} \times \left((\mathbf{J} + \mathbf{J}_a)\boldsymbol{\omega} + \boldsymbol{\Gamma}\mathbf{V}_a\right)\right) = \mathbf{0} \tag{5.61}$$

$$\mathbf{V}_a^T\left(\boldsymbol{\omega} \times \left(\left(\mathbf{M}_a + (m + \frac{1}{3}\rho_t r)\mathbf{I}_3\right)\mathbf{V}_a + \boldsymbol{\Gamma}^T\boldsymbol{\omega}\right)\right)$$

$$= -\boldsymbol{\omega}^T\left(\mathbf{V}_a \times \left(\left(\mathbf{M}_a + (m + \frac{1}{3}\rho_t r)\mathbf{I}_3\right)\mathbf{V}_a + \boldsymbol{\Gamma}^T\boldsymbol{\omega}\right)\right) \tag{5.62}$$

Therefore, the time derivative of T_a can be further simplified as follows

$$\dot{T}_a = \mathbf{V}_a^T\mathbf{Q}_t + \boldsymbol{\omega}^T\mathbf{Q}_r \tag{5.63}$$

Moreover, consider the potential energies of the undersea kite energy system, which consists of

two parts, the gravitational and buoyancy potential energies and velocity potential energies

$$U = -\mathbf{G}^T\mathbf{r}_C + \mathbf{B}^T(\mathbf{r}_C + \mathbf{L}_{CB}\mathbf{d}) \tag{5.64}$$

$$U_v = -\frac{1}{2}\mathbf{W}_B^T\mathbf{M}_a\mathbf{W}_B \tag{5.65}$$

For the constant current condition, both U and U_v are bounded by constant value, i.e.

$$|U| \leq (\|\mathbf{G}\| + \|\mathbf{B}\|)r_{max} + \|\mathbf{B}\|\|\mathbf{d}\| \tag{5.66}$$

$$|U_v| \leq \frac{1}{2}\lambda_m\|\mathbf{W}\|^2 \tag{5.67}$$

Under the assumption 4, there exist a minimum nonzero kite apparent speed, i.e. $\|\mathbf{V}_a\| \geq V_{min}$, there must exist a constant C_U such that

$$|U| + |U_v| \leq C_U\|\mathbf{V}_a\|^2 \tag{5.68}$$

Taking the time derivative of the potential energies gives that

$$\dot{U} + \dot{U}_v = \mathbf{V}_C^T\frac{\partial U}{\partial\mathbf{r}_C} + \dot{\mathbf{\Theta}}^T\frac{\partial U}{\partial\mathbf{\Theta}} + \dot{\mathbf{\Theta}}^T\frac{\partial U_v}{\partial\mathbf{\Theta}} \tag{5.69}$$

Recall the definition of $\mathbf{G}_t$, $\mathbf{G}_r$ and $\mathbf{G}_v$,

$$\mathbf{G}_t = -\frac{\partial U}{\partial\mathbf{r}_C}, \quad \mathbf{G}_r = -\frac{\partial U}{\partial\mathbf{\Theta}}, \quad \mathbf{G}_v = -\frac{\partial U_v}{\partial\mathbf{\Theta}}$$

Hence the derivative of U_T can be simplified as follows

$$\dot{U} + \dot{U}_v = -\mathbf{V}_C^T\mathbf{G}_t - \dot{\mathbf{\Theta}}^T(\mathbf{G}_r + \mathbf{G}_v) \tag{5.70}$$

Further define the the kite artificial rotational potential energy as

$$U_r = \frac{1}{2}(\mathbf{\Theta} - \mathbf{\Theta}_d)^T\mathbf{K}_\Theta(\mathbf{\Theta} - \mathbf{\Theta}_d) \tag{5.71}$$

The time derivative of U_r, if the desired kite attitudes $\mathbf{\Theta}_d$ is constant, is given by

$$\dot{U}_r = \dot{\mathbf{\Theta}}^T \mathbf{K}_\Theta (\mathbf{\Theta} - \mathbf{\Theta}_d) \tag{5.72}$$

Rewrite the kinematic relation of the kite rotation using attitude error $\mathbf{\Theta}_e = \mathbf{\Theta} - \mathbf{\Theta}_d$, the undersea kite system dynamics become

$$\left(\mathbf{M}_a + (m + \frac{1}{3}\rho_t r)\mathbf{I}_3\right)\dot{\mathbf{V}}_a + \mathbf{\Gamma}^T \dot{\boldsymbol{\omega}} + \boldsymbol{\omega} \times \left(\left(\mathbf{M}_a + (m + \frac{1}{3}\rho_t r)\mathbf{I}_3\right)\mathbf{V}_a + \mathbf{\Gamma}^T \boldsymbol{\omega}\right)$$
$$= \mathbf{L}_{BC}\mathbf{G}_t + \mathbf{H} + \mathbf{T}_B \tag{5.73}$$

$$\dot{\mathbf{\Theta}}_e = \mathbf{R}^{-1}\boldsymbol{\omega} \tag{5.74}$$

$$(\mathbf{J} + \mathbf{J}_a)\dot{\boldsymbol{\omega}} + \mathbf{\Gamma}\dot{\mathbf{V}}_a + \boldsymbol{\omega} \times \left((\mathbf{J} + \mathbf{J}_a)\boldsymbol{\omega} + \mathbf{\Gamma}\mathbf{V}_a\right) + \mathbf{V}_a \times \left(\left(\mathbf{M}_a + (m + \frac{1}{3}\rho_t r)\mathbf{I}_3\right)\mathbf{V}_a + \mathbf{\Gamma}^T \boldsymbol{\omega}\right)$$
$$= \mathbf{u}'_B + (\mathbf{R}^{-1})^T(\mathbf{G}_r + \mathbf{G}_v) \tag{5.75}$$

Choose the Lyapunov function candidate as follows

$$E_a = T_a + U + U_v + U_r + |U| + |U_v| \tag{5.76}$$

Notice that both T_a and U_r take positive definite quadratic form,

$$(\sigma_a)_{min}(\|\mathbf{V}_a\|^2 + \|\boldsymbol{\omega}\|^2) \leq T_a \leq (\sigma_a)_{max}(\|\mathbf{V}_a\|^2 + \|\boldsymbol{\omega}\|^2) \tag{5.77}$$

$$(\sigma_\Theta)_{min}\|\mathbf{\Theta}_e\|^2 \leq U \leq (\sigma_\Theta)_{max}\|\mathbf{\Theta}_e\|^2 \tag{5.78}$$

Therefore, the Lyapunov function (5.76) is bounded by two class $\mathcal{K}$ functions

$$(\sigma_a)_{min}(\|\mathbf{V}_a\|^2 + \|\boldsymbol{\omega}\|^2) + (\sigma_\Theta)_{min}\|\mathbf{\Theta}_e\|^2 \leq E_a$$
$$\leq (\sigma_a)_{max}(\|\mathbf{V}_a\|^2 + \|\boldsymbol{\omega}\|^2) + (\sigma_\Theta)_{max}\|\mathbf{\Theta}_e\|^2 + C_U\|\mathbf{V}_a\|^2 \tag{5.79}$$

Take the time derivative of the Lyapunov function E_a along the system trajectories (5.73)-(5.75) gives that

$$\dot{E}_a = \dot{T}_a + \dot{U} + \dot{U}_v + \dot{U}_r$$

$$= \mathbf{V}_a^T \mathbf{Q}_t + \boldsymbol{\omega}^T \mathbf{Q}_r + \mathbf{V}_C^T \frac{\partial U}{\partial \mathbf{r}_C} + \dot{\boldsymbol{\Theta}}^T \frac{\partial U}{\partial \boldsymbol{\Theta}} + \dot{\boldsymbol{\Theta}}^T \frac{\partial U_v}{\partial \boldsymbol{\Theta}} + \dot{\boldsymbol{\Theta}}^T \mathbf{K}_\Theta (\boldsymbol{\Theta} - \boldsymbol{\Theta}_d)$$

$$= \mathbf{V}_a^T \mathbf{Q}_t + \boldsymbol{\omega}^T \mathbf{Q}_r - \mathbf{V}_C^T \mathbf{G}_t - \dot{\boldsymbol{\Theta}}^T \mathbf{G}_r - \dot{\boldsymbol{\Theta}}^T \mathbf{G}_v + \dot{\boldsymbol{\Theta}}^T \mathbf{K}_\Theta (\boldsymbol{\Theta} - \boldsymbol{\Theta}_d) \tag{5.80}$$

By substituting equations (5.56), (5.59) and (5.60) into equation (5.80), the time derivative of E_a along the system trajectories (5.73)-(5.75) becomes

$$\dot{E}_a = \mathbf{V}_a^T (\mathbf{H} + \mathbf{T}_B) + \boldsymbol{\omega}^T \mathbf{u}_B' + \dot{\boldsymbol{\Theta}}^T \mathbf{K}_\Theta (\boldsymbol{\Theta} - \boldsymbol{\Theta}_d) \tag{5.81}$$

Choose the rotational control signal such that the last two term in equation (5.81) is negative definite

$$\boldsymbol{\omega}^T \mathbf{u}_B' + \dot{\boldsymbol{\Theta}}^T \mathbf{K}_\Theta (\boldsymbol{\Theta} - \boldsymbol{\Theta}_d) = -\dot{\boldsymbol{\Theta}}^T \mathbf{K}_\Omega \dot{\boldsymbol{\Theta}} \tag{5.82}$$

Solving equation (5.82) gives the augmented rotational control signal as

$$\mathbf{u}_B' = \mathbf{R}^{-1} \big(- \mathbf{K}_\Omega \dot{\boldsymbol{\Theta}} - \mathbf{K}_\Theta (\boldsymbol{\Theta} - \boldsymbol{\Theta}_d) \big) \tag{5.83}$$

Therefore, the kite rotational control signal $\mathbf{u}_B$ is given by

$$\mathbf{u}_B = \mathbf{R}^{-1} \big(- \mathbf{K}_\Omega \dot{\boldsymbol{\Theta}} - \mathbf{K}_\Theta (\boldsymbol{\Theta} - \boldsymbol{\Theta}_d) \big) + \mathbf{W}_B \times (\mathbf{M}_a \mathbf{V}_a + \boldsymbol{\Gamma}^T \boldsymbol{\omega}) \tag{5.84}$$

Under the control signal (5.84), the time derivative of E_a is bounded by the following inequality

$$\dot{E}_a \leq \mathbf{V}_a^T (\mathbf{H} + \mathbf{T}_B) \tag{5.85}$$

Furthermore, since the tether length is constant, the total force acting on the kite is balanced in the tether direction, i.e.

$$\mathbf{V}_B^T \mathbf{T}_B = 0 \tag{5.86}$$

83

Therefore, the bound of the time derivative of E_a can be further simplified

$$\dot{E}_a \leq \mathbf{V}_a^T\mathbf{H} + (\mathbf{V}_B - \mathbf{W}_B)^T\mathbf{T}_B = \mathbf{V}_a^T\mathbf{H} - \mathbf{W}_B^T\mathbf{T}_B \tag{5.87}$$

If the tether tension satisfies the following assumption,

Assumption 6. Assume the tether tension is bounded by a quadratic function of the kite apparent velocity

$$\|\mathbf{T}_B\| \leq K_T\|\mathbf{V}_a\|^2 \tag{5.88}$$

Then the expansion of equation (5.87) becomes

$$\begin{aligned}\dot{E}_a \leq & \mathbf{V}_a^T\mathbf{H} - \mathbf{W}_B^T\mathbf{T}_B \\ = & -\frac{1}{2}\rho_t S\|\mathbf{V}_a\|^3 C_a + K_T\|\mathbf{V}_a\|^2\end{aligned} \tag{5.89}$$

Therefore, the undersea kite energy system dynamics (5.73)-(5.75) are ultimately bounded, i.e.

$$\dot{E}_a < 0 \quad \text{if} \quad \|\mathbf{V}_a\| > \frac{2K_T}{\rho_f SC_{min}} \tag{5.90}$$

where C_{min} is the positive minimum of the coefficient C_a. It is clear that the lower bound of the parameter C_a has a significant influence of the performance of the kite apparent velocity. It is also very important to notice that under the steady aerodynamics condition, the parameter C_a is function kite apparent velocity α and β as shown in equation (**??**). Therefore, to satisfies the minimum value assumption of C_a, the control strategies that controlling the α and β needs to be developed.

For a thin finite wing undersea kite, matrices $\mathbf{M}_a$ and $\mathbf{J}_a$ take the diagonal form

$$\mathbf{M}_a = \begin{pmatrix} 0 & 0 & 0 \\ 0 & 0 & 0 \\ 0 & 0 & \lambda_1 \end{pmatrix} ; \quad \mathbf{J}_a = \begin{pmatrix} \lambda_2 & 0 & 0 \\ 0 & \lambda_3 & 0 \\ 0 & 0 & 0 \end{pmatrix} ; \quad \mathbf{\Gamma} = \mathbf{0}_{3\times3}$$

Table 5.4: Input and Control Parameters.

parameter	value	parameter	value	parameter	value
m	10000kg	J_x	$2.3\times10^5\text{kgm}^2$	(q_2^-, q_2^+)	$(-20°, +20°)$
J_y	$9.4\times10^3\text{kgm}^2$	J_z	$2.4\times10^5\text{kgm}^2$	(ϕ_d^-, ϕ_d^+)	$(-70°, +70°)$
S	35m^2	AR	2	(θ_d^-, θ_d^+)	$5°$
S_T	7m^2	ρ_t	0.64kg/m	(ψ_d^-, ψ_d^+)	$(-40°, +40°)$
$\mathbf{W}$	[2,0,0]m/s	ρ_w	1025kg/m^3	$\mathbf{K}_\Theta$	$1.79\times10^5\mathbf{I}$
c_l		κ_1	0.075	$\mathbf{K}_\Omega$	$1.79\times10^5\mathbf{I}$
κ_2	-0.005	κ_3	0.01		
N		d	-0.1m		

where λ_1, λ_2 and λ_3 are added mass parameters with kite chord length is c and kite area S, then the added mass coefficients are defined as,

$$\kappa_1 = \frac{\lambda_1}{\rho_w c S}; \quad \kappa_2 = \frac{\lambda_2}{\rho_w c^3 S}; \quad \kappa_3 = \frac{\lambda_3}{\rho_w c^3 S}$$

where ρ_w is the volume density of the surrounding fluid, and the coefficients depend on planform. The key undersea kite system input parameters for the baseline simulation are given in Table 5.4. The aspect ratio represent kite wing span compared to chord length, $AR = \frac{b^2}{S} = \frac{S}{c^2}$. To form a figure eight kite trajectory, we propose a switching law for rotational control. The desired Euler angle $\boldsymbol{\Theta}_d$ is switched when the cross current positions of the kite CG reaches (q_1^+, q_1^-) which are set cross current angles:

$$\boldsymbol{\Theta}_d = \begin{cases} (\phi_d^+ \ \theta_d^+ \ \psi_d^+) & q_2 > q_2^+ \\ (\phi_d^- \ \theta_d^- \ \psi_d^-) & q_2 < q_2^- \end{cases} \tag{5.91}$$

The control design parameters are also listed in Table 5.4. The simulation result of the Lyapunov based control signal to the undersea kite energy systems are shown in the following figures. To test the robustness of the control system, simulations are run under two different current speed with three kite mass and area. In all cases, the Lyapunov based control generates figure-eight trajectory of the kite motion. The corresponding power output is listed in Table 5.5.
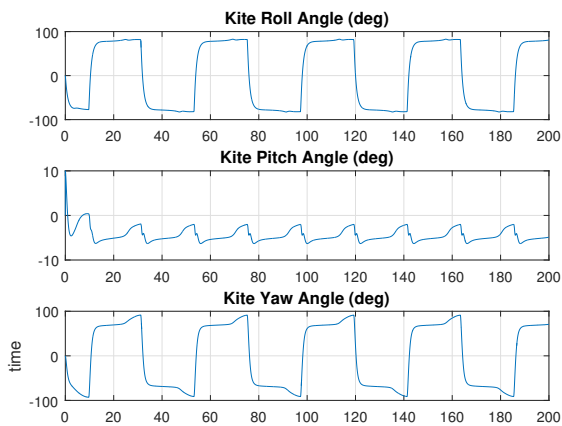
Table 5.5: Power Output

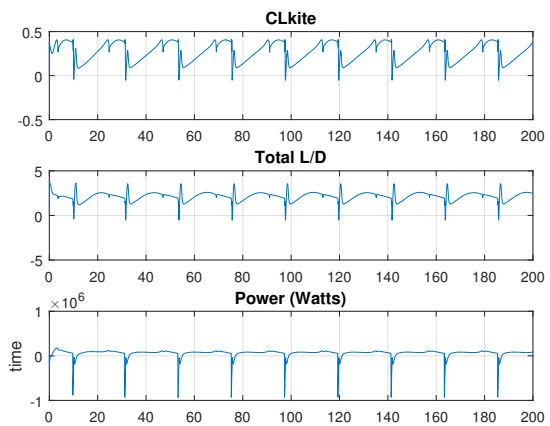| Current Speed(m/s)	Area(m^2)	mass(ton)	Power(kW)
	30	3.4	31.98
2	35	4.0	29.79
	40	4.6	28.27
	30	3.4	58.06
2.5	35	4.0	55.10
	40	4.6	43.42
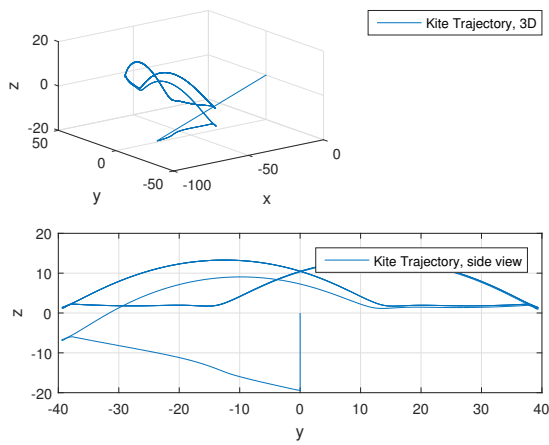
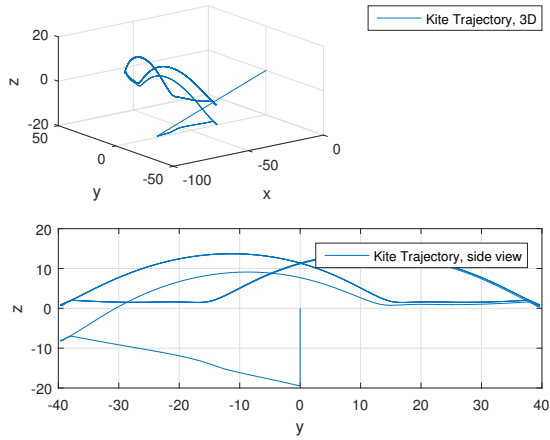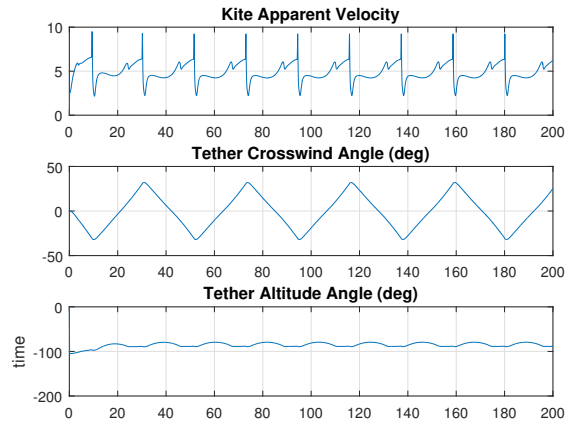*(a) 3D Translational Trajectory*
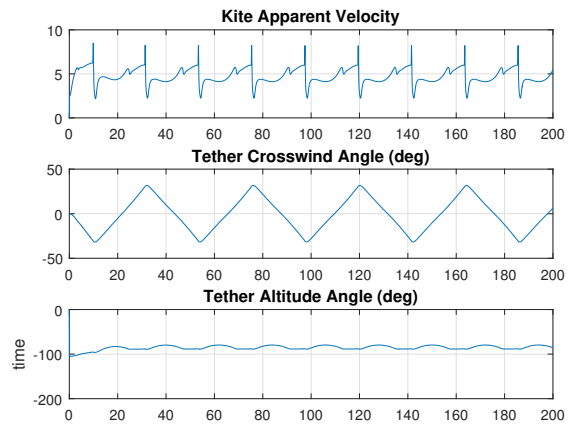
(b) Spherical Trajectory

(c) Kite Rotational Trajectory
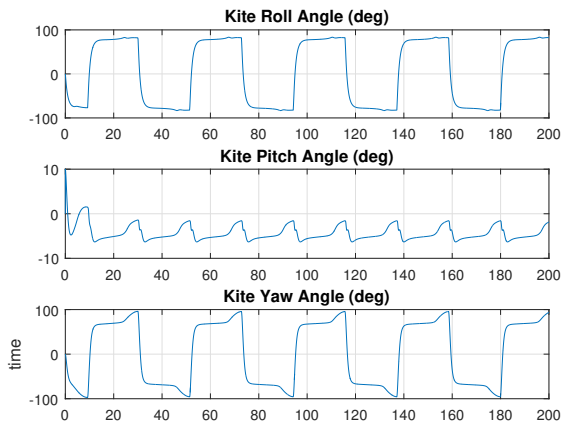
(d) Hydrodynamic Coefficient and Power Production

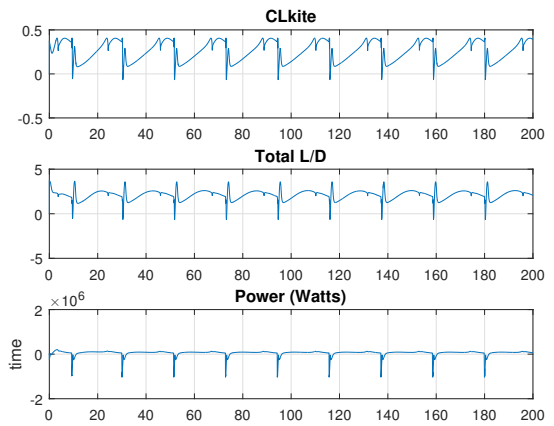*Figure 5.8: Current Speed = 2.5m/s, Mass = 3.4ton, Area = 30m^2*

(a) Kite Translational Trajectory
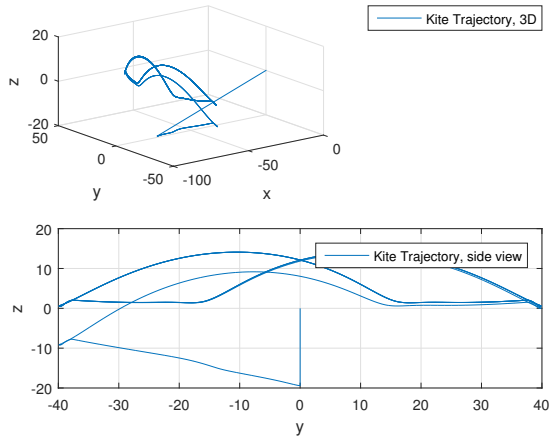

(b) Kite Euler Angles Trajectory
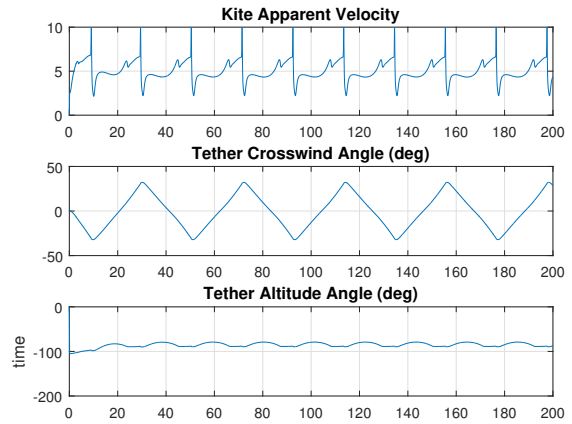

(c) Kite apparent Attitude

(d) Kite Angular Velocity

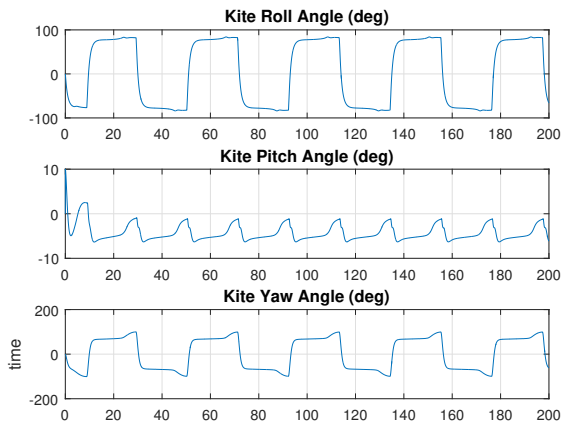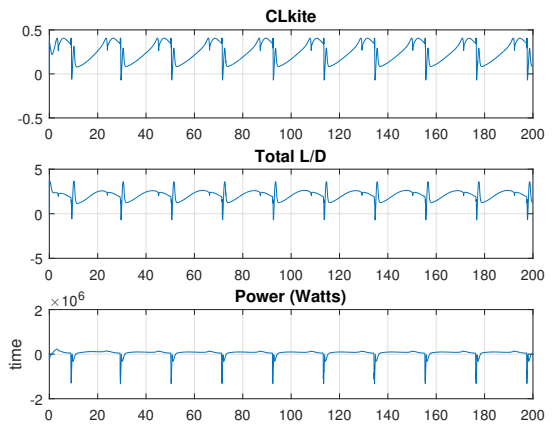*Figure 5.9: Current Speed = 2.5m/s, Mass = 4.0ton, Area = 35m^2*

(a) Kite Translational Trajectory

(b) Kite Euler Angles Trajectory

(c) Kite apparent Attitude

(d) Kite Angular Velocity

Figure 5.10: Current Speed = 2.5m/s, Mass = 4.6ton, Area = 40m^2

(a) 3D Translational Trajectory

(b) Spherical Trajectory

(c) Kite Rotational Trajectory
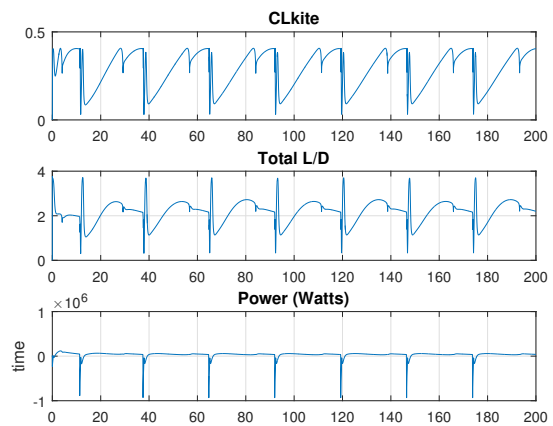
(d) Hydrodynamic Coefficient and Power Production

Figure 5.11: Current Speed = 2m/s, Mass = 3.4ton, Area = 30m^2
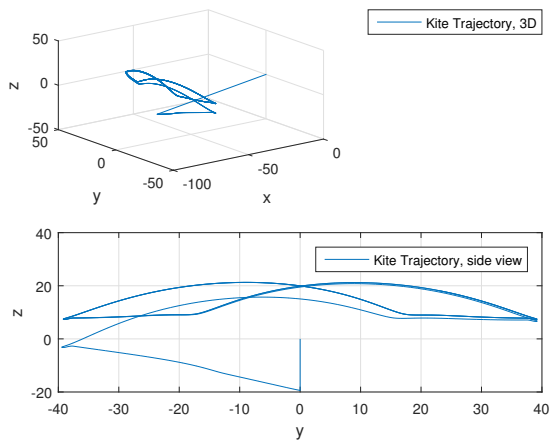
(a) Kite Translational Trajectory
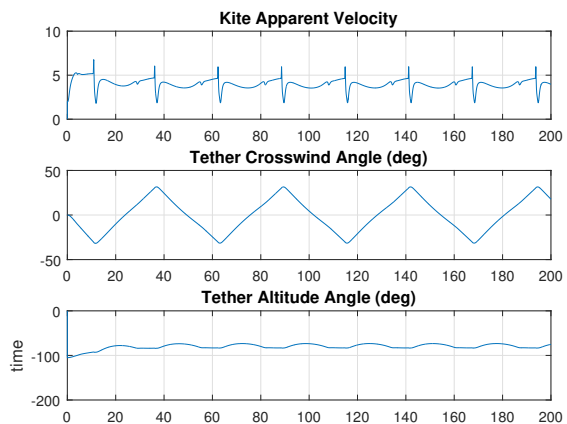
(b) Kite Euler Angles Trajectory

(c) Kite apparent Attitude

(d) Kite Angular Velocity

Figure 5.12: Current Speed = 2m/s, Mass = 4.0ton, Area = $35m^2$
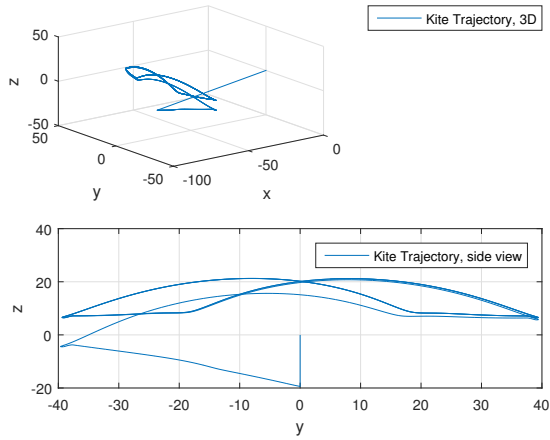
90

(a) Kite Translational Trajectory

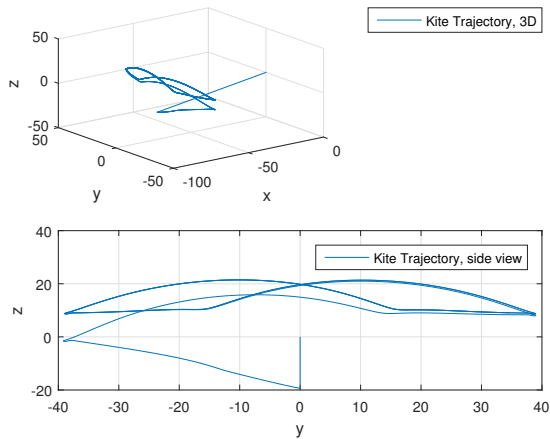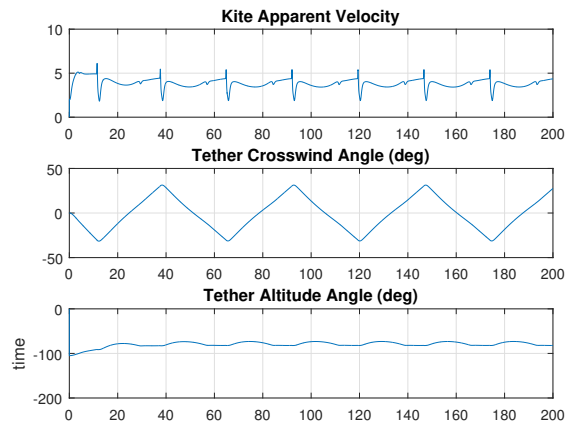*(b) Kite Euler Angles Trajectory*

(c) Kite apparent Attitude

(d) Kite Angular Velocity

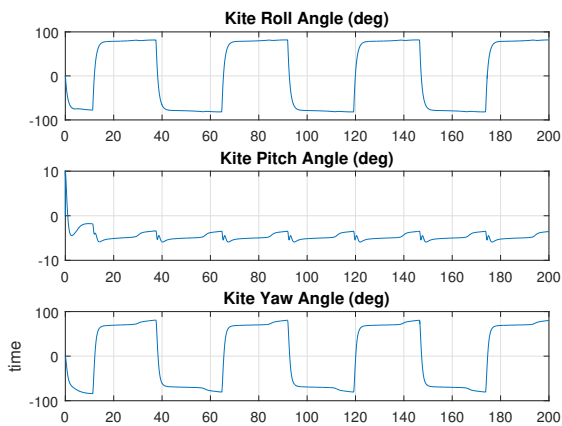*Figure 5.13: Current Speed = 2m/s, Mass = 4.6ton, Area = 40m^2*

Chapter 6

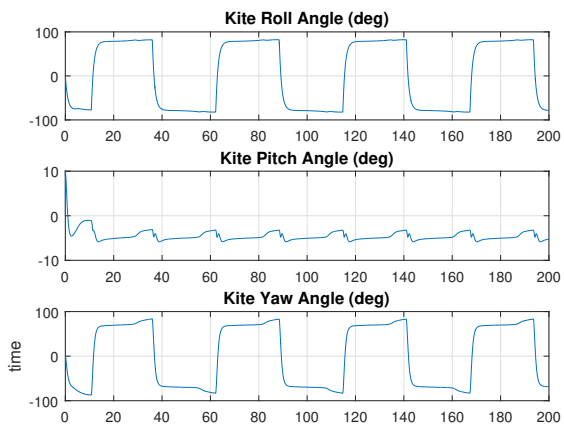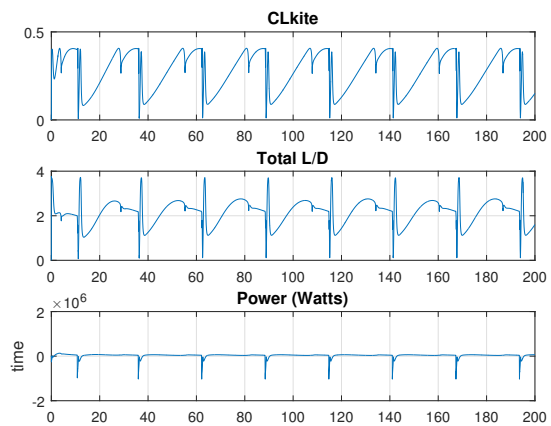# Dynamic Apparent Attitude Tracking

In the previous chapter, the influence of the tether tension on kite translational motion is studied. Although the boundedness of the kite apparent velocity can be guaranteed from the Lyapunov analysis, no conclusion can be drawn on the detailed information of the kite apparent velocity. For a FlyGen airborne kite energy system, the power production by the on board turbine can be formulated as follows

$$P = \frac{1}{2}\rho_{air}C_p S_t(\|\mathbf{V}_a\| \cos\alpha \cos\beta)^3 \tag{6.1}$$

where C_p is the power harvesting coefficient of the on board turbine. On the one hand, for a constant apparent wind speed, the maximum power production is achieve by $\alpha = \beta = 0$. On the other hand, to maintain the power generation in flight, the angle of attack α needs to be kept large enough to provide lift force. To achieve the balance between the sustainability and optimality of the kite power generation, control schemes that regulate the kite apparent attitudes, α and β need to be developed.

6.1   System Dynamics Transformation

If the wind velocity is constant, the kite apparent velocity obey the same dynamics as the kite absolute velocity as shown in Lemma 7,

$$(m + \frac{1}{3}\rho_t r)(\dot{\mathbf{V}}_B + \boldsymbol{\omega} \times \mathbf{V}_B) = (m + \frac{1}{3}\rho_t r)(\dot{\mathbf{V}}_a + \boldsymbol{\omega} \times \mathbf{V}_a)$$

The airborne kite system dynamics in frame **B** is given by

$$(m + \frac{1}{3}\rho_t r)(\dot{\mathbf{V}}_B + \boldsymbol{\omega} \times \mathbf{V}_B) = \mathbf{H}_B + \mathbf{L}_{BC}\mathbf{G}_t + \mathbf{T}_B$$

Therefore, the kite apparent translational dynamics are given by

$$(m + \frac{1}{3}\rho_t r)(\dot{\mathbf{V}}_a + \boldsymbol{\omega} \times \mathbf{V}_a) = \mathbf{H}_B + \mathbf{L}_{BC}\mathbf{G}_t + \mathbf{T}_B \tag{6.2}$$

Moreover, the kite apparent speed $\|\mathbf{V}_a\|$ and apparent attitudes α, β are the spherical coordinates of the kite apparent velocity.

$$\mathbf{V}_a = V_a \begin{pmatrix} \cos\alpha\cos\beta & \sin\beta & \sin\alpha\cos\beta \end{pmatrix}^T \tag{6.3}$$

Taking the time derivative of equation (6.3) gives the kite apparent acceleration transformation

$$\dot{\mathbf{V}}_a = \boldsymbol{\Lambda}_B \dot{\boldsymbol{\xi}}_B \quad \boldsymbol{\Lambda}_B = \begin{pmatrix} \cos\alpha\cos\beta & -V_a\sin\alpha\cos\beta & -V_a\cos\alpha\sin\beta \\ \sin\beta & 0 & V_a\cos\beta \\ \sin\alpha\cos\beta & V_a\cos\alpha\cos\beta & -V_a\sin\alpha\sin\beta \end{pmatrix} \tag{6.4}$$

where $\boldsymbol{\xi}_B = \begin{pmatrix} V_a & \alpha & \beta \end{pmatrix}$. Substituting the velocity and acceleration transformations (6.3) and (6.4) into kite apparent dynamics (6.2) yields that

$$(m + \frac{1}{3}\rho_t r)(\boldsymbol{\Lambda}_B \dot{\boldsymbol{\xi}}_B - [\mathbf{V}_a]_\times \boldsymbol{\omega}) = \mathbf{H}_B + \mathbf{L}_{BC}\mathbf{G}_t + \mathbf{T}_B \tag{6.5}$$

where $[\mathbf{V}_a]_\times$ is the cross product matrix,

$$[\mathbf{V}_a]_\times = \begin{pmatrix} 0 & -w_a & v_a \\ w_a & 0 & -u_a \\ -v_a & u_a & 0 \end{pmatrix} = V_a \begin{pmatrix} 0 & -\sin\alpha\cos\beta & \sin\beta \\ \sin\alpha\cos\beta & 0 & -\cos\alpha\cos\beta \\ -\sin\beta & \cos\alpha\cos\beta & 0 \end{pmatrix} \quad (6.6)$$

Taking the inversion of the acceleration transformation matrix is

$$\mathbf{\Lambda}_B^{-1} = \begin{pmatrix} \cos\alpha\cos\beta & \sin\beta & \sin\alpha\cos\beta \\ \frac{\sin\alpha}{V_a\cos\beta} & 0 & \frac{\cos\alpha}{V_a\cos\beta} \\ \frac{\cos\alpha\sin\beta}{V_a} & \frac{\cos\beta}{V_a} & -\frac{\sin\alpha\sin\beta}{V_a} \end{pmatrix} \quad (6.7)$$

Therefore, the kite system dynamics in $\boldsymbol{\xi}_B$ is given by

$$\dot{\boldsymbol{\xi}}_B = \mathbf{\Lambda}_B^{-1}[\mathbf{V}_a]_\times\boldsymbol{\omega} + \frac{1}{m + \frac{1}{3}\rho_t r}\mathbf{\Lambda}_B^{-1}\left(\mathbf{H}_B + \mathbf{L}_{BC}\mathbf{G}_t + \mathbf{T}_B\right) \quad (6.8)$$

The equation (6.8) can be further simplified by noticing that the gravitational force

$$\mathbf{G}_t = (m + \frac{1}{2}\rho_t r)\mathbf{g} \quad (6.9)$$

where $\mathbf{g} = \begin{pmatrix} 0 & 0 & g \end{pmatrix}$. Therefore, equation (6.8) can be further simplified as follows

$$\dot{\boldsymbol{\xi}}_B = \mathbf{D}_V\boldsymbol{\omega} + \frac{1}{m + \frac{1}{3}\rho_t r}\mathbf{D}_H\mathbf{C}_B + \frac{m + \frac{1}{2}\rho_t r}{m + \frac{1}{3}\rho_t r}\mathbf{\Lambda}_B^{-1}\mathbf{L}_{BC}\mathbf{g} + \frac{1}{m + \frac{1}{3}\rho_t r}\mathbf{\Lambda}_B^{-1}\mathbf{T}_B \quad (6.10)$$

If the kite mass is much greater than the tether mass, then equation (6.10) can be further simplified

$$\dot{\boldsymbol{\xi}}_B = \mathbf{D}_V\boldsymbol{\omega} + \frac{\frac{1}{2}\rho_{air}S}{m + \frac{1}{3}\rho_t r}V_a^2\mathbf{D}_H\mathbf{C}_B + \mathbf{\Lambda}_B^{-1}\mathbf{L}_{BC}\mathbf{g} + \frac{1}{m + \frac{1}{3}\rho_t r}\mathbf{\Lambda}_B^{-1}\mathbf{T}_B \quad (6.11)$$

where the matrices $\mathbf{D}_V$ and $\mathbf{D}_H$ are given by

$$
\mathbf{D}_V = \begin{pmatrix} 0 & 0 & 0 \\ -c_\alpha \tan\beta & 1 & -s_\alpha \tan\beta \\ s_\alpha & 0 & -c_\alpha \end{pmatrix} \quad \mathbf{D}_H = \begin{pmatrix} 0 & -\sin\beta & -\cos\beta \\ -\frac{1}{V_a c_\beta} & 0 & 0 \\ 0 & \frac{\cos\beta}{V_a} & \frac{\sin\beta}{V_a} \end{pmatrix} \tag{6.12}
$$

Denote $\mathbf{D}_T = \mathbf{\Lambda}_B^{-1}\mathbf{L}_{BC}\mathbf{g} + \frac{1}{m+\frac{1}{3}\rho_t r}\mathbf{\Lambda}_B^{-1}\mathbf{T}_B$, the complete airborne kite energy system dynamics are given by

$$
\dot{\boldsymbol{\xi}}_B = \mathbf{D}_V\boldsymbol{\omega} + \frac{\frac{1}{2}\rho_{air}S}{m + \frac{1}{3}\rho_t r}V_a^2\mathbf{D}_H\mathbf{C}_B + \mathbf{D}_T \tag{6.13}
$$

$$
\dot{\boldsymbol{\omega}} = \mathbf{J}^{-1}(\mathbf{u}_B - \boldsymbol{\omega} \times \mathbf{J}\boldsymbol{\omega}) \tag{6.14}
$$

It is important to notice that the resulting system dynamics (6.13)-(6.14) is cascade. Therefore, the back stepping methods can be used for control design.

6.2 Back-stepping Control Design

To design the back-stepping controller, the control signal for translational dynamics (6.13) needs to be designed first. It is important to notice that there is no control signal acting on V_a as shown in definition (6.12), where the first row of $\mathbf{D}_V$ is zero. Hence, choose the following Lyapunov function candidate

$$
V_\xi = \frac{1}{2}\alpha_e^2 \cos^2\beta + \frac{1}{2}\beta_e^2 \tag{6.15}
$$

where the error apparent attitudes are defined as $\alpha_e = \alpha - \alpha_d, \beta_d = \beta - \beta_d$ for some constant desired apparent attitudes α_d and β_d. The gradient of the Lyapunov function is

$$
\nabla V_\xi = \begin{pmatrix} 0 & \alpha_e \cos^2\beta & -\alpha_e^2 \sin\beta \cos\beta + \beta_e \end{pmatrix} \tag{6.16}
$$

The time derivative of the Lyapunov function (6.15) then becomes

$$
\dot{V}_\xi = \boldsymbol{\nabla} V_\xi^T \Big(\mathbf{D}_V \boldsymbol{\omega} + \frac{\frac{1}{2}\rho_{air}S}{m + \frac{1}{3}\rho_t r} V_a^2 \mathbf{D}_H \mathbf{C}_B + \mathbf{D}_T \Big) \tag{6.17}
$$

By substitution, the time derivative of the V_ξ can be rewritten as follows

$$
\dot{V}_\xi = \boldsymbol{\delta}_e^T \Big(\boldsymbol{\Xi}\boldsymbol{\omega} + \frac{\frac{1}{2}\rho_{air}S}{m + \frac{1}{3}\rho_t r} V_a^2 \boldsymbol{\Xi}_H \mathbf{C}_B + \frac{1}{V_a} \boldsymbol{\Xi}_T (\mathbf{L}_{BC}\mathbf{g} + \frac{1}{m + \frac{1}{3}\rho_t r} \mathbf{T}_B) \Big) \tag{6.18}
$$

where $\boldsymbol{\delta}_e = \begin{pmatrix} \beta_e & \alpha_e \cos^2\beta & \alpha_e \cos\beta\sin\beta \end{pmatrix}^T$ and matrices in equation (6.18) are defined as follows

$$
\boldsymbol{\Xi} = \begin{pmatrix} \sin\alpha & 0 & -\cos\alpha \\ 0 & 1 & 0 \\ -\cos\alpha - \alpha_e \sin\alpha & 0 & \alpha_e \cos\alpha - \sin\alpha \end{pmatrix} \tag{6.19}
$$

$$
\boldsymbol{\Xi}_H = \begin{pmatrix} 0 & \cos\beta & \sin\beta \\ -\cos\beta & -\alpha_e \sin\beta & 0 \\ -\sin\beta & 0 & -\alpha_e \sin\beta \end{pmatrix} \tag{6.20}
$$

$$
\boldsymbol{\Xi}_T = \begin{pmatrix} -\cos\alpha\sin\beta & \cos\beta & -\sin\alpha\sin\beta \\ -\sin\alpha\cos\beta & -\alpha_e \sin\beta & \cos\alpha\cos\beta \\ (\alpha_e \cos\alpha - \sin\alpha)\sin\beta & 0 & (\cos\alpha + \alpha_e \sin\alpha)\sin\beta \end{pmatrix} \tag{6.21}
$$

The desired angular velocity can then be calculated by the following equality,

$$
-\boldsymbol{\zeta}_e = \boldsymbol{\Xi}\boldsymbol{\omega}_d + \frac{\frac{1}{2}\rho_{air}S}{m + \frac{1}{3}\rho_t r} V_a^2 \boldsymbol{\Xi}_H \mathbf{C}_B + \frac{1}{V_a} \boldsymbol{\Xi}_T (\mathbf{L}_{BC}\mathbf{g} + \frac{1}{m + \frac{1}{3}\rho_t r} \mathbf{T}_B) \tag{6.22}
$$

where $\boldsymbol{\zeta}_e = \begin{pmatrix} k_1\beta_e & k_2\alpha_e & 0 \end{pmatrix}^T$. The desired angular velocity $\boldsymbol{\omega}_d$ then becomes

$$
\boldsymbol{\omega}_d = -\boldsymbol{\Xi}^{-1} \Big(\boldsymbol{\zeta}_e + \frac{\frac{1}{2}\rho_{air}S}{m + \frac{1}{3}\rho_t r} V_a^2 \boldsymbol{\Xi}_H \mathbf{C}_B + \frac{1}{V_a} \boldsymbol{\Xi}_T (\mathbf{L}_{BC}\mathbf{g} + \frac{1}{m + \frac{1}{3}\rho_t r} \mathbf{T}_B) \Big) \tag{6.23}
$$

The resulting time derivative is

$$\dot{V}_\xi = - k_1\beta_e^2 - k_2\alpha_e^2 \cos^2\beta \leq -2\min(k_1, k_2)V_\xi \tag{6.24}$$

Using Barbalat's lemma the apparent attitudes converge to the desired value asymptotically. The rotational dynamics (6.14) can also be transformed into the error dynamics form.

$$\mathbf{J}\dot{\boldsymbol{\omega}}_e + \boldsymbol{\omega}_e \times \mathbf{J}\boldsymbol{\omega} = \mathbf{u}_e$$

where the angular velocity tracking error and error dynamics control signal are given by $\boldsymbol{\omega}_e = \boldsymbol{\omega} - \boldsymbol{\omega}_d$ and $\mathbf{u}_e = \mathbf{u}_B + \mathbf{J}\dot{\boldsymbol{\omega}}_d + \boldsymbol{\omega}_d \times \mathbf{J}\boldsymbol{\omega}$.

Substituting the desired angular velocity $\boldsymbol{\omega}_d$ into translational dynamics (6.13) and combining the error rotational dynamics gives that

$$\dot{\boldsymbol{\xi}}_B = \mathbf{D}_V\boldsymbol{\omega}_e + \mathbf{D}_V\boldsymbol{\omega}_d + \frac{\frac{1}{2}\rho_{air}S}{m + \frac{1}{3}\rho_t r}V_a^2\mathbf{D}_H\mathbf{C}_B + \mathbf{D}_T \tag{6.25}$$

$$\mathbf{J}\dot{\boldsymbol{\omega}}_e = \mathbf{u}_e - \boldsymbol{\omega}_e \times \mathbf{J}\boldsymbol{\omega} \tag{6.26}$$

Choose the Lyapunov function of the error dynamics (6.25) and (6.26) as follows

$$\tilde{V}_\xi = \frac{1}{2}\alpha_e^2\cos^2\beta + \frac{1}{2}\beta_e^2 + \frac{1}{2}\boldsymbol{\omega}_e^T\mathbf{J}\boldsymbol{\omega}_e \tag{6.27}$$

Taking the time derivative of equation (6.27) along system trajectories (6.25)-(6.26) gives that

$$\begin{aligned}
\dot{\tilde{V}}_\xi &= \boldsymbol{\delta}_e^T\boldsymbol{\Xi}\boldsymbol{\omega}_e - k_1\beta_e^2 - k_2\alpha_e^2\cos^2\beta + \boldsymbol{\omega}_e^T\mathbf{u}_e \\
&= \boldsymbol{\omega}_e^T(\mathbf{u}_e + \boldsymbol{\Xi}^T\boldsymbol{\delta}_e) - k_1\beta_e^2 - k_2\alpha_e^2\cos^2\beta
\end{aligned} \tag{6.28}$$

Choose the error rotational control signal as follows,

$$\mathbf{u}_e = -\boldsymbol{\Xi}^T\boldsymbol{\delta}_e - \mathbf{K}_e\boldsymbol{\omega}_e \tag{6.29}$$

The resulting time derivative of the Lyapunov function (6.28) then becomes

$$\dot{\tilde{V}}_\xi = -\boldsymbol{\omega}_e^T \mathbf{K}_e \boldsymbol{\omega}_e - k_1 \beta_e^2 - k_2 \alpha_e^2 \cos^2 \beta < 0 \tag{6.30}$$

Then the rotational control signal in body frame is then given by

$$\mathbf{u}_B = \mathbf{J}\dot{\boldsymbol{\omega}}_d + \boldsymbol{\omega}_d \times \mathbf{J}\boldsymbol{\omega} - \boldsymbol{\Xi}^T \boldsymbol{\delta}_e - \mathbf{K}_e \boldsymbol{\omega}_e \tag{6.31}$$

Although the control signal (6.31) guarantee the stability of the tracking error α_e and β_e, the achievable angular velocity of a kite is limited. In order to handle the saturation issue in the desired angular velocity, the following scaling is applied in the control system implementation,

$$\tilde{\boldsymbol{\omega}}_d = \omega_{sat} \frac{\boldsymbol{\omega}_d}{\|\boldsymbol{\omega}_d\|} \tag{6.32}$$

Moreover, the first order time derivative of the desired angular velocity is required in control signal (6.31), the high gain observer is applied to provide the real time signal differentiation.

$$\dot{\hat{\mathbf{x}}}_1 = \hat{\mathbf{x}}_2 + \frac{\sigma_1}{\epsilon}(\tilde{\boldsymbol{\omega}}_d - \hat{\mathbf{x}}_1)$$
$$\dot{\hat{\mathbf{x}}}_2 = \frac{\sigma_2}{\epsilon}(\tilde{\boldsymbol{\omega}}_d - \hat{\mathbf{x}}_1)$$

the σ_1, σ_2 are coefficients of the Huwitzs polynomial $s^2 + \sigma_1 s + \sigma_2$ and ϵ is a small positive number. The states $\hat{\mathbf{x}}_1, \hat{\mathbf{x}}_1$ are estimation of the desired angular velocity $\tilde{\boldsymbol{\omega}}_d$ and its first order derivative $\dot{\tilde{\boldsymbol{\omega}}}_d$, the estimation error converge to zero as ϵ goes to zero. Hence, the actual control signal that applied on the kite rotation is given by

$$\mathbf{u}_B = \mathbf{J}\dot{\hat{\tilde{\boldsymbol{\omega}}}}_d + \tilde{\boldsymbol{\omega}}_d \times \mathbf{J}\boldsymbol{\omega} - \boldsymbol{\Xi}^T \boldsymbol{\delta}_e - \mathbf{K}_e \tilde{\boldsymbol{\omega}}_e \tag{6.33}$$

where $\tilde{\boldsymbol{\omega}}_e = \boldsymbol{\omega} - \tilde{\boldsymbol{\omega}}_d$. In the baseline simulation, it is clear that the limitation on the kite desired angular velocity will results in nonzero residue errors in kite apparent attitudes. Hence, to achieve the desired apparent attitudes, a different control approach is required.

The kite system parameters simulated for the baseline condition is list in table 6.1, and the key

parameter	value	paramter	value	paramter	value
Kite Mass	70kg	Turbine Mass	35kg	$\mathbf{K}_\delta$	$20\mathbf{I}$
Kite Area	$15m^2$	Turbine Area	$3m^2$	ϵ	0.05
Aspect Ratio	3.27	J_x	$1715kg \cdot m^2$	$\mathbf{K}_e$	$10\mathbf{I}$
J_y	$160kg \cdot m^2$	J_z	$1875kg \cdot m^2$	$[\sigma_1, \sigma_2]$	$[8, 16]$
$\mathbf{W}_{ref}$	$[0, 0, -6]$	z_{ref}	10m	ω_{sat}	$0.05°/s$
α_d	$10°$	β_d	$5°$		

control parameters are also listed in table 6.1. The kite moment of inertial are label as J_x, J_y and J_z. The wind field is modeled using the exponential formular

$$\mathbf{W} = \mathbf{W}_{ref}\Big(\frac{z_E}{z_{ref}}\Big)^{\frac{1}{7}}$$
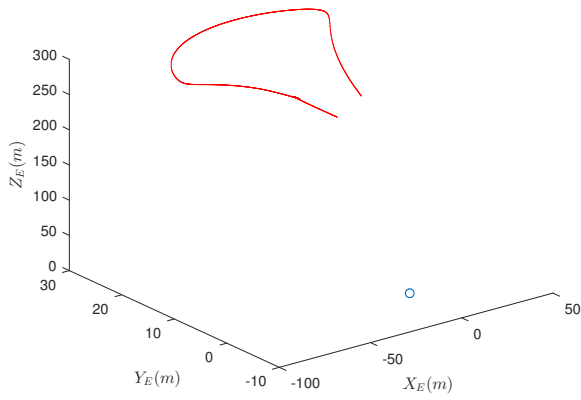
99

(a) Kite Translational Trajectory
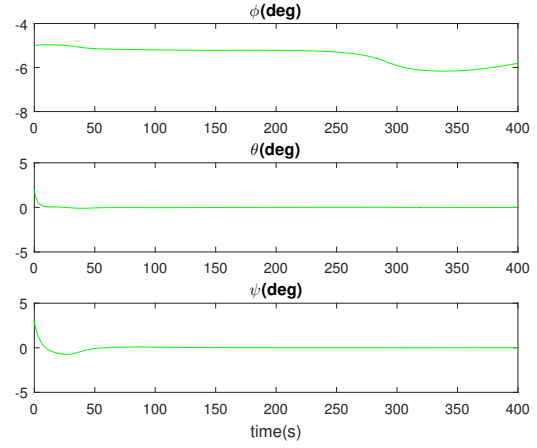
(b) Kite Euler Angles Trajectory

(c) Kite apparent Attitude

(d) Kite Angular Velocity

Chapter 7

Geometric Apparent Attitude Tracking

In the previous chapter, an apparent attitude tracking control scheme is designed based on the kite system dynamics transformation. However, sin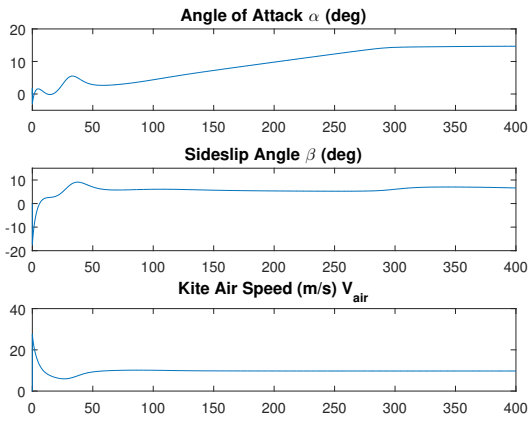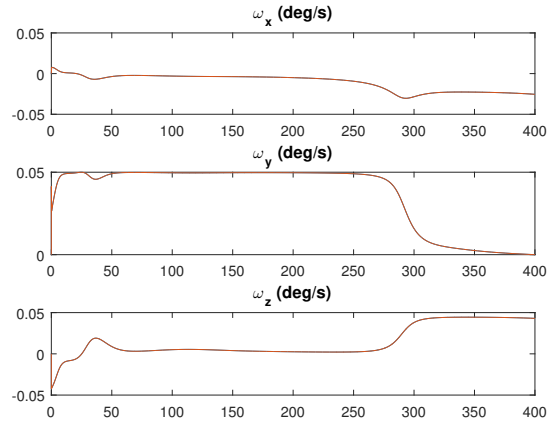ce the achievable kite angular velocity is limited, the saturation of the desired angular velocity will cause nonzero residue error. In other words, the control input, which is angular velocity in this case, is small compare to other physical effects in the system, such as the tether tension and aerodynamic force. Therefore, a different apparent attitude tracking control method needs to be developed. By definition, the kite apparent velocity and apparent attitudes are given in the following equations

$$\mathbf{V}_a = \mathbf{L}_{BC}(\mathbf{V}_C - \mathbf{W}) \tag{7.1}$$

$$\alpha = \arctan\frac{u_a}{w_a}; \quad \beta = \arcsin\frac{v_a}{V_a} \tag{7.2}$$

Therefore, the generation of the kite apparent attitudes can be summarized as the following non-linear process The new apparent attitude tracking control design is motivated by treating the kite geometric attitudes as inputs and kite apparent velocity in the inertial reference frame as measurements. It is clear that if the apparent velocity measurement in the inertial reference frames can be obtained, then it is possible to adjust the kite geometric attitudes Θ such that the desired apparent attitudes can be achieved.
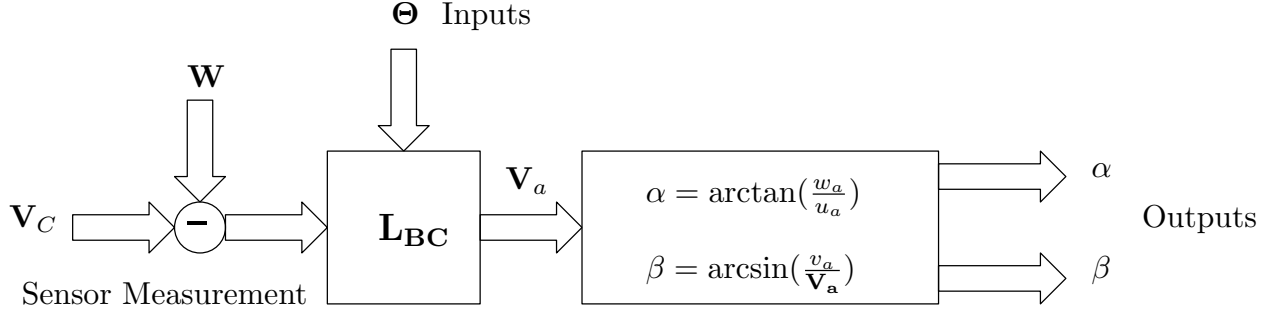
Figure 7.1: Generation of Apparent Attitudes

7.1 Apparent Attitude Tracking Theorem

In this section, the attitude trajectory for apparent attitude tracking is proposed. The given the desired apparent attitude α_d, β_d can be achieved by a desired kite attitude Θ_d. Denote the kite apparent velocity in a inertial reference frame as follows

$$\mathbf{V} = \begin{pmatrix} u & v & w \end{pmatrix} = (\mathbf{V}_C - \mathbf{W})^T. \tag{7.3}$$

The velocity angles can be further defined as

$$\gamma_1 = \arctan\left(\frac{v}{u}\right) \tag{7.4}$$

$$\gamma_2 = \arctan\left(\frac{w}{\sqrt{u^2 + v^2}}\right) \tag{7.5}$$

where the inverse tangent function takes value from interval $\left(-\frac{\pi}{2}, \ \frac{\pi}{2}\right)$. The velocity angles γ_1 and γ_2 are the spherical representation of the kite apparent velocity $\mathbf{V}$ as shown in Figure 7.2. For desired apparent attitude α_d and β_d, the desired kite attitude Θ_d can be derived using velocity angles γ_1 and γ_2.

Theorem 8 (Apparent Attitude Tracking). *To achieve the desired apparent attitude* $\alpha_d, \beta_d \in \left(-\frac{\pi}{2}, \ \frac{\pi}{2}\right), \alpha_d \neq 0$, *the desired kite geometric attitude is given by:*

$$\psi_d = \gamma_1 \tag{7.6}$$

$$\theta_d = \frac{\alpha_d}{|\alpha_d|} \arccos(\cos \alpha_d \cos \beta_d) - \frac{|u|}{u} \gamma_2 \tag{7.7}$$
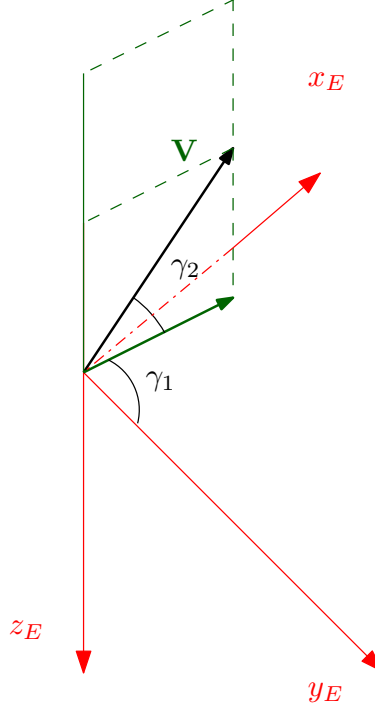
Figure 7.2: Velocity Angles

$$\phi_d = \frac{|u|}{u} \arctan\left(\frac{\tan \beta_d}{\sin \alpha_d}\right) \tag{7.8}$$

Especially, if $\alpha_d, \beta_d = 0$ the desired kite attitude becomes

$$\psi_d = \gamma_1 \tag{7.9}$$

$$\theta_d = -\frac{|u|}{u}\gamma_2 \tag{7.10}$$

and kite roll can be assigned to any value in the interval $\phi \in \left(-\frac{\pi}{2}, \ \frac{\pi}{2}\right)$.

Proof. Consider the generation of kite apparent attitudes α and β as shown in Figure 7.1. Using equation (7.3) and the definition of matrix $\mathbf{L}_{BC}$, the kite apparent velocity $\mathbf{V}_a$ is given by

$$\begin{pmatrix} u_a \\ v_a \\ w_a \end{pmatrix} = \begin{pmatrix} \cos\theta\cos\psi & \cos\theta\sin\psi & -\sin\theta \\ \sin\phi\sin\theta\cos\psi - \cos\phi\sin\psi & \sin\phi\sin\theta\sin\psi + \cos\phi\cos\psi & \sin\phi\cos\theta \\ \cos\phi\sin\theta\cos\psi + \sin\phi\sin\psi & \cos\phi\sin\theta\sin\psi - \sin\phi\sin\psi & \cos\phi\cos\theta \end{pmatrix} \begin{pmatrix} u \\ v \\ w \end{pmatrix}$$

103

By rearrangement, the transformation from $\mathbf{V}$ to $\mathbf{V}_a$ becomes:

$$u_a = (v \sin \psi + u \cos \psi) \cos \theta - w \sin \theta, \tag{7.11}$$

$$v_a = \Big((v \sin \psi + u \cos \psi) \sin \theta + w \cos \theta\Big) \sin \phi - (u \sin \psi - v \cos \psi) \cos \phi, \tag{7.12}$$

$$w_a = \Big((v \sin \psi + u \cos \psi) \sin \theta + w \cos \theta\Big) \cos \phi + (u \sin \psi - v \sin \psi) \sin \phi. \tag{7.13}$$

The linear combination of the sine and cosine function can be simplified as follows

$$v \sin \psi + u \cos \psi = \frac{|u|}{u} \cos (\psi - \gamma_1) \sqrt{u^2 + v^2}, \tag{7.14}$$

$$u \sin \psi - v \cos \psi = - \frac{|u|}{u} \sin (\psi - \gamma_1) \sqrt{u^2 + v^2}. \tag{7.15}$$

Substitute equations (7.14) and (7.15) into equations (7.11)-(7.13),

$$u_a = \Big(\frac{|u|}{u} \cos (\psi - \gamma_1) \sqrt{u^2 + v^2}\Big) \cos \theta - w \sin \theta,$$

$$v_a = \Big((\frac{|u|}{u} \cos (\psi - \gamma_1) \sqrt{u^2 + v^2}) \sin \theta + w \cos \theta\Big) \sin \phi + (\frac{|u|}{u} \sin (\psi - \gamma_1) \sqrt{u^2 + v^2}) \cos \phi,$$

$$w_a = \Big((\frac{|u|}{u} \cos (\psi - \gamma_1) \sqrt{u^2 + v^2}) \sin \theta + w \cos \theta\Big) \cos \phi + (\frac{|u|}{u} \sin (\psi - \gamma_1) \sqrt{u^2 + v^2}) \sin \phi.$$

Let $\psi = \gamma_1$; then, the transformation from $\mathbf{V}$ to $\mathbf{V}_a$ becomes

$$u_a = \frac{|u|}{u} \sqrt{u^2 + v^2} \cos \theta - w \sin \theta, \tag{7.16}$$

$$v_a = \Big(\frac{|u|}{u} \sqrt{u^2 + v^2} \sin \theta + w \cos \theta\Big) \sin \phi, \tag{7.17}$$

$$w_a = \Big(\frac{|u|}{u} \sqrt{u^2 + v^2} \sin \theta + w \cos \theta\Big) \cos \phi. \tag{7.18}$$

Using the linear combination of the trigonometric functions,

$$\frac{|u|}{u} \sqrt{u^2 + v^2} \cos \theta - w \sin \theta = \frac{|u|}{u} \|\mathbf{V}\| \cos \Big(\theta + \frac{|u|}{u} \gamma_2\Big) \tag{7.19}$$

$$\frac{|u|}{u} \sqrt{u^2 + v^2} \sin \theta + w \cos \theta = \frac{|u|}{u} \|\mathbf{V}\| \sin \Big(\theta + \frac{|u|}{u} \gamma_2\Big) \tag{7.20}$$
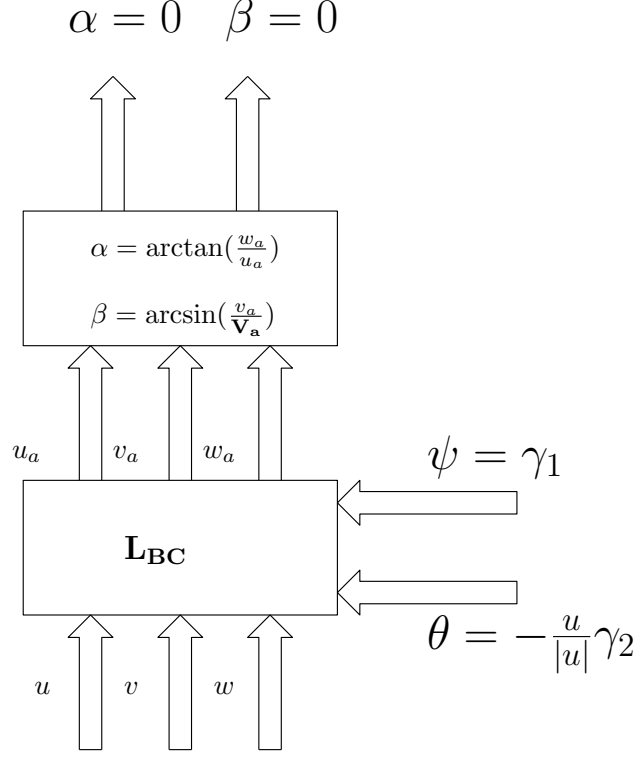
Figure 7.3: Tracking Local Wind

Substitute equations (7.19) and (7.20) into equations (7.16)-(7.18), and notice that $\|\mathbf{V}\| = \|\mathbf{V}_a\|$

$$u_a = \frac{|u|}{u}\|\mathbf{V}_a\| \cos\left(\theta + \frac{|u|}{u}\gamma_2\right),$$

$$v_a = \frac{|u|}{u}\|\mathbf{V}_a\| \sin\left(\theta + \frac{|u|}{u}\gamma_2\right)\sin\phi,$$

$$w_a = \frac{|u|}{u}\|\mathbf{V}_a\| \sin\left(\theta + \frac{|u|}{u}\gamma_2\right)\cos\phi.$$

By definition, the kite angle of attack and side slip angle are given by

$$\tan\alpha = \tan\left(\theta + \frac{|u|}{u}\gamma_2\right)\cos\phi \tag{7.21}$$

$$\sin\beta = \frac{|u|}{u}\sin\left(\theta + \frac{|u|}{u}\gamma_2\right)\sin\phi. \tag{7.22}$$

Thereby, if $\alpha_d = 0; \beta_d = 0$, the corresponding desired kite attitude is $\psi_d = \gamma_1, \theta_d = -\frac{|u|}{u}\gamma_2$. This result is shown in Figure 7.3.

If desired apparent attitude $\alpha_d, \beta_d \in \left(-\frac{\pi}{2}, \ \frac{\pi}{2}\right), \alpha_d \neq 0$ the desired kite attitude can be solved

105

from equalities (7.21) and (7.22). Rewrite equations (7.21) and (7.22) as follows,

$$\cos\left(\theta + \frac{|u|}{u}\gamma_2\right)\tan\alpha = \sin\left(\theta + \frac{|u|}{u}\gamma_2\right)\cos\phi \tag{7.23}$$

$$\sin\beta = \frac{|u|}{u}\sin\left(\theta + \frac{|u|}{u}\gamma_2\right)\sin\phi \tag{7.24}$$

Take the square sum of equations (7.23) and (7.24):

$$\sin^2\beta + \cos^2\left(\theta + \frac{|u|}{u}\gamma_2\right)\tan^2\alpha = 1 - \cos^2\left(\theta + \frac{|u|}{u}\gamma_2\right).$$

By rearrangement, the equation above becomes

$$\cos^2\left(\theta + \frac{|u|}{u}\gamma_2\right)(1 + \tan^2\alpha) = 1 - \sin^2\beta$$

Hence, the desired pitch angle must satisfy the following equation

$$\cos^2\left(\theta_d + \frac{|u|}{u}\gamma_2\right) = \cos^2\alpha\cos^2\beta. \tag{7.25}$$

Take the square ratio of equations (7.22) to (7.21):

$$\frac{\sin^2\beta}{\tan^2\alpha} = \cos^2\left(\theta + \frac{|u|}{u}\gamma_2\right)\tan^2\phi$$

Use equation (7.25), the desired roll angle must satisfies that

$$\tan^2\phi_d = \frac{\tan^2\beta}{\sin^2\alpha}. \tag{7.26}$$

Assume all angles in equations (7.21) and (7.22) are inside the interval $\left(-\frac{\pi}{2}, \frac{\pi}{2}\right)$ then the sign relation of equations (7.21) and (7.22) becomes:

$$\mathrm{sgn}(\alpha_d) = \mathrm{sgn}\left(\theta_d + \frac{|u|}{u}\gamma_2\right) \tag{7.27}$$

$$\mathrm{sgn}(\beta_d) = \mathrm{sgn}(u)\mathrm{sgn}\left(\theta_d + \frac{|u|}{u}\gamma_2\right)\mathrm{sgn}(\phi_d) \tag{7.28}$$

Combining equations (7.25)-(7.28), the desired kite attitude can be obtained as:

$$\theta_d = \frac{\alpha_d}{|\alpha_d|} \arccos(\cos \alpha_d \cos \beta_d) - \frac{|u|}{u}\gamma_2 \tag{7.29}$$

$$\phi_d = \frac{|u|}{u} \arctan \left(\frac{\tan \beta_d}{\sin \alpha_d} \right). \tag{7.30}$$

The inverse cosine function takes value from interval $\left(0, \quad \frac{\pi}{2} \right)$ and inverse tangent takes value from $\left(-\frac{\pi}{2}, \quad \frac{\pi}{2} \right)$. $\qquad\qquad\square$

The kite attitude trajectory (7.29) and (7.30) are sum of (7.9), (7.10) and a constant offset. Discontinuity will be introduced if sudden change occurred in the desired apparent attitude α_d and β_d. A smoother kite attitude trajectory can be achieved by using the roll angle, ϕ, information in the desired pitch angle , θ_d.

Theorem 9 (Smoothing Apparent Attitude Tracking). *For $\alpha_d, \beta_d \in \left(-\frac{\pi}{2}, \quad \frac{\pi}{2} \right)$, a smoothing kite geometric attitude is given by:*

$$\psi_d = \gamma_1 \tag{7.31}$$

$$\theta_d = \arctan \left(\tan \alpha_d \sec \phi \right) - \frac{|u|}{u}\gamma_2 \tag{7.32}$$

$$\phi_d = \frac{|u|}{u} \arctan \left(\frac{\tan \beta_d}{\sin \alpha_d} \right) \tag{7.33}$$

Proof. The desired pitch angle θ_d is obtained by directly solving the equation (7.21) by treating θ as unknown,

$$\tan \alpha = \tan(\theta + \frac{|u|}{u}\gamma_2) \cos \phi$$

$$\theta = \arctan \left(\tan \alpha \sec \phi \right) - \frac{|u|}{u}\gamma_2 \tag{7.34}$$

Comparing equation (7.34) with equation (7.29), the desired pitch angle θ_d is equivalent if and only if

$$\arctan(\tan \alpha \sec \phi) = \frac{|\alpha|}{\alpha} \arccos(\cos \alpha \cos \beta). \tag{7.35}$$

107

The equivalent relation can be obtained by substituting the desired roll angle (7.33) into the left hand side of the equation (7.35). Rearrange equation (7.35) to the following form,

$$\tan \alpha \sec \phi = \frac{|\alpha|}{\alpha} \tan \left(\arccos(\cos \alpha \cos \beta) \right) \tag{7.36}$$

where the inverse cosine takes value from interval $(0, \frac{\pi}{2})$. Substitute equation (7.33) into equation (7.36),

$$\tan \alpha \sec \left(\frac{|u|}{u} \arctan \left(\frac{\tan \beta}{\sin \alpha} \right) \right) = \frac{|\alpha|}{\alpha} \tan \left(\arccos(\cos \alpha \cos \beta) \right) \tag{7.37}$$

The secant of the inverse tangent function is given by $\sec(\arctan \xi) = \sqrt{1 + \xi^2}$, therefore, the left hand side of equation (7.37) can be simplified as follows,

$$\begin{aligned}
\tan \alpha_d \sec \left(\arctan \left(\frac{\tan \beta_d}{\sin \alpha_d} \right) \right) &= \tan \alpha_d \sqrt{1 + \left(\frac{\tan \beta_d}{\sin \alpha_d} \right)^2} \\
&= \frac{|\alpha_d|}{\alpha_d} \sqrt{\tan^2 \alpha_d + \sec^2 \alpha_d \tan^2 \beta_d} \tag{7.38}
\end{aligned}$$

Moreover, the tangent of the inverse cosine function is given by $\tan(\arccos \xi) = \frac{\sqrt{1 - \xi^2}}{\xi}$, the right hand side of equation (7.37) can be simplified as follows

$$\begin{aligned}
\frac{|\alpha_d|}{\alpha_d} \tan \left(\arccos(\cos \alpha_d \cos \beta_d) \right) &= \frac{|\alpha_d|}{\alpha_d} \sqrt{\frac{1 - \cos^2 \alpha_d \cos^2 \beta_d}{\cos^2 \alpha_d \cos^2 \beta_d}} \\
&= \frac{|\alpha_d|}{\alpha_d} \sqrt{\sec^2 \alpha_d \sec^2 \beta_d - 1} \\
&= \frac{|\alpha_d|}{\alpha_d} \sqrt{\sec^2 \alpha_d (\sec^2 \beta_d - 1) + \tan^2 \alpha_d} \\
&= \frac{|\alpha_d|}{\alpha_d} \sqrt{\sec^2 \alpha_d \tan^2 \beta_d + \tan^2 \alpha_d} \tag{7.39}
\end{aligned}$$

Comparing equations (7.38) and (7.39), it is clear that the equation (7.37) holds if the roll angle achieves the desired value. $\qquad \square$

7.2 Back-Stepping Rotational Control Design

In the previous section, two equivalent time varying trajectories for Euler angles Θ are given in equations (7.6)-(7.8) and (7.31)-(7.33). To achieve the desired geometric attitudes, a rotational control signal needs to be designed. To facilitate the derivation, Assumption 2 needs to be adopted, i.e. the rotational transformation matrix $\mathbf{R}$ is invertible

$$\exists \theta_\epsilon \ni -\frac{\pi}{2} + \theta_\epsilon \leq \theta \leq \frac{\pi}{2} - \theta_\epsilon \tag{7.40}$$

where the constant $\theta_\epsilon \in (0, \frac{\pi}{2})$. Then, the inverse of the rotational transformation matrix is

$$\mathbf{R}^{-1} = \begin{pmatrix} 1 & \sin\phi\tan\theta & \cos\phi\tan\theta \\ 0 & \cos\phi & -\sin\phi \\ 0 & \sec\theta\sin\phi & \sec\theta\cos\phi \end{pmatrix}. \tag{7.41}$$

Combining the rotational kinematics and the Euler rotational dynamics,

$$\dot{\Theta} = \mathbf{R}^{-1}\boldsymbol{\omega} \tag{7.42}$$

$$\mathbf{J}\dot{\boldsymbol{\omega}} = \mathbf{u}_B - \boldsymbol{\omega} \times \mathbf{J}\boldsymbol{\omega} \tag{7.43}$$

The structure of attitude dynamics is cascade. The angular velocity $\boldsymbol{\omega}$ is the input to kinematic equation (7.42) and the output of the Euler equation (7.43). The rotational tracking control signal can be designed using a back-stepping method. Denote the kite attitudes and angular velocity tracking error as follows

$$\Theta_e = \Theta - \Theta_d; \qquad \boldsymbol{\omega}_e = \boldsymbol{\omega} - \boldsymbol{\omega}_d. \tag{7.44}$$

where $\boldsymbol{\omega}_d$ is defined by the following equation

$$\boldsymbol{\omega}_d = \mathbf{R}\big(\dot{\Theta}_d - \mathbf{K}_\Theta(\Theta - \Theta_d)\big) \quad \mathbf{K}_\Theta > 0 \tag{7.45}$$

Then the rotational control signal can be designed as in the following theorem,

Theorem 10. *Assume the kite pitch angle is bounded away from the singularity as in (7.40). Given the kite attitude dynamics (7.42) and (7.43), the rotational control signal can be chosen in the following form*

$$\mathbf{u}_B = \mathbf{J}\dot{\boldsymbol{\omega}}_d + \boldsymbol{\omega}_d \times \mathbf{J}\boldsymbol{\omega} - \mathbf{K}_\omega \boldsymbol{\omega}_e - (\mathbf{R}^T)^{-1}\boldsymbol{\Theta}_e \tag{7.46}$$

where $\mathbf{K}_\omega$ is a positive definite design matrix. Then the attitude tracking error $\boldsymbol{\Theta}_e$ is locally asymptotically stable.

Proof. Rewrite the rotational kinematic relation as follows

$$\dot{\boldsymbol{\Theta}} = \mathbf{R}^{-1}\boldsymbol{\omega}_d + \mathbf{R}^{-1}\boldsymbol{\omega}_e$$
$$= \dot{\boldsymbol{\Theta}}_d - \mathbf{K}_\Theta(\boldsymbol{\Theta} - \boldsymbol{\Theta}_d) + \mathbf{R}^{-1}\boldsymbol{\omega}_e$$

Therefore, the attitude tracking error satisfies the following error dynamics

$$\dot{\boldsymbol{\Theta}}_e = -\mathbf{K}_\Theta \boldsymbol{\Theta}_e + \mathbf{R}^{-1}\boldsymbol{\omega}_e \tag{7.47}$$

Furthermore, rewrite the angular velocity dynamics into the form of equation (6.26) as follows

$$\mathbf{J}\dot{\boldsymbol{\omega}}_e + \boldsymbol{\omega}_e \times \mathbf{J}\boldsymbol{\omega} = \mathbf{u}_e \tag{7.48}$$

where $\mathbf{u}_e = \mathbf{u}_B - \mathbf{J}\dot{\boldsymbol{\omega}}_d - \boldsymbol{\omega}_d \times \mathbf{J}\boldsymbol{\omega}$. Therefore, instead of designing control signal using the original rotational dynamics, the attitude tracking control signal can be designed using error dynamics (7.47) and (7.48). Choose the following Lyapunov function,

$$V_e = \frac{1}{2}\boldsymbol{\omega}_e^T \mathbf{J}\boldsymbol{\omega}_e + \frac{1}{2}\boldsymbol{\Theta}_e^T \boldsymbol{\Theta}_e \tag{7.49}$$

Take the time derivative of Lyapunov function (7.49) along system trajectories (7.47) and (7.48),

$$\dot{V}_e = \boldsymbol{\omega}_e^T \mathbf{J}\dot{\boldsymbol{\omega}}_e + \boldsymbol{\Theta}_e^T \dot{\boldsymbol{\Theta}}_e$$
$$= \boldsymbol{\omega}_e^T(-\boldsymbol{\omega}_e \times \mathbf{J}\boldsymbol{\omega} + \mathbf{u}_e) + \boldsymbol{\Theta}_e^T(-\mathbf{K}_\Theta \boldsymbol{\Theta}_e + \mathbf{R}^{-1}\boldsymbol{\omega}_e)$$

$$=\boldsymbol{\omega}_e^T \mathbf{u}_e - \boldsymbol{\Theta}_e^T \mathbf{K}_\Theta \boldsymbol{\Theta}_e + \boldsymbol{\Theta}_e^T \mathbf{R}^{-1} \boldsymbol{\omega}_e \tag{7.50}$$

The rotational control signal can be solved from the following equation

$$\boldsymbol{\omega}_e^T \mathbf{u}_e + \boldsymbol{\Theta}_e^T \mathbf{R}^{-1} \boldsymbol{\omega}_e = -\boldsymbol{\omega}_e^T \mathbf{K}_\omega \boldsymbol{\omega}_e \tag{7.51}$$

where the matrix $\mathbf{K}_\omega$ is a positive definite design matrix. Therefore, the error control signal $\mathbf{u}_e$ becomes

$$\mathbf{u}_e = -\mathbf{K}_\omega \boldsymbol{\omega}_e - (\mathbf{R}^T)^{-1} \boldsymbol{\Theta}_e \tag{7.52}$$

The original control signal $\mathbf{u}_B$ then can be obtained as

$$\mathbf{u}_B = \mathbf{J}\dot{\boldsymbol{\omega}}_d + \boldsymbol{\omega}_d \times \mathbf{J}\boldsymbol{\omega} - \mathbf{K}_\omega \boldsymbol{\omega}_e - (\mathbf{R}^T)^{-1} \boldsymbol{\Theta}_e$$

Using Barbarlet lemma, the attitudes tracking error $\boldsymbol{\Theta}_e$ is then locally asymptotically stable. $\quad\square$

Moreover, the form of control signal can be further simplified by choosing the design matrix $\mathbf{K}_\Theta$ and $\mathbf{K}_\omega$ properly. This result is given in the following corollary,

Corollary 5. *Assume the kite pitch angle is bounded away from the singularity as in* (7.40). *Given the kite attitude dynamics* (7.42) *and* (7.43), *the rotational control signal can be chosen in the following form*

$$\mathbf{u}_B = \mathbf{J}\dot{\boldsymbol{\omega}}_d + \boldsymbol{\omega}_d \times \mathbf{J}\boldsymbol{\omega} - \mathbf{K}_\omega \boldsymbol{\omega}_e \tag{7.53}$$

where $\mathbf{K}_\omega$ is a positive definite design matrix. Then the attitude tracking error $\boldsymbol{\Theta}_e$ is locally asymptotically stable.

Proof. Choose the same Lyapunov function as in equation (7.49), take the time derivative along the system trajectories (7.47) and (7.48) yields,

$$\dot{V}_e = \boldsymbol{\omega}_e^T \mathbf{u}_e - \boldsymbol{\Theta}_e^T \mathbf{K}_\Theta \boldsymbol{\Theta}_e + \boldsymbol{\Theta}_e^T \mathbf{R}^{-1} \boldsymbol{\omega}_e$$

Notice the following equivalent relation,

$$\|\boldsymbol{\Theta}_e - \mathbf{R}^{-1}\boldsymbol{\omega}_e\|^2 = \boldsymbol{\Theta}_e^T\boldsymbol{\Theta}_e - 2\boldsymbol{\Theta}_e^T\mathbf{R}^{-1}\boldsymbol{\omega}_e + \boldsymbol{\omega}_e^T(\mathbf{R}\mathbf{R}^T)^{-1}\boldsymbol{\omega}_e \geq 0$$

Therefore, the following inequality holds,

$$\boldsymbol{\Theta}_e^T\mathbf{R}^{-1}\boldsymbol{\omega}_e \leq \frac{1}{2}\left(\boldsymbol{\Theta}_e^T\boldsymbol{\Theta}_e + \boldsymbol{\omega}_e^T(\mathbf{R}\mathbf{R}^T)^{-1}\boldsymbol{\omega}_e\right) \tag{7.54}$$

By definition (7.41), the largest eigenvalue of the matrix $(\mathbf{R}\mathbf{R}^T)^{-1}$ can be obtained as follows

$$\sigma_R = \max\left(1 \quad \frac{1}{\left(\cos(\frac{\theta}{2})-\sin(\frac{\theta}{2})\right)^2} \quad \frac{1}{\left(\cos(\frac{\theta}{2})+\sin(\frac{\theta}{2})\right)^2}\right) < \infty \tag{7.55}$$

The second inequality holds due to Assumption (7.40), therefore, the time derivative of the Lyapunov function can be simplified as follows

$$\begin{aligned}
\dot{V}_e &= \boldsymbol{\omega}_e^T\mathbf{u}_e - \boldsymbol{\Theta}_e^T\mathbf{K}_\Theta\boldsymbol{\Theta}_e + \boldsymbol{\Theta}_e^T\mathbf{R}^{-1}\boldsymbol{\omega}_e \\
&\leq \boldsymbol{\omega}_e^T\mathbf{u}_e - \boldsymbol{\Theta}_e^T\mathbf{K}_\Theta\boldsymbol{\Theta}_e + \frac{1}{2}\boldsymbol{\Theta}_e^T\boldsymbol{\Theta}_e + \frac{1}{2}\sigma_R\boldsymbol{\omega}_e^T\boldsymbol{\omega}_e
\end{aligned} \tag{7.56}$$

Therefore, by choosing the design matrices $\mathbf{K}_\Theta$ and $\mathbf{K}_\omega$ satisfies that

$$\mathbf{K}_\Theta - \frac{1}{2}\mathbf{I}_3 > 0 \quad \mathbf{K}_\omega - \frac{1}{2}\sigma_R\mathbf{I}_3 > 0 \tag{7.57}$$

the time derivative of the Lyapunov function along the trajectories of closed loop system becomes

$$\begin{aligned}
\dot{V}_e &\leq -\boldsymbol{\omega}_e^T\mathbf{K}_\omega\boldsymbol{\omega}_e - \boldsymbol{\Theta}_e^T\mathbf{K}_\Theta\boldsymbol{\Theta}_e + \frac{1}{2}\boldsymbol{\Theta}_e^T\boldsymbol{\Theta}_e + \frac{1}{2}\sigma_R\boldsymbol{\omega}_e^T\boldsymbol{\omega}_e \\
&= -\boldsymbol{\omega}_e^T(\mathbf{K}_\omega - \frac{1}{2}\sigma_R\mathbf{I}_3)\boldsymbol{\omega}_e - \boldsymbol{\Theta}_e^T(\mathbf{K}_\Theta - \frac{1}{2}\mathbf{I}_3)\boldsymbol{\Theta}_e
\end{aligned} \tag{7.58}$$

Using Barbarlet lemma, the angular velocity and attitude tracking errors are also asymptotically converge. □

To implement the control signal (7.53) into the simulation, the equivalent form in Euler angles

need to be obtained. Taking the derivative of desired angular velocity gives

$$\dot{\boldsymbol{\omega}}_d = \dot{\mathbf{R}}(\dot{\boldsymbol{\Theta}}_d - \mathbf{K}_\Theta \boldsymbol{\Theta}_e) + \mathbf{R}(\ddot{\boldsymbol{\Theta}}_d - \mathbf{K}_\Theta \dot{\boldsymbol{\Theta}}_e) \tag{7.59}$$

Further denote the cross product matrix as follows

$$[\mathbf{J}\boldsymbol{\omega}]_\times \boldsymbol{\omega}_d = \mathbf{J}\boldsymbol{\omega} \times \boldsymbol{\omega}_d \tag{7.60}$$

Expending the proposed control signal (7.53) gives that

$$\mathbf{u}_B = \mathbf{J}\big(\dot{\mathbf{R}}(\dot{\boldsymbol{\Theta}}_d - \mathbf{K}_\Theta \boldsymbol{\Theta}_e) + \mathbf{R}(\ddot{\boldsymbol{\Theta}}_d - \mathbf{K}_\Theta \dot{\boldsymbol{\Theta}}_e)\big) - [\mathbf{J}\boldsymbol{\omega}]_\times \mathbf{R}(\dot{\boldsymbol{\Theta}}_d - \mathbf{K}_\Theta \boldsymbol{\Theta}_e) - \mathbf{K}_\omega \mathbf{R}(\dot{\boldsymbol{\Theta}}_e + \mathbf{K}_\Theta \boldsymbol{\Theta}_e)$$

$$= (\mathbf{J}\dot{\mathbf{R}} - [\mathbf{J}\boldsymbol{\omega}]_\times \mathbf{R})\dot{\boldsymbol{\Theta}}_d - (\mathbf{K}_e \mathbf{R} + \mathbf{J}\mathbf{R}\mathbf{K}_\Theta)\dot{\boldsymbol{\Theta}}_e + (-\mathbf{K}_e \mathbf{R} - \mathbf{J}\dot{\mathbf{R}} + [\mathbf{J}\boldsymbol{\omega}]_\times \mathbf{R})\mathbf{K}_\Theta \boldsymbol{\Theta}_e + \mathbf{J}\mathbf{R}\ddot{\boldsymbol{\Theta}}_d$$

By rearrangement, the proposed control signal can be simplified as follows:

$$\mathbf{u}_B = \mathbf{K}_1 \dot{\boldsymbol{\Theta}}_d + \mathbf{K}_2 \ddot{\boldsymbol{\Theta}}_d + \mathbf{K}_3 \boldsymbol{\Theta}_e + \mathbf{K}_4 \dot{\boldsymbol{\Theta}}_e \tag{7.61}$$

$$\mathbf{K}_1 = \mathbf{J}\dot{\mathbf{R}} - [\mathbf{J}\boldsymbol{\omega}]_\times \mathbf{R} \tag{7.62}$$

$$\mathbf{K}_2 = \mathbf{J}\mathbf{R} \tag{7.63}$$

$$\mathbf{K}_3 = (-\mathbf{K}_\omega \mathbf{R} - \mathbf{J}\dot{\mathbf{R}} + [\mathbf{J}\boldsymbol{\omega}]_\times \mathbf{R})\mathbf{K}_\Theta \tag{7.64}$$

$$\mathbf{K}_4 = -\mathbf{K}_\omega \mathbf{R} - \mathbf{J}\mathbf{R}\mathbf{K}_\Theta \tag{7.65}$$

Remark 1. If the kite desired attitude $\boldsymbol{\Theta}_d$ is bounded, first order differentiable and $\boldsymbol{\Theta}_d$ is also bounded then the kite angular velocity $\boldsymbol{\omega}$ is bounded under the control signal (7.53). By definition, the kite angular velocity is the sum of $\boldsymbol{\omega}_e$ and $\boldsymbol{\omega}_d$, i.e.

$$\boldsymbol{\omega} = \boldsymbol{\omega}_e + \boldsymbol{\omega}_d = \boldsymbol{\omega}_e + \mathbf{R}\big(\dot{\boldsymbol{\Theta}}_d - \mathbf{K}_\Theta \boldsymbol{\Theta}_e\big)$$

Using trigonometric inequality, the bound of kite angular velocity is given by

$$\|\boldsymbol{\omega}\| \leq \|\boldsymbol{\omega}_e\| + \|\mathbf{R}\|\big(\|\dot{\boldsymbol{\Theta}}_d\| + \|\mathbf{K}_\Theta\|\|\boldsymbol{\Theta}_e\|\big) \leq \infty$$

In practice, the kite rotational control moment is generated by the control surfaces such as ailerons, elevators and rudders whose deflection is limited. Thereby, the available control moment is also limited. The first two terms of the resulting control structure (7.61) is linear with respect to $\dot{\Theta}_d$ and $\ddot{\Theta}_d$ and the control gains $\mathbf{K}_3$ and $\mathbf{K}_4$ is proportional to the design matrices $\mathbf{K}_e$ and $\mathbf{K}_\Theta$. Hence, by proper choice of the desired kite attitude Θ_d and design matrices $\mathbf{K}_e$ and $\mathbf{K}_\Theta$, the control signal can be made accessible to the limited kite control moment. In other words, for slow varying desired attitude Θ_d and design matrix $\mathbf{K}_\Theta$, the desired angular velocity $\boldsymbol{\omega}_d$ can be made feasible to the kite rotation in practice.

The first and second order time derivative of the desired attitudes, $\dot{\Theta}_d$ and $\ddot{\Theta}_d$, are required in the control signal (7.61), therefore the real time differentiation are required. Assume that the desired tracking angles Θ_d is third order differentiable, then the first and second order derivatives of the desired tracking angle can be obtained using the high gain observer, [36]:

$$\dot{y}_1 = y_2 + \frac{\sigma_1}{\epsilon}(\Theta_d - y_1)$$
$$\dot{y}_2 = y_3 + \frac{\sigma_2}{\epsilon}(\Theta_d - y_1)$$
$$\dot{y}_3 = \frac{\sigma_3}{\epsilon}(\Theta_d - y_1)$$

where ϵ is a small number and $\sigma_i, i = 1, 2$ are the coefficient of a design Hurwitz polynomial $s^2 + \sigma_1 s + \sigma_2$. The estimate of the first and second order of the desired tracking angle are denoted as $\hat{\dot{\Theta}}_d$ and $\hat{\ddot{\Theta}}_d$, which can be obtained as:

$$\left(\hat{\dot{\Theta}}_d \quad \hat{\ddot{\Theta}}_d \right) = \left(y_2 \quad y_3 \right)$$

The estimation errors vanish as ϵ vanishes. Substituting the estimation of first and second order derivative of the tracking attitude into the control signal (7.61) results in

$$\mathbf{u}_B = \mathbf{K}_1 \hat{\dot{\Theta}}_d + \mathbf{K}_2 \hat{\ddot{\Theta}}_d + \mathbf{K}_3(\Theta - \Theta_d) + \mathbf{K}_4(\dot{\Theta} - \hat{\dot{\Theta}}_d) \tag{7.66}$$

The desired kite angle of attack is chosen to be a constant value α^* while the desired side slip

Table 7.1: Input and Control Parameters

parameter	value	paramter	value	parameter	value	paramter	value
Kite Mass	40kg	Tether Density	0.003kg/m	$\mathbf{K}_\omega$	0.5J	$\mathbf{K}_\Theta$	$5\mathbf{I}_3$
Kite Area	$30m^2$	Tether Length	300m	ϵ	0.1	σ_1	12
Turbine Mass Ratio	50%	Tether Diameter	0.002m	σ_2	48	σ_3	64
Turbine Area Ratio	20%	$\bar{W}$	6m/s	α^*	10°	β^+	3.8°
Aspect Ratio	3.3	C_t	0.072	β^-	−3.8°	ΔT	4s
Induction Factor	0.1	C_p	0.324				

angle is chosen according to the following switching law

$$\beta_d = \begin{cases} \beta^+ & \text{if } q_1 > q_1^+ \\ \\ \beta^- & \text{if } q_1 < q_1^- \end{cases},$$

where q_1^- and q_1^+ are specified cross wind limit angles. To meet the continuity requirement of the kite desired attitude in the control signal , cosine smoothing is applied at the switch as follows. Suppose the switching time for the ith cycle is t_i^+ and t_i^- and $t_i^+ > t_i^-$, in the transient period ΔT of the switching that occurs at t_i^-, the desired side slip angle is

$$\beta_d(t) = \frac{\beta^+ + \beta^-}{2} - \frac{\beta^+ - \beta^-}{2} \cos \frac{\pi}{\Delta T}(t - t_i^-),$$

where $t \in [t_i^-, t_i^- + \Delta T]$ and $\Delta T < t_i^+ - t_i^-$. The smoothing desired angle at t_i^+ can be obtained similarly. The parameters for rotational control signal are shown in Table 7.1. The following figures show that the apparent attitude tracking control system forms consecutive figure-eight trajectory of the kite translation. The power output greatly increase compared to the Lyapunov based control.

7.3 Inertial Apparent Dynamics

In previous section, an attitude trajectory that track the desired kite apparent attitudes, α_d and β_d, is proposed. In this section, the proposed attitude trajectory (7.6) - (7.8) is applied on the kite

Table 7.2: Power Output

Wind Speed(m/s)	ϕ(degree)	Power(kW)
	25	9.99
6	30	19.5
	35	24.3
	25	14.4
7	30	30.2
	35	36.4

Figure 7.4: Wind Speed = 6m/s, $\phi = 25°$

(a) Kite Translational Trajectory

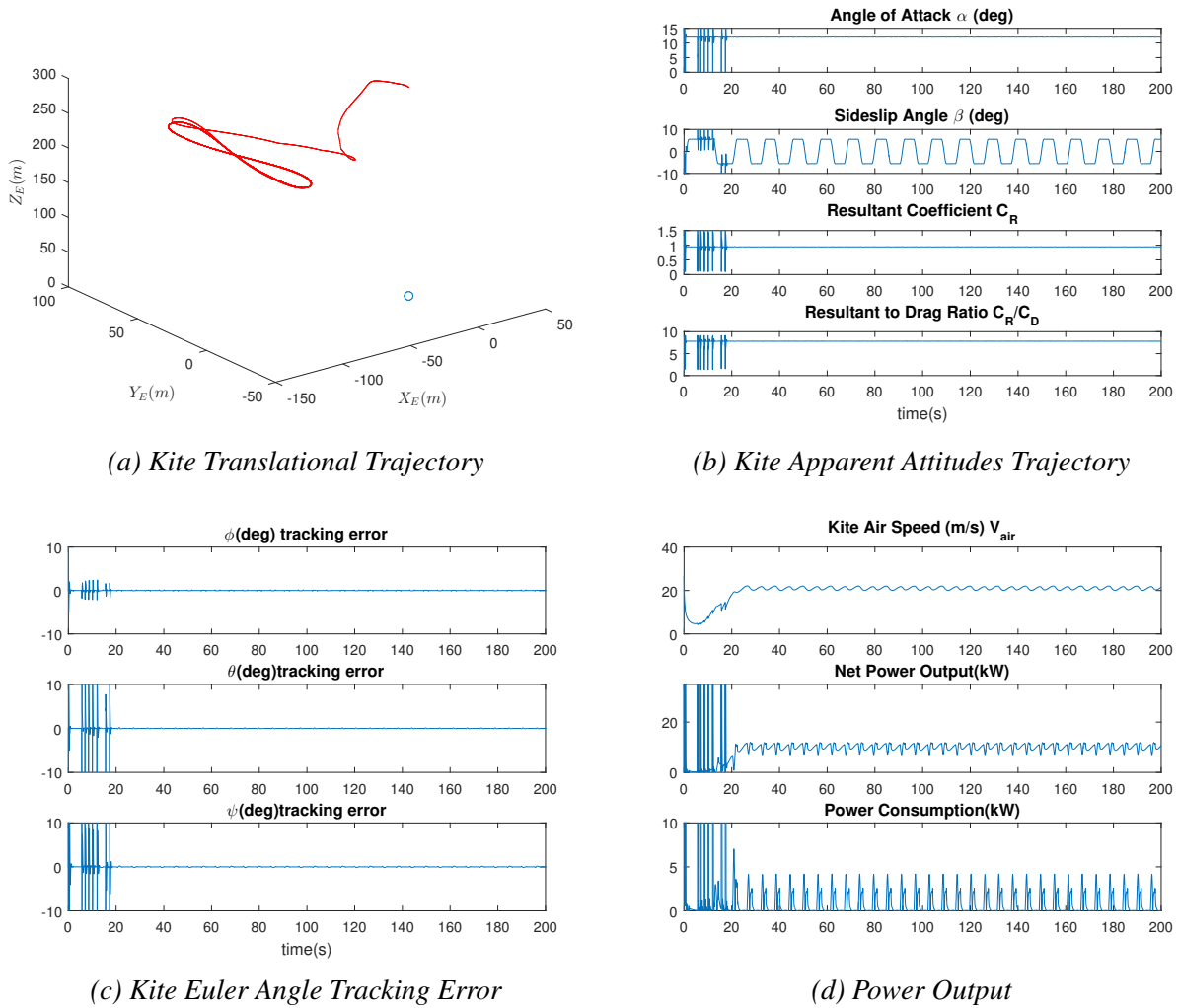*(b) Kite Apparent Attitudes Trajectory*
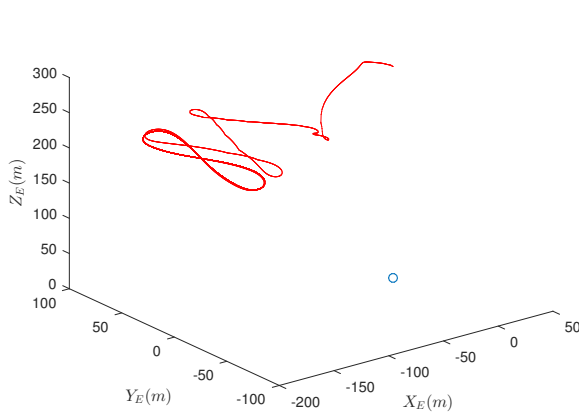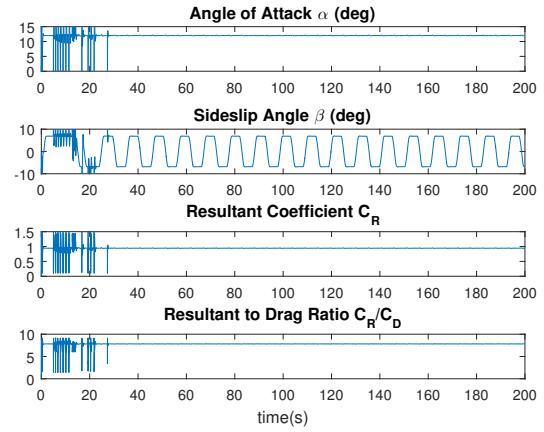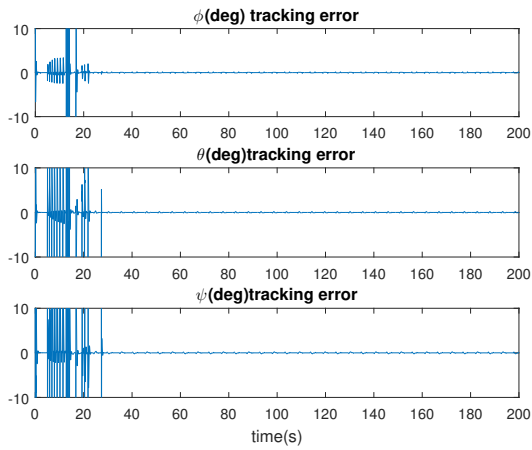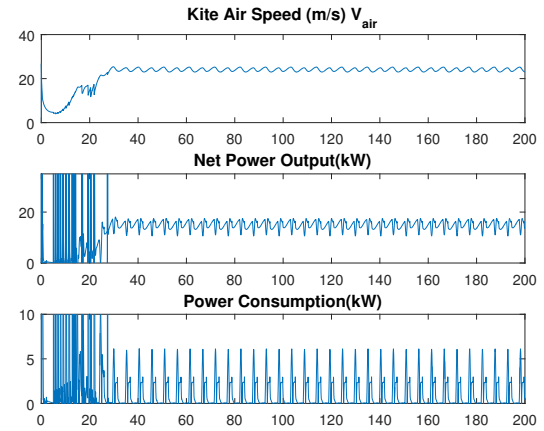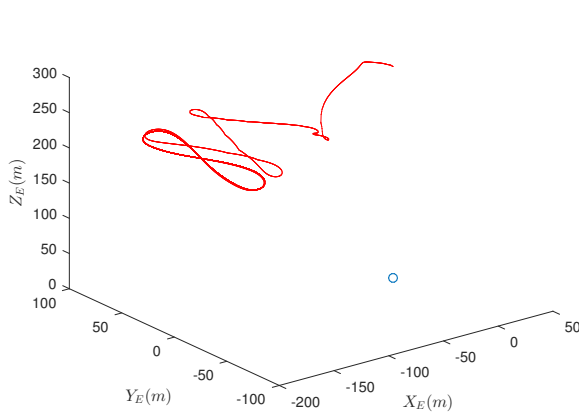

(c) Kite Euler Angle Tracking Error

(d) Power Output

116

Figure 7.5: Wind Speed = 6m/s, $\phi = 30°$

(a) Kite Translational Trajectory

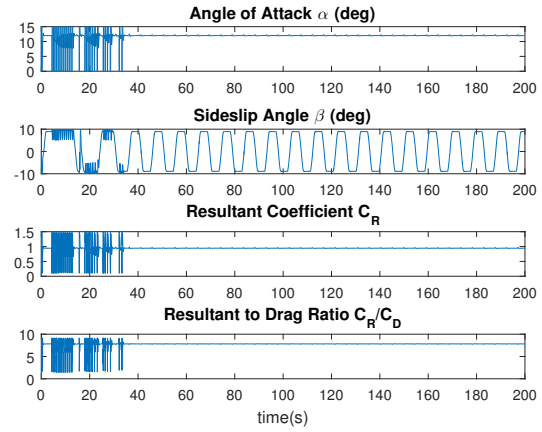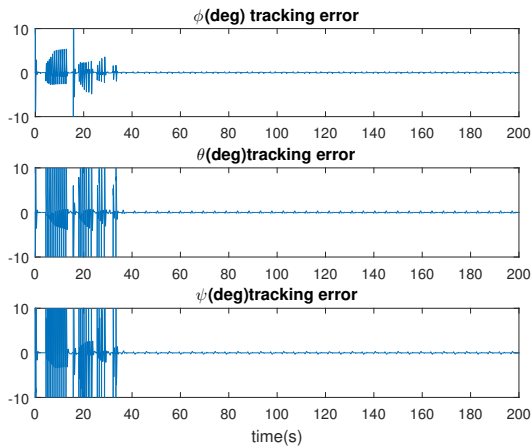*(b) Kite Apparent Attitudes Trajectory*

(c) Kite Euler Angle Tracking Error

(d) Power Output

Figure 7.6: Wind Speed = 6m/s, $\phi = 35°$

(a) Kite Translational Trajectory

(b) Kite Apparent Attitudes Trajectory

(c) Kite Euler Angle Tracking Error

(d) Power Output

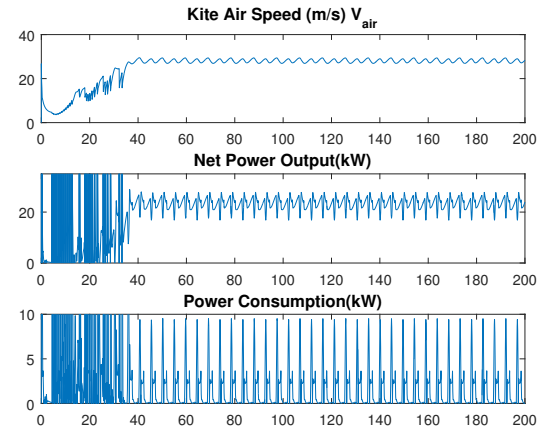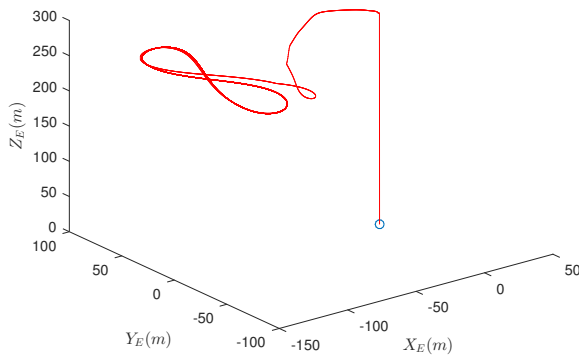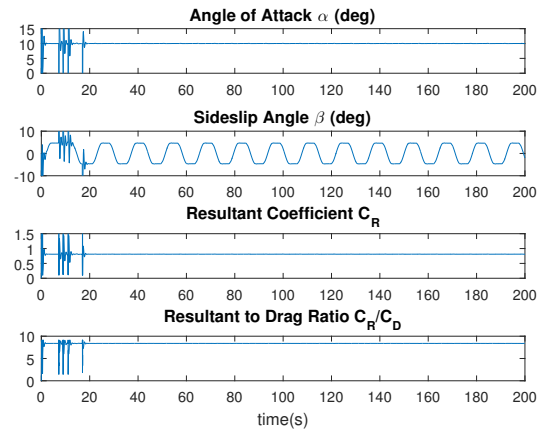*Figure 7.7: Wind Speed = 7m/s, $\phi = 25°$*

(a) Kite Translational Trajectory

(b) Kite Apparent Attitudes Trajectory

(c) Kite Euler Angle Tracking Error

(d) Power Output

119

Figure 7.8: Wind Speed = 7m/s, $\phi = 30°$

(a) Kite Translational Trajectory

(b) Kite Apparent Attitudes Trajectory

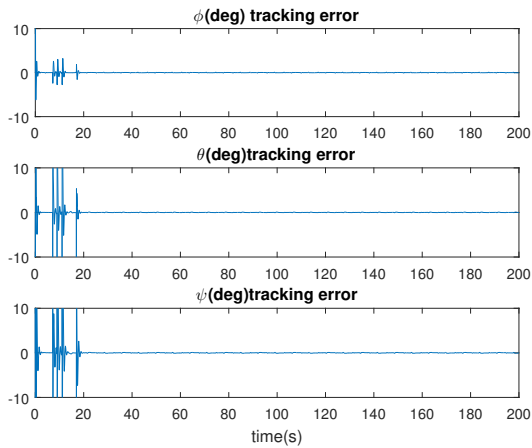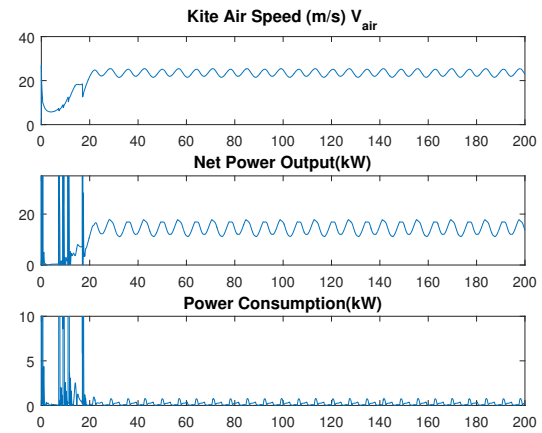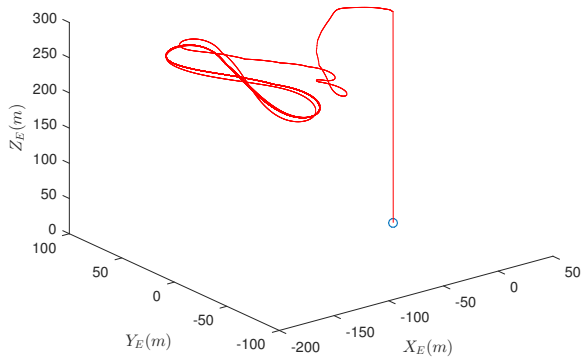*(c) Kite Euler Angle Tracking Error*

(d) Power Output

Figure 7.9: Wind Speed = 7m/s, $\phi = 35°$

(a) Kite Translational Trajectory

(b) Kite Apparent Attitudes Trajectory
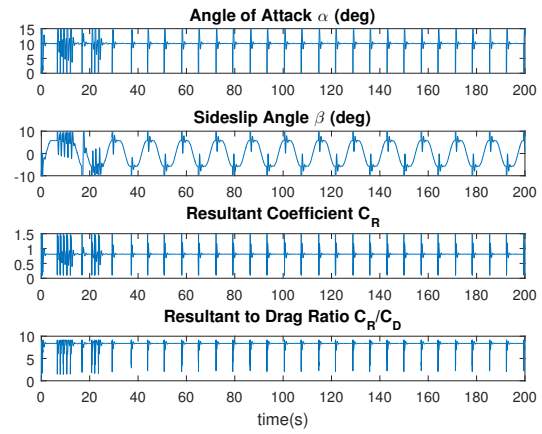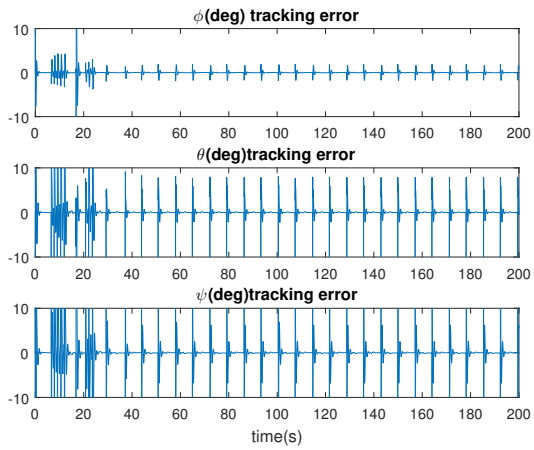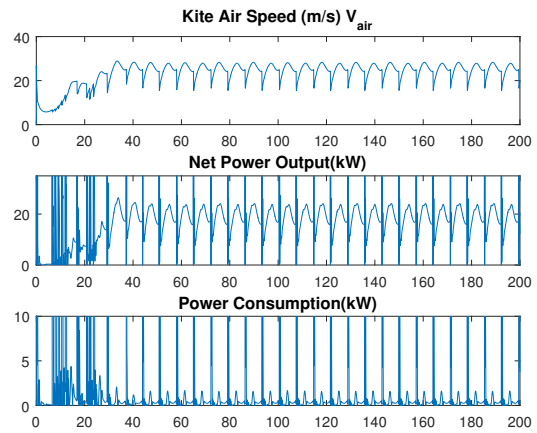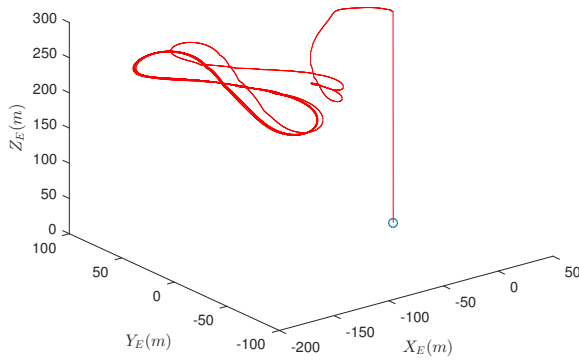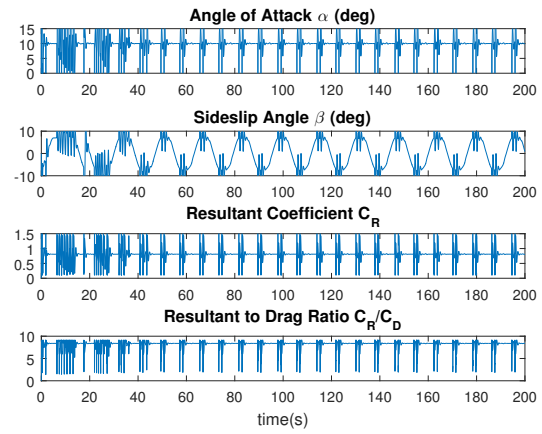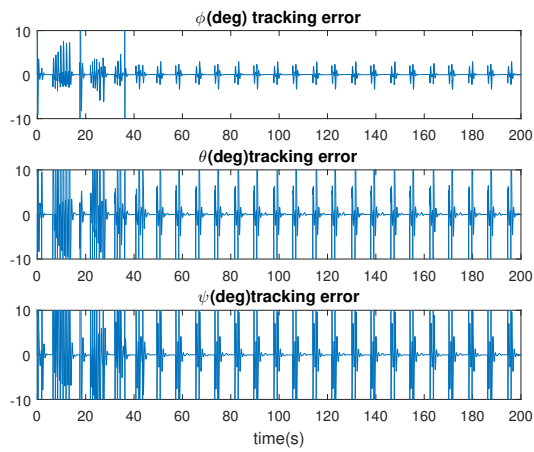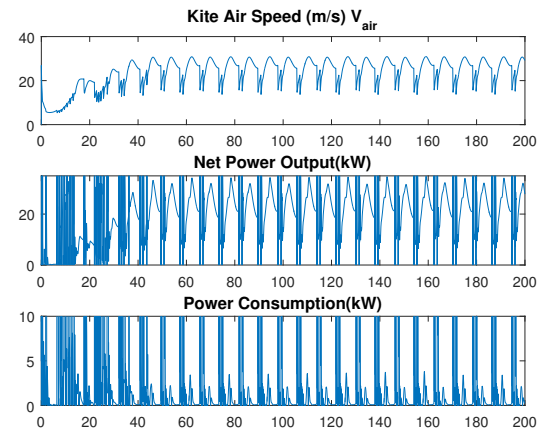
(c) Kite Euler Angle Tracking Error

(d) Power Output

translational dynamics. It can be shown that under the desired kite attitudes, the aerodynamic force can be decoupled and explicit control signal can be introduced to the kite translational dynamics.

Recall that the glider apparent velocity in frame $\mathbf{C}$ as $\mathbf{V} = \mathbf{V}_C - \mathbf{W}$, then the apparent velocity angles can be defined as follows

$$\gamma_1 = \arctan\left(\frac{v}{u}\right) \tag{7.67}$$

$$\gamma_2 = \arcsin\left(\frac{w}{V}\right) \tag{7.68}$$

where u, v and w are the components of the apparent velocity, i.e. $\mathbf{V} = \begin{pmatrix} u & v & w \end{pmatrix}$, and V is the glider apparent speed, i.e. $V = \|\mathbf{V}\|$. The apparent attitude tracking trajectory can be developed using velocity angles as follows

$$
\begin{pmatrix} \phi \\ \theta \\ \psi \end{pmatrix} = \begin{pmatrix} \frac{|u|}{u}\arctan\left(\frac{\tan\beta}{\sin\alpha}\right) \\ \frac{|\alpha|}{\alpha}\arccos\left(\cos\alpha\cos\beta\right) - \frac{|u|}{u}\gamma_2 \\ \gamma_1 \end{pmatrix} \tag{7.69}
$$

Notice that the apparent velocity angles can be treated as the spherical coordinates of the apparent velocity, i.e.

$$\mathbf{V}_C = \mathbf{V} + \mathbf{W} \qquad \mathbf{V} = V\left(\frac{u}{|u|}\cos\gamma_1\cos\gamma_2 \quad \frac{u}{|u|}\sin\gamma_1\cos\gamma_2 \quad \sin\gamma_2\right) \tag{7.70}$$

Using the notation $\boldsymbol{\xi}_C = \begin{pmatrix} V & \gamma_1 & \gamma_2 \end{pmatrix}$, the apparent acceleration can be found by taking the time derivative of equation (7.70):

$$\dot{\mathbf{V}} = \boldsymbol{\Lambda}\dot{\boldsymbol{\xi}}_C \qquad \boldsymbol{\Lambda} = \begin{pmatrix} \frac{u}{|u|}\cos\gamma_1\cos\gamma_2 & -\frac{u}{|u|}V\sin\gamma_1\cos\gamma_2 & -\frac{u}{|u|}V\cos\gamma_1\sin\gamma_2 \\ \frac{u}{|u|}\sin\gamma_1\cos\gamma_2 & \frac{u}{|u|}V\cos\gamma_1\cos\gamma_2 & -\frac{u}{|u|}V\sin\gamma_1\sin\gamma_2 \\ \sin\gamma_2 & 0 & V\cos\gamma_2 \end{pmatrix} \tag{7.71}$$

Therefore, the inverse acceleration transformation becomes

$$\dot{\boldsymbol{\xi}}_C = \mathbf{\Lambda}^{-1}\dot{\mathbf{V}} \qquad \mathbf{\Lambda}^{-1} = \frac{1}{V}\begin{pmatrix} \frac{u}{|u|}V\cos\gamma_1\cos\gamma_2 & \frac{u}{|u|}V\sin\gamma_1\cos\gamma_2 & V\sin\gamma_2 \\ -\frac{u}{|u|}\sin\gamma_1\sec\gamma_2 & \frac{u}{|u|}\cos\gamma_1\sec\gamma_2 & 0 \\ -\frac{u}{|u|}\cos\gamma_1\sin\gamma_2 & -\frac{u}{|u|}\sin\gamma_1\sin\gamma_2 & \cos\gamma_2 \end{pmatrix} \qquad (7.72)$$

If the wind velocity is constant, $\dot{\mathbf{V}} = \dot{\mathbf{V}}_C$, then the dynamical equation for apparent velocity $\mathbf{V}$ is given by

$$(m + \frac{1}{3}\rho_t r)\dot{\mathbf{V}} = \mathbf{A}_C + \mathbf{G}_C + \mathbf{T}_C \qquad (7.73)$$

Combining equations (7.72) and (7.73), the dynamical equation for variable $\boldsymbol{\xi}_C$ becomes

$$(m + \frac{1}{3}\rho_t r)\dot{\boldsymbol{\xi}}_C = \mathbf{\Lambda}^{-1}(\mathbf{H}_C + \mathbf{G}_C + \mathbf{T}_C)$$

Using the generalized force transformation $\mathbf{H}_C = \mathbf{L}_{CB}\mathbf{H}_B$, we have

$$(m + \frac{1}{3}\rho_t r)\dot{\boldsymbol{\xi}}_C = \mathbf{\Lambda}^{-1}(\mathbf{L}_{CB}\mathbf{H}_B + \mathbf{G}_C + \mathbf{T}_C) \qquad (7.74)$$

Additionally, the rotational matrix $\mathbf{L}_{BC}$ can be decomposed into three elementary rotational matrices

$$\mathbf{L}_{BC} = \mathbf{L}_1(\phi)\mathbf{L}_2(\theta)\mathbf{L}_3(\psi) \qquad (7.75)$$

$$\mathbf{L}_1(\phi) = \begin{pmatrix} 1 & 0 & 0 \\ 0 & c_\phi & s_\phi \\ 0 & -s_\phi & c_\phi \end{pmatrix} \qquad \mathbf{L}_2(\theta) = \begin{pmatrix} c_\theta & 0 & -s_\theta \\ 0 & 1 & 0 \\ s_\theta & 0 & c_\theta \end{pmatrix} \qquad \mathbf{L}_3(\psi) = \begin{pmatrix} c_\psi & s_\psi & 0 \\ -s_\psi & c_\psi & 0 \\ 0 & 0 & 1 \end{pmatrix}$$

Since the rotational matrix is orthogonal, the rotational matrix from frame $\mathbf{B}$ to frame $\mathbf{C}$ is

$$\mathbf{L}_{CB} = \mathbf{L}_3^T(\psi)\mathbf{L}_2^T(\theta)\mathbf{L}_1^T(\phi) \qquad (7.76)$$

For angle χ_1 and χ_2, each elementary rotational matrix $\mathbf{L}_i$ satisfies the following properties

$$\mathbf{L}_i^T(\chi_1) = \mathbf{L}_i(-\chi_1) \tag{7.77}$$

$$\mathbf{L}_i(\chi_1 + \chi_2) = \mathbf{L}_i(\chi_1)\mathbf{L}_i(\chi_2) = \mathbf{L}_i(\chi_2)\mathbf{L}_i(\chi_1) \tag{7.78}$$

where $i = 1, 2, 3$. Under the apparent attitude tracking, the rotational matrix $\mathbf{L}_{CB}$ becomes

$$\mathbf{L}_{CB} = \mathbf{L}_3\left(-\gamma_1\right)\mathbf{L}_2\left(\frac{|u|}{u}\gamma_2\right)\mathbf{L}_2\left(-\frac{|\alpha|}{\alpha}\arccos\left(\cos\alpha\cos\beta\right)\right)\mathbf{L}_1\left(-\frac{|u|}{u}\arctan(\frac{\tan\beta}{\sin\alpha})\right) \tag{7.79}$$

Moreover, the steady aerodynamic force on kite is given by

$$\mathbf{H}_B = \frac{1}{2}\rho_{air}V^2 S\mathbf{C}_B$$

By substitution of equation (7.79) into equation (7.74), the glider translational dynamics under the apparent attitude tracking is given by

$$\dot{\boldsymbol{\xi}}_C = \frac{1}{m + \frac{1}{3}\rho_t r}\left(\mathbf{D}(\boldsymbol{\xi}_C)\boldsymbol{\tau} + \boldsymbol{\Lambda}^{-1}(\mathbf{G}_C + \mathbf{T}_C)\right)$$

$$\mathbf{D}(\boldsymbol{\xi}_C) = \frac{1}{2}\rho_{air}SV^2\boldsymbol{\Lambda}^{-1}\mathbf{L}_3\left(-\gamma_1\right)\mathbf{L}_2\left(\frac{|u|}{u}\gamma_2\right) \tag{7.80}$$

$$\boldsymbol{\tau} = \mathbf{L}_2\left(-\frac{|\alpha|}{\alpha}\arccos\left(\cos\alpha\cos\beta\right)\right)\mathbf{L}_1\left(-\frac{|u|}{u}\arctan(\tan\beta\csc\alpha)\right)\mathbf{C}_B$$

Through coordinate transformation, the glider apparent attitudes are introduced into apparent dynamics (7.80) as control inputs. Yet (7.80) is too complicated that simplification is needed for further analysis.

Substituting equation (7.72) to equation (7.80), the control gain matrix $\mathbf{D}$ can be simplified as

follows

$$
\mathbf{D} = \frac{1}{2}\rho_{air}SV \begin{pmatrix} \frac{u}{|u|}V & 0 & 0 \\ 0 & \frac{u}{|u|}\sec\gamma_2 & 0 \\ 0 & 0 & 1 \end{pmatrix} \tag{7.81}
$$

Recall the aerodynamic coefficient in frame **B** is given by

$$
\mathbf{C}_B = \begin{pmatrix} 1 & 0 & 0 \\ 0 & 1 & 0 \\ 0 & 0 & -1 \end{pmatrix} \begin{pmatrix} \sin\alpha & 0 & -\cos\alpha \\ 0 & 1 & 0 \\ \cos\alpha & 0 & \sin\alpha \end{pmatrix} \begin{pmatrix} C_L \\ C_y \\ C_D \end{pmatrix} - \begin{pmatrix} C_t \\ 0 \\ 0 \end{pmatrix}
$$

which can be put into matrix form

$$
\mathbf{C}_B = -\mathbf{L}_3(\pi)\mathbf{L}_2(\frac{\pi}{2} - \alpha)\mathbf{C}_n - \mathbf{C}_t \tag{7.82}
$$

where $\mathbf{C}_n = \begin{pmatrix} C_L & C_y & C_D \end{pmatrix}$ and $\mathbf{C}_t = \begin{pmatrix} C_t & 0 & 0 \end{pmatrix}$. Then the vector $\boldsymbol{\tau}$ in equation (7.80) can be expressed in the following way

$$
\boldsymbol{\tau} = \boldsymbol{\Gamma}_n\mathbf{C}_n - \boldsymbol{\Gamma}_t\mathbf{C}_t \tag{7.83}
$$

$$
\boldsymbol{\Gamma}_t = \mathbf{L}_2\left(-\frac{|\alpha|}{\alpha}\arccos\left(\cos\alpha\cos\beta\right)\right)\mathbf{L}_1\left(-\frac{|u|}{u}\arctan(\tan\beta\csc\alpha)\right)
$$

$$
\boldsymbol{\Gamma}_n = \boldsymbol{\Gamma}_t\mathbf{I}_-\mathbf{L}_2(\frac{\pi}{2} - \alpha)
$$

By substitution, it can be shown that

$$
\boldsymbol{\Gamma}_t\mathbf{C}_t = C_t \begin{pmatrix} \cos\alpha\cos\beta \\ 0 \\ -\frac{\alpha}{|\alpha|}\sqrt{1 - \cos^2\alpha\cos^2\beta} \end{pmatrix} \tag{7.84}
$$

Denote the trigonometric functions $\eta_1 = \sqrt{1 - \cos^2\alpha\cos^2\beta}$ and $\eta_2 = \sqrt{1 + \csc^2\alpha\tan^2\beta}$, then

$$
\mathbf{\Gamma}_n =
\begin{pmatrix}
\sin\alpha\cos\alpha\cos\beta - \frac{\alpha}{|\alpha|}\frac{\eta_1}{\eta_2}\cos\alpha & \frac{u}{|u|}\frac{\alpha}{|\alpha|}\frac{\eta_1}{\eta_2}\csc\alpha\tan\beta & -\cos^2\alpha\cos\beta - \frac{\alpha}{|\alpha|}\frac{\eta_1}{\eta_2}\sin\alpha \\
\frac{u}{|u|}\frac{1}{\eta_2}\cot\alpha\tan\beta & \frac{1}{\eta_2} & \frac{u}{|u|}\frac{1}{\eta_2}\tan\beta \\
-\frac{\alpha}{|\alpha|}\eta_1\sin\alpha - \frac{1}{\eta_2}\cos^2\alpha\cos\beta & \frac{u}{|u|}\frac{1}{\eta_2}\cot\alpha\sin\beta & \frac{\alpha}{|\alpha|}\eta_1\cos\alpha - \frac{1}{\eta_2}\sin\alpha\cos\alpha\cos\beta
\end{pmatrix}
\tag{7.85}
$$

Additionally, using trigonometric identities, the following equation can be proven

$$
\begin{aligned}
1 + \csc^2\alpha\tan^2\beta &= 1 + \csc^2\alpha(\sec^2\beta - 1) \\
&= 1 + \csc^2\alpha\sec^2\beta - \csc^2\alpha \\
&= \csc^2\alpha\sec^2\beta(\sin^2\alpha\cos^2\beta + 1 - \cos^2\beta) \\
&= \csc^2\alpha\sec^2\beta\left((\sin^2\alpha - 1)\cos^2\beta + 1\right) \\
&= \csc^2\alpha\sec^2\beta(1 - \cos^2\alpha\cos^2\beta)
\end{aligned}
$$

Therefore, for $\alpha, \beta \in (-\frac{\pi}{2}, \frac{\pi}{2})$,

$$
\eta_1 = \frac{\alpha}{|\alpha|}\eta_2\sin\alpha\cos\beta
\tag{7.86}
$$

Using equation (7.86), the matrix $\mathbf{\Gamma}_n$ can be simplified as follows

$$
\mathbf{\Gamma}_n =
\begin{pmatrix}
0 & \frac{u}{|u|}\sin\beta & -\cos\beta \\
\frac{u}{|u|}\frac{\alpha}{|\alpha|}\frac{1}{\eta_1}\cos\alpha\sin\beta & \frac{\alpha}{|\alpha|}\frac{1}{\eta_1}\sin\alpha\cos\beta & \frac{u}{|u|}\frac{\alpha}{|\alpha|}\frac{1}{\eta_1}\sin\alpha\sin\beta \\
-\frac{\alpha}{|\alpha|}\frac{1}{\eta_1}\sin\alpha & \frac{u}{|u|}\frac{\alpha}{|\alpha|}\frac{1}{\eta_1}\cos\alpha\sin\beta\cos\beta & \frac{\alpha}{|\alpha|}\frac{1}{\eta_1}\cos\alpha\sin^2\beta
\end{pmatrix}
\tag{7.87}
$$

Under the apparent attitude tracking (7.69), the airborne kite system translational apparent dynamics are given by

$$
\dot{\boldsymbol{\xi}}_C = \frac{1}{m + \frac{1}{3}\rho_t r}\left(\mathbf{D}(\mathbf{\Gamma}_n\mathbf{C}_n - \mathbf{\Gamma}_t\mathbf{C}_t) + \mathbf{\Lambda}^{-1}(\mathbf{G}_C + \mathbf{T}_C)\right)
\tag{7.88}
$$

$$\mathbf{D} = \frac{1}{2}\rho_{air}SV \begin{pmatrix} \frac{u}{|u|}V & 0 & 0 \\ 0 & \frac{u}{|u|}\sec\gamma_2 & 0 \\ 0 & 0 & 1 \end{pmatrix}$$

$$\mathbf{\Gamma}_n = \begin{pmatrix} 0 & \frac{u}{|u|}\sin\beta & -\cos\beta \\ \frac{u}{|u|}\frac{\alpha}{|\alpha|}\frac{1}{\eta_1}\cos\alpha\sin\beta & \frac{\alpha}{|\alpha|}\frac{1}{\eta_1}\sin\alpha\cos\beta & \frac{u}{|u|}\frac{\alpha}{|\alpha|}\frac{1}{\eta_1}\sin\alpha\sin\beta \\ -\frac{\alpha}{|\alpha|}\frac{1}{\eta_1}\sin\alpha & \frac{u}{|u|}\frac{\alpha}{|\alpha|}\frac{1}{\eta_1}\cos\alpha\sin\beta\cos\beta & \frac{\alpha}{|\alpha|}\frac{1}{\eta_1}\cos\alpha\sin^2\beta \end{pmatrix}$$

$$\mathbf{\Gamma}_t\mathbf{C}_t = C_t \begin{pmatrix} \cos\alpha\cos\beta \\ 0 \\ -\frac{\alpha}{|\alpha|}\sqrt{1-\cos^2\alpha\cos^2\beta} \end{pmatrix}$$

The glider apparent velocity dynamics can be further simplified using the following lemma:

Lemma 8. *If the glider geometric attitude follows the desired attitude given in (7.69), then the following sign equation holds*

$$\frac{u_a}{|u_a|} = \frac{u}{|u|} \tag{7.89}$$

Proof. According to the apparent velocity transformation $\mathbf{V}_a = \mathbf{L}_{BC}\mathbf{V}$, the apparent velocity component u_a can be rewritten as follows

$$u_a = (v\sin\psi + u\cos\psi)\cos\theta - w\sin\theta \tag{7.90}$$

Using the following trigonometric identity,

$$v\sin\psi + u\cos\psi = \frac{u}{|u|}\sqrt{u^2+v^2}\cos(\psi-\gamma_1) \tag{7.91}$$

Therefore, under the desired glider geometric attitude $\psi = \gamma_1$, the u_a can be simplified as

$$u_a = \frac{u}{|u|}\sqrt{u^2+v^2}\cos\theta - w\sin\theta \tag{7.92}$$

Using the trigonometric identity of sum of the sine and cosine function, the u_a can be further

simplified as

$$u_a = \frac{u}{|u|} \|V_a\| \cos\left(\theta - \frac{u}{|u|}\gamma_2\right) \tag{7.93}$$

Substituting the desired pitch angle $\theta = \frac{u}{|u|}\gamma_2 + \frac{\alpha}{|\alpha|} \arccos(\cos\alpha\cos\beta)$, equation (7.93) becomes

$$u_a = \frac{u}{|u|} \|V_a\| \cos\alpha\cos\beta \tag{7.94}$$

Since $\alpha, \beta \in (-\frac{\pi}{2}, \frac{\pi}{2})$, $\cos\alpha\cos\beta > 0$, hence

$$\frac{u_a}{|u_a|} = \frac{u}{|u|}$$

$\square$

In modeling of the glider aerodynamics, it is assumed that the glider apparent velocity along $\mathbf{i}_B$ axis is positive, i.e. $u_a > 0$. Using lemma 8, this implies that $u > 0$, hence the glider apparent velocity dynamics becomes

$$\dot{\boldsymbol{\xi}}_C = \frac{1}{m + \frac{1}{3}\rho_t r}\left(\mathbf{D}(\boldsymbol{\Gamma}_n\mathbf{C}_n - \boldsymbol{\Gamma}_t\mathbf{C}_t) + \boldsymbol{\Lambda}^{-1}(\mathbf{G}_C + \mathbf{T}_C)\right)$$

$$\mathbf{C}_n = \begin{pmatrix} C_L & C_y & C_D \end{pmatrix} \qquad \mathbf{C}_t = \begin{pmatrix} 0 & 0 & C_t \end{pmatrix}$$

$$\mathbf{D} = \frac{1}{2}\rho_{air}SV\begin{pmatrix} V & 0 & 0 \\ 0 & \sec\gamma_2 & 0 \\ 0 & 0 & 1 \end{pmatrix}$$

$$\boldsymbol{\Gamma}_n = \begin{pmatrix} 0 & \sin\beta & -\cos\beta \\ \frac{\alpha}{|\alpha|}\frac{1}{\eta_1}\cos\alpha\sin\beta & \frac{\alpha}{|\alpha|}\frac{1}{\eta_1}\sin\alpha\cos\beta & \frac{\alpha}{|\alpha|}\frac{1}{\eta_1}\sin\alpha\sin\beta \\ -\frac{\alpha}{|\alpha|}\frac{1}{\eta_1}\sin\alpha & \frac{\alpha}{|\alpha|}\frac{1}{\eta_1}\cos\alpha\sin\beta\cos\beta & \frac{\alpha}{|\alpha|}\frac{1}{\eta_1}\cos\alpha\sin^2\beta \end{pmatrix} \tag{7.95}$$

$$\boldsymbol{\Gamma}_t\mathbf{C}_t = C_t\begin{pmatrix} \cos\alpha\cos\beta \\ 0 \\ -\frac{\alpha}{|\alpha|}\sqrt{1 - \cos^2\alpha\cos^2\beta} \end{pmatrix}$$

Combining the apparent velocity dynamics (7.95) and the kinematic relation (4.5), a cascade dy-
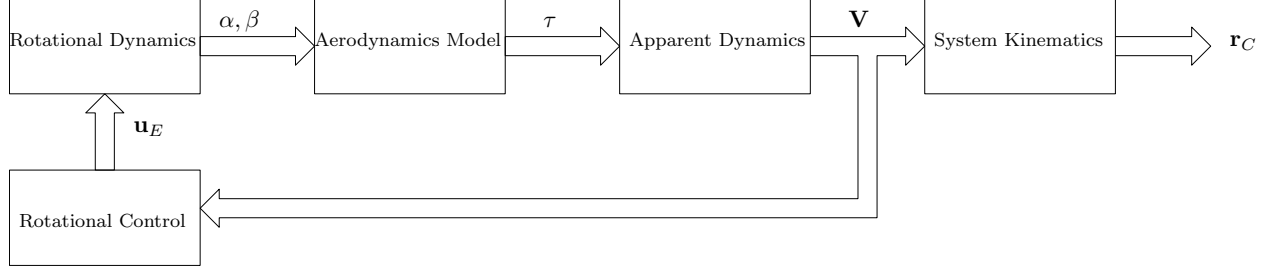
Figure 7.10: Inertial Apparent Velocity System Diagram

namical system can be proposed under the apparent attitude tracking as shown in the following theorem:

Theorem 11. *Denote the glider position vector in Cartesian earth frame C as $\mathbf{r}_C = \begin{pmatrix} x_C & y_C & z_C \end{pmatrix}$ and velocity vector as $\mathbf{V}_C = \begin{pmatrix} u_C & v_C & w_C \end{pmatrix}$. If the glider apparent velocity component $u_a > 0$, then the glider attitudes follow the apparent attitude tracking trajectories*

$$
\begin{pmatrix} \phi \\ \theta \\ \psi \end{pmatrix} = \begin{pmatrix} \frac{|u|}{u} \arctan\left(\frac{\tan \beta}{\sin \alpha} \right) \\ \frac{|\alpha|}{\alpha} \arccos\left(\cos \alpha \cos \beta \right) - \frac{|u|}{u} \gamma_2 \\ \gamma_1 \end{pmatrix}
$$

where the $\begin{pmatrix} \alpha & \beta \end{pmatrix}$ are the desired apparent attitudes and $\begin{pmatrix} \gamma_1 & \gamma_2 \end{pmatrix} = \begin{pmatrix} \arctan(\frac{v}{u}) & \frac{w}{V} \end{pmatrix}$ are apparent velocity angles. Denote the state variables $\boldsymbol{\xi}_C = \begin{pmatrix} V & \gamma_1 & \gamma_2 \end{pmatrix}$, the glider translational dynamics becomes a cascade dynamical system

$$
\dot{\mathbf{r}}_C = \mathbf{V} + \mathbf{W} \tag{7.96}
$$

$$
\mathbf{V} = V \begin{pmatrix} \cos \gamma_1 \cos \gamma_2 & \sin \gamma_1 \cos \gamma_2 & \sin \gamma_2 \end{pmatrix} \tag{7.97}
$$

$$
\dot{\boldsymbol{\xi}}_C = \frac{1}{m + \frac{1}{3}\rho_t r} \left(\mathbf{D}\boldsymbol{\tau} + \boldsymbol{\Lambda}^{-1}(\mathbf{G}_C + \mathbf{T}_C) \right) \tag{7.98}
$$

Under the apparent attitude tracking, the aerodynamic forces on glider motion are decoupled. The angle of attack α and sideslip angle β are introduced into the apparent velocity dynamics as control inputs. The resulting dynamical system possess a cascade structure as shown in Figure 7.10.

Chapter 8

Conclusion and Future Works

In this dissertation, the modeling and control of the kite energy system are studied. The fundamental aspects of the kite energy system are first considered. Four different coordinate systems are established to describe the kite motion. The kinematic relations of the kite motion in different coordinate systems are derived. Four important aspect of the physics acting on the kite energy systems are investigated, including the steady aerodynamics, added mass effects, conservative force and tether tension. Based on the kinematic relations of the aerodynamics, the passivity property of the steady aerodynamic force with respect to the kite apparent velocity is established. This property reflects the dissipativity of the steady aerodynamic force. The power generation limits of the kite energy system is then derived in the three dimensional case.

Based on Euler-Lagrange dynamics and system kinematic relations, the dynamical equation of the kite energy systems are established. It can be shown that the kite system dynamics are equivalent in different reference frames, therefore, a unified simulation model for airborne and undersea kite energy system can be established. The structures of kite rotational and translational dynamics are studied based on the established dynamical model. In the airborne case, the overall system dynamics is cascade and the rotational motion can be treated as inputs to the kite translational motion. On the other hand, the rotational and translational dynamics are fully coupled in the undersea kite energy systems.

The Lyapunov and passivity methods are used to studied the stability of the kite translational

motion. In airborne kite energy system, by choosing the apparent energy function as storage function for kite translational motion, the ultimately boundedness and boundedness of the kite apparent velocity are established and three different tether control algorithms are designed. Using the rotational energy function as Lyapunov function candidate, the stability of the kite rotational motion about a constant desirable attitude can be established. By switching the desired kite attitudes, a figure eight kite translational trajectory can be formed which results in net power output. In undersea kite energy systems, the total energy of the kite and surrounding fluid is chosen as the Lyapunov function of the system. The ultimately boundedness of the undersea kite energy system is established using Lyapunov method.

Although the boundedness property of the kite translation can be established through Lyapunov and passivity analysis, there is no direct control input in kite translational dynamics. To achieve better performance in translational motion, the transformation of the kite translational dynamics into relative motion frame is investigated. The system dynamics transformation allows the kite angular velocity appears in the equations of motion as direct control inputs. The back-stepping method is used to design the rotational control input to achieve desirable translational states. However, the simulation shows that the control signal cause a large error in tracking performance since the magnitude of the control input is very limited.

To achieve the tracking performance in translational motion, the apparent attitude tracking theorem is proposed. Using geometric relations of the kite apparent attitudes, a desired trajectory of the Euler angles is derived. The back-stepping method is used to designed the rotational control signal for achieving desired angle of attack and side-slip angle. Based on the geometric apparent attitude tracking control, the apparent dynamics of the kite energy system is proposed where the angle of attack and side-slip angle are introduced into the translational dynamics as control inputs.

In summary, the following contributions are made in this research of kite energy systems,

- The physics and fundamental power generation limit of the kite energy systems are studied.

- A unified simulation model of both airborne and undersea kite motion is proposed.

- Three different control systems are designed for the kite energy systems.

- A modified kite system dynamic is proposed and the direct control input is introduced into the kite translational motion.

Although the geometric apparent attitude tracking control system achieves the desired kite apparent attitudes, there are several drawbacks in the proposed algorithm. From the modeling perspective, the following aspects needs to be addressed, the unsteady aerodynamics caused by the switching of the kite attitudes needs to be modeled. The stability issue of the kite motion needs to be considered if the unsteady aerodynamics are included in the model. From the control perspective, the following issues need to be addressed in the future. First the apparent attitude tracking is given in terms of the Euler angles, which have the singularity issues that may cause the failure of the control system. Second, the geometric apparent attitude tracking depends on the global measurement of the kite apparent velocity, which is difficult to obtained from the local sensing device mounted on the kite. Therefore, the apparent attitude tracking algorithm needs to be modified so that only the local measurement is required for tracking. Based on the modified kite translational dynamics, the optimal power harvesting strategy of the kite energy system can be design.

Bibliography

[1] Makani power. [Online]. Available: http://www.makanipower.com

[2] Minesto. [Online]. Available: http://minesto.com/deep-green/

[3] Ampyx power. [Online]. Available: http://www.ampyxpower.com

[4] Delft kite power. [Online]. Available: http://www.lr.tudelft.nl/en/

[5] Joby energy. [Online]. Available: http://www.jobyenergy.com/haw

[6] M. L. Loyd, "Crosswind kite power,," *Journal of Energy*, vol. 4(3), 1980.

[7] M. Landberg, "Submersible plant," Patent US 8 246 293, Aug 21, 2012.

[8] Enerkíte. [Online]. Available: http://www.enerkite.com

[9] Kitenrg. [Online]. Available: http://www.kitenergy.net/

[10] M. Canale, L. Fagiano, and M. Milanese, "High altitude wind energy generation using controlled power kites," *IEEE Transactions on Control Systems Technology*, vol. 18, no. 2, March 2010.

[11] L. Fagiano, M. Milanese, and D. Piga, "Optimization of airborne wind energy generators," *Int. J. Robust. Nonlinear Control*, vol. 22, 2011.

[12] L. Fagiano, M. Milanese, V. Razza, and M. Bonansone, "High-altitude wind energy for sustainable marine transportation," *IEEE Transactions on Intelligent Transportation Systems*, vol. 13, no. 2, June 2012.

[13] M. Erhard and H. Strauch, "Control of towing kites for seagoing vessels," *IEEE Trans. on Control Systems Technology*, vol. 21(5), 2013.

[14] M. Erhard, G. Horn, and M. Diehl, "A quaternion-based model for optimal control of an airborne wind energy system," *ZAMM - Journal of Applied Mathematics and Mechanics / Zeitschrift fr Angewandte Mathematik und Mechanik*, vol. 97, no. 1, 2017.

[15] F. L., H. K., B. B., and K. M., "On sensor fusion for airborne wind energy systems," *IEEE Transactions on Control Systems Technology*, vol. 22, no. 3, May 2014.

[16] L. Fagiano, A. Zgraggen, M. Morari, and M. Khammash, "Automatic crosswind flight of tethered wings for airborne wind energy: Modeling, control design, and experimental results," *IEEE Transactions on Control Systems Technology*, vol. 22, no. 4, July 2014.

[17] A. Zgraggen, L. Fagiano, and M. Morari, "Real-time optimization and adaptation of the crosswind flight of tethered wings for airborne wind energy," *IEEE Transactions on Control Systems Technology*, vol. 23, no. 2, March 2015.

[18] A. U. Zgraggen, L. Fagiano, and M. Morari, "Automatic retraction and full-cycle operation for a class of airborne wind energy generators," *IEEE Transactions on Control Systems Technology*, vol. 24, no. 2, March 2016.

[19] T. A. Wood, H. Hesse, A. U. Zgraggen, and R. S. Smith, "Model-based identification and control of the velocity vector orientation for autonomous kites," in *2015 American Control Conference (ACC)*, July 2015.

[20] ——, "Model-based flight path planning and tracking for tethered wings," in *2015 54th IEEE Conference on Decision and Control (CDC)*, Dec 2015.

[21] A. Millane, H. Hesse, T. A. Wood, and R. S. Smith, "Range-inertial estimation for airborne wind energy," in *2015 54th IEEE Conference on Decision and Control (CDC)*, Dec 2015.

[22] P. Williams, B. Lansdorp, and W. Ockels, "Nonlinear control and estimation of a tethered kite in changing wind conditions," *AIAA Journal of Guidance, Control and Dynamics*, vol. 31, no. 3, 2008.

[23] ——, "Optimal crosswind towing and power generation with tethered kites," *AIAA Journal of Guidance, Control and Dynamics*, vol. 31, no. 1, 2008.

[24] C. Jehle and R. Schmehl, "Applied tracking control for kite power systems," *AIAA Journal of Guidance, Control and Dynamics*, vol. 37, no. 4, 2014.

[25] L. Fagiano and C. Novara, "Learning a nonlinear controller from data: Theory, computation, and experimental results," *IEEE Transactions on Automatic Control*, vol. 61, no. 7, July 2016.

[26] C. Vermillion, T. Grunnagle, R. Lim, and I. Kolmanovsky, "Model-based plant design and hierarchical control of a prototype lighter-than-air wind energy system, with experimental flight test results," *IEEE Transactions on Control Systems Technology*, vol. 22, no. 2, March 2014.

[27] A. Bafandeh and C. Vermillion, "Altitude optimization of airborne wind energy systems via switched extremum seeking–design, analysis, and economic assessment," *IEEE Transactions on Control Systems Technology*, vol. PP, no. 99, 2016.

[28] M. Kehs, C. Vermillion, and H. Fathy, "Online energy maximization of an airborne wind energy turbine in simulated periodic flight," *IEEE Transactions on Control Systems Technology*, vol. PP, no. 99, 2017.

[29] H. Li, D. J. Olinger, and M. A. Demetriou, "Control of an airborne wind energy system using an aircraft dynamics model," in *2015 American Control Conference (ACC)*, July 2015.

[30] ——, "Attitude tracking control of a groundgen airborne wind energy system," in *2016 American Control Conference (ACC)*, July 2016.

[31] ——, "Control of a tethered undersea kite energy system using a six degree of freedom model," in *2015 54th IEEE Conference on Decision and Control (CDC)*, Dec 2015.

[32] ——, "Passivity based control of a tethered undersea kite energy system," in *2016 American Control Conference (ACC)*, July 2016.

[33] ——, "Attitude tracking control of an airborne wind energy system," in *2015 European Control Conference (ECC)*, July 2015.

[34] ——, "Modeling of tethered kite apparent velocity dynamics based on effective attitude tracking," in *35th Wind Energy Symposium*, January 2017.

[35] M. Diehl, "Airborne wind energy," ser. Green Energy and Technology. Springer, 2013.

[36] H. K. Khalil, *Nonlinear Systems.*, 3rd ed. Upper Saddle River, NJ: Prentice Hall, 2001.